

Electronic Thesis and Dissertation Repository

---

4-27-2015 12:00 AM

## Molecular identification and characterization of host DEAD-box RNA helicases that are associated with Turnip mosaic virus infection

Yinzi Li, *The University of Western Ontario*

Supervisor: Dr. Aiming Wang, *The University of Western Ontario*

Joint Supervisor: Dr. Mark Bernards, *The University of Western Ontario*

A thesis submitted in partial fulfillment of the requirements for the Doctor of Philosophy degree in Biology

© Yinzi Li 2015

Follow this and additional works at: <https://ir.lib.uwo.ca/etd>



Part of the [Plant Pathology Commons](#)

---

### Recommended Citation

Li, Yinzi, "Molecular identification and characterization of host DEAD-box RNA helicases that are associated with Turnip mosaic virus infection" (2015). *Electronic Thesis and Dissertation Repository*. 2824.

<https://ir.lib.uwo.ca/etd/2824>

This Dissertation/Thesis is brought to you for free and open access by Scholarship@Western. It has been accepted for inclusion in Electronic Thesis and Dissertation Repository by an authorized administrator of Scholarship@Western. For more information, please contact [wlsadmin@uwo.ca](mailto:wlsadmin@uwo.ca).

MOLECULAR IDENTIFICATION AND CHARACTERIZATION OF  
HOST DEAD-BOX RNA HELICASES THAT ARE ASSOCIATED WITH  
TURNIP MOSAIC VIRUS INFECTION

(Thesis format: Monograph)

By

**Yinzi Li**

Graduate Program in Biology

A thesis submitted in partial fulfillment of the requirements for the degree of  
Doctor of Philosophy

The School of Graduate and Postdoctoral Studies  
The University of Western Ontario  
London, Ontario, Canada

© Yinzi Li 2015

## ABSTRACT

Plant viruses have small and compact genomes whose coding capacity is not sufficient to fulfil the viral life cycle. Thus, they are largely dependent on the host by recruiting many host components such as proteins and membranes. Many efforts have been made towards understanding the role of host factors and recent progress has led to the identification and characterization of a number of important host factors recruited for plant virus replication. DEAD-box RNA helicases (RHs) have been shown to play multiple roles in RNA metabolism, including remodeling RNA structures and promoting RNA-protein association/dissociation. During viral replication, RHs are implicated in several key steps of the infection process, such as viral genome translation, unwinding double-stranded RNA intermediates, and maintaining viral gene integrity by suppression of viral RNA recombination. Here, we used *Turnip mosaic virus* (TuMV), a member of potyviruses, as a model virus to explore RHs' role in viral infection. Firstly, we screened *Arabidopsis* T-DNA insertion mutants corresponding to *RHs* and identified three *Arabidopsis* DEAD-box RNA helicases (*AtRHs*) that are associated with TuMV infection. We further characterized an *Arabidopsis* DEAD-box RNA helicase, PRH75, which is required for TuMV infection as downregulation of *PRH75* in *Arabidopsis* impedes the viral infection. We also found that PRH75 interacts with several viral proteins including TuMV helicase CI, RNA-dependent RNA polymerase (RdRP) NIb and viral genome-linked protein VPg. In TuMV-infected cells, PRH75 colocalizes with the 6K2-induced viral replication complex (VRC) and viral dsRNA. The recruitment of PRH75 to the VRC is possibly through its interactions with viral replicase components CI, NIb and VPg. As an RNA helicase, PRH75 may assist in unwinding viral RNA duplexes during TuMV replication. Moreover, the work here also presents evidence demonstrating that the nuclear transport of TuMV viral proteins is mediated by *Arabidopsis* importin  $\alpha$ . Taken together, these data suggest that PRH75 is an essential host factor required for TuMV infection.

**Keywords:** plant viruses, potyviruses, *Turnip mosaic virus* (TuMV), viral replication and translation, viral replication complex (VRC), recessive resistance, host factor(s), *Arabidopsis* DEAD-box RNA helicase (*AtRH*), nuclear transport, *Arabidopsis* importin  $\alpha$ .

## ACKNOWLEDGMENTS

First, I would like to give my heartfelt gratitude to my supervisor and mentor, Dr. Aiming Wang for his guidance, patience and encouragement. It was an invaluable and deeply rewarding experience to learn from him and work in his team. His supervision and intelligence inspired me to complete my journey of pursuing my Ph.D degree. More than anything, his diligence, generosity and wisdom have been instrumental in my personal growth.

I am truly grateful to my co-supervisor, Dr. Mark Bernards for his mentoring, assistance and support throughout the years. Thanks for all the valuable advice and discussions on my project. Without his help, I wouldn't have made it this far. Genuine thanks to my advisory committee, Dr. Jim Karagiannis and Dr. Susanne Kohalmi, for the helpful ideas and support during my studies.

My earnest thanks go to my group fellows, Dr. Ruyi Xiong, Dr. Changwei Zhang, Dr. Chowda Reddy, Dr. Hui Chen, Dr. Lingrui Zhang, Dr. Xiaofei Cheng and Dr. Hongguang Cui. It was a great pleasure to work with them. Also, I am grateful towards other group members and friends for their companionship and help. I have learned and benefited so much from them.

I would like to express my sincere thanks to Jamie McNeil, Huaiyu Wang and Dr. Cinta Hernández Sebastià for their assistance and support. Thanks for the time and all the effort you put into my project. I greatly appreciate that! I warmly thank Alex Molnar, Ted Blazejowski and Lisa Amyot from AAFC for their technical support.

I am deeply indebted to my parents and my husband. It was their endless love and sacrifices to enable me to succeed. I am so proud of my baby girl who changed my life and makes it joyful.



# TABLE OF CONTENTS

ABSTRACT.....	II
KEYWORDS.....	II
ACKNOWLEDGMENTS.....	III
TABLE OF CONTENTS.....	IV
LIST OF TABLES.....	X
LIST OF FIGURES.....	XI
LIST OF APPENDICES.....	XIV
LIST OF ABBREVIATIONS.....	XV
<b>Chapter 1: Introduction.....</b>	<b>1</b>
1.1 An overview of plant viruses.....	1
1.1.1 Replication of positive-sense RNA viruses.....	4
1.1.2 Picorna-like plant viruses, <i>Potyviridae</i> .....	6
1.1.3 Genome organization of potyviruses.....	7
1.1.4 Functions of potyviral proteins.....	7
1.1.5 <i>Turnip mosaic virus</i> (TuMV).....	13
1.2 Host factors required for viral infection.....	14
1.2.1 Host factors.....	14
1.2.2 Eukaryotic translation initiation factors (eIFs).....	16

1.2.3	Eukaryotic translation initiation factor 4A, eIF4A.....	16
1.3	DEAD-box RNA helicase.....	17
1.3.1	Structure and functions.....	17
1.3.2	Association with abiotic stress.....	19
1.3.3	Association with viral infection.....	20
1.4	Plant defense responses against viral pathogens.....	22
1.4.1	Dominant resistance.....	22
1.4.2	Recessive resistance.....	24
1.4.3	RNA silencing and its suppression.....	26
1.5	Research objectives and goals.....	29
<b>Chapter 2: Materials and Methods.....</b>		<b>31</b>
2.1	Plant materials and growth conditions.....	31
2.2	Virus materials.....	31
2.3	Bacterial strains and growth conditions.....	31
2.4	Yeast strains and cell culture.....	32
2.5	Plasmid construction.....	32
2.6	Bacterial transformations .....	37
2.6.1	<i>E. coli</i> transformation.....	37
2.6.2	<i>Agrobacterium</i> transformation.....	39
2.7	Plant genomic DNA extraction.....	39

2.8	RNA isolation.....	39
2.9	Functional analysis of <i>Arabidopsis</i> T-DNA insertion lines of <i>AtRHs</i> .....	40
2.9.1	Selection of <i>Arabidopsis</i> T-DNA insertion lines of <i>AtRHs</i> .....	40
2.9.2	Screening for homozygous <i>Arabidopsis</i> T-DNA insertion lines of <i>AtRHs</i> .....	40
2.9.3	Gene expression analysis of <i>Arabidopsis</i> T-DNA insertion lines of <i>AtRHs</i> .....	42
2.10	Polymerase chain reaction (PCR).....	42
2.10.1	Polymerase chain reaction (PCR).....	42
2.10.2	RT-PCR.....	42
2.10.3	Real-time quantitative RT-PCR (qRT-PCR).....	42
2.11	Gateway-based cloning.....	44
2.12	Yeast transformation.....	46
2.13	Yeast two-hybrid assay.....	46
2.14	Transient expression in <i>N. benthamiana</i> .....	47
2.15	Confocal microscopy.....	48
2.16	Quantification of Fluorescence Resonance Energy Transfer (FRET) efficiency by acceptor photobleaching.....	48
2.17	dsRNA-binding dependent fluorescence complementation (dRBFC) assay.....	49
2.18	TuMV infection assay.....	49
2.19	Triple-antibody sandwich enzyme-linked immunosorbent assay (TAS-ELISA).....	50

2.20	TRV-based virus-induced gene silencing (VIGS).....	50
2.21	Gene structure and multiple sequence alignments.....	52
2.22	Statistical analysis.....	52
<b>Chapter 3: Results.....</b>		<b>53</b>
3.1	Identification of <i>Arabidopsis</i> DEAD-box RNA helicase ( <i>AtRH</i> ) genes essential for TuMV infection.....	53
3.1.1	Screening for homozygous T-DNA insertion lines of <i>AtRH</i> genes in <i>Arabidopsis</i> .....	53
3.1.2	Identification of <i>AtRH</i> genes associated with TuMV infection.....	56
3.2	Characterization of <i>Arabidopsis atrh9</i> T-DNA insertion line.....	60
3.2.1	Verification of <i>Arabidopsis atrh9</i> T-DNA insertion line.....	60
3.2.2	The accumulation of TuMV was reduced in <i>atrh9</i> mutant plants.....	63
3.2.3	Knock down of <i>AtRH9</i> expression in <i>Arabidopsis</i> by VIGS.....	63
3.2.4	Subcellular localization of <i>Arabidopsis AtRH9</i> .....	66
3.2.5	<i>Arabidopsis AtRH9</i> interacts with TuMV NIa-Pro <i>in planta</i> .....	66
3.3	Characterization of <i>Arabidopsis atrh26</i> T-DNA insertion line.....	71
3.3.1	Verification of <i>Arabidopsis atrh26</i> T-DNA insertion line.....	71
3.3.2	<i>Arabidopsis AtRH26</i> is necessary for TuMV infection.....	71
3.3.3	Subcellular localization of <i>Arabidopsis AtRH26</i> .....	71
3.4	Characterization of <i>Arabidopsis prh75</i> T-DNA insertion line.....	75

3.4.1	PRH75 was required for TuMV infection.....	75
3.4.2	Silencing of <i>PRH75</i> in <i>Arabidopsis</i> by VIGS confers resistance to TuMV.....	78
3.5	Molecular characterization of PRH75 and TuMV interactions.....	83
3.5.1	The DEAD-box RNA helicase PRH75 is conserved in many plants.....	83
3.5.2	PRH75 is a nuclear protein.....	88
3.5.3	PRH75 directly interacts with multiple TuMV viral replicase proteins....	88
3.5.4	<i>Arabidopsis</i> importin $\alpha$ interacts with PRH75 and TuMV viral replicase proteins.....	97
3.5.5	PRH75 colocalizes with <i>Arabidopsis</i> importin $\alpha$ , eIF(iso)4E and TuMV viral replicase proteins.....	105
3.5.6	Distribution of BiFC signals between PRH75 and TuMV viral replicase proteins is altered in the presence of TuMV infection.....	105
3.5.7	PRH75 is associated with TuMV replication vesicles that are bound to chloroplasts and contain dsRNA.....	110
<b>Chapter 4: Discussion.....</b>		<b>118</b>
4.1	Identification of <i>Arabidopsis</i> DEAD-box RNA helicases as host factors required for <i>Turnip mosaic virus</i> (TuMV) infection.....	118
4.2	AtRH9 and its recruitment for TuMV infection.....	119
4.3	PRH75 and its roles in TuMV infection.....	120
4.3.1	PRH75 is a nuclear-localized ATP-dependent DEAD-box RNA helicase.....	120

4.3.2 PRH75 interacts with multiple viral proteins that are essential for TuMV replication.....	120
4.3.3 Localization of PRH75 and its recruitment to the viral replication complex (VRC).....	123
4.3.4 <i>Arabidopsis</i> PRH75 is highly dynamic.....	125
4.4 Nucleus, nucleolus and virus life cycle.....	126
4.4.1 The nucleolus functions as a stress sensor in response to viral infection.....	126
4.4.2 Nuclear import of TuMV viral proteins is mediated by <i>Arabidopsis</i> importin $\alpha$ .....	126
4.5 Major findings and future directions.....	129
<b>Reference.....</b>	<b>131</b>
<b>Appendices.....</b>	<b>154</b>
<b><i>Curriculum Vitae</i>.....</b>	<b>159</b>

## LIST OF TABLES

Table 1 Primers used for plasmid construction to express TuMV viral proteins in plants.....	33
Table 2 Primers used for construction of plasmids to express <i>Arabidopsis</i> proteins...34	
Table 3 Primers used for construction of plasmids for PRH75 domain analysis.....36	
Table 4 Primers used to amplify <i>AtRH9</i> and <i>PRH75</i> DNA fragments that are inserted into the TRV-based vector.....38	
Table 5 Primers used for PCR-screening of homozygous <i>Arabidopsis atrh</i> T-DNA insertion lines.....41	
Table 6 Primers for RT-PCR.....43	
Table 7 Primers for real-time quantitative RT-PCR (qRT-PCR).....45	
Table 8 List of <i>AtRH</i> genes and corresponding <i>Arabidopsis atrh</i> T-DNA insertion lines.....54	
Table 9 List of homozygous <i>Arabidopsis atrh</i> T-DNA insertion lines for ELISA analysis.....57	
Table 10 Summary of tested protein-protein interactions.....104	

## LIST OF FIGURES

Figure 1 Schematic depiction of potyvirus infection cycle.....	3
Figure 2 Potyviral genome organization and polyprotein processing strategy.....	8
Figure 3 Methodology of triple-antibody sandwich enzyme-linked immunosorbent assay (TAS-ELISA).....	51
Figure 4 ELISA analysis of candidate <i>Arabidopsis atrh</i> T-DNA mutants.....	59
Figure 5 Genotyping and RT-PCR analysis of <i>Arabidopsis atrh9</i> T-DNA insertion lines.....	62
Figure 6 TuMV accumulation was reduced in <i>atrh9</i> mutant plants.....	65
Figure 7 Knockdown of <i>AtRH9</i> expression affects TuMV infection in <i>Arabidopsis</i> .....	68
Figure 8 Subcellular localization of <i>Arabidopsis AtRH9</i> .....	69
Figure 9 The BiFC assay for detection of the interaction between <i>AtRH9</i> and TuMV NIa-Pro <i>in planta</i> .....	70
Figure 10 Characterization of <i>Arabidopsis atrh26</i> homozygous T-DNA insertion line...	73
Figure 11 Subcellular localization of <i>Arabidopsis AtRH26</i> .....	74
Figure 12 Genotyping and RT-PCR analysis of <i>Arabidopsis prh75</i> T-DNA insertion lines.....	77
Figure 13 Relative TuMV accumulation in <i>prh75</i> mutant and wild-type plants.....	80
Figure 14 <i>PRH75</i> -silenced plants exhibit partial resistance to TuMV infection.....	82
Figure 15 Multi-sequence alignment of <i>PRH75</i> amino acid sequence with corresponding domains from different plant species.....	86
Figure 16 Characterization of <i>Arabidopsis PRH75</i> .....	87



Figure 17	PRH75 is localized in the nucleus.....	89
Figure 18	Analysis of truncated PRH75 proteins.....	90
Figure 19	The BiFC assay for detection of the interactions between PRH75 and different TuMV viral proteins <i>in planta</i> .....	93
Figure 20	The yeast two-hybrid assay for detection of the interactions between PRH75 and TuMV viral proteins.....	94
Figure 21	Quantification of FRET efficiency between PRH75 and TuMV viral proteins.....	96
Figure 22	The BiFC assay for detection of the interactions between PRH75 and <i>Arabidopsis</i> IMPA1 and IMPA2 <i>in planta</i> .....	98
Figure 23	The yeast two-hybrid assay for detection of the interactions between PRH75 and <i>Arabidopsis</i> IMPA1 and IMPA2.....	99
Figure 24	The BiFC assay for detection of the interactions between IMPA1 and TuMV viral proteins <i>in planta</i> .....	100
Figure 25	The yeast two-hybrid assay for detection of the interactions between <i>Arabidopsis</i> IMPA1 and TuMV viral proteins.....	101
Figure 26	The BiFC assay for detection of the interactions between IMPA2 and TuMV viral proteins <i>in planta</i> .....	102
Figure 27	The yeast two-hybrid assay for detection of the interactions between <i>Arabidopsis</i> IMPA2 and TuMV viral proteins.....	103
Figure 28	Colocalization of PRH75 and <i>Arabidopsis</i> importin $\alpha$ .....	106
Figure 29	Colocalization of PRH75 and <i>Arabidopsis</i> host proteins.....	107
Figure 30	Colocalization of PRH75 and TuMV viral proteins.....	109

Figure 31 The BiFC assay of the interactions between PRH75 and TuMV viral proteins during TuMV infection.....	112
Figure 32 PRH75-CFP colocalized with the chloroplast-bound 6K-YFP vesicles.....	114
Figure 33 PRH75-CFP colocalized with dsRNA-containing foci.....	115
Figure 34 PRH75-CFP colocalized with dsRNA-containing foci in the presence of TuMV infection.....	117
Figure 35 Working model for <i>Arabidopsis</i> PRH75 associated with TuMV infection.....	130

## LIST OF APPENDICES

Appendix I: List of DEAD-box RNA helicases in <i>Arabidopsis</i> .....	154
Appendix II: Negative controls of the BiFC assays.....	155

## LIST OF ABBREVIATIONS

::	fused to (in the context of reporter-gene fusion constructs)
°C	Degrees Celsius
35S	<i>Cauliflower mosaic virus</i> 35S RNA promoter
[A]	poly(A) tail
At	<i>Arabidopsis thaliana</i>
aa	amino acids
AAFC	Agriculture and Agri-Food Canada
ABRC	Arabidopsis Biological Resource Center
ACT	<i>Arabidopsis Actin2</i>
AD	activation domain
Ade	adenine
AGO	Argonaute protein
AtRH	<i>Arabidopsis</i> DEAD-box RNA helicase
ATP	adenosine 5'-triphosphate
AV-3	<i>Asparagus virus 3</i>
Avr	avirulence gene
BiFC	bimolecular fluorescence complementation
BK	binding domain
BLAST	basic local alignment search tool
BMV	<i>Brome mosaic virus</i>
bp	base pair
CaMV	<i>Cauliflower mosaic virus</i>
cDNA	complementary DNA
CFP	cyan fluorescent protein
Chl	chloroplast autofluorescence
CI	the cylindrical inclusion protein
CIYVV	<i>Clover yellow vein virus</i>
cm	centimeter (s)
CMV	<i>Cucumber mosaic virus</i>
Col-0	ecotype Columbia
CP	coat protein or viral capsid
CTAB	cetyltrimethyl-ammonium bromide
C-terminal	carboxyl-terminal
CVYV	<i>Cucumber vein yellowing virus</i>
DBP1	DNA-binding protein phosphatase 1
Dbp3	DEAD-box protein 3
Dbp5	DEAD-box protein 5
Dbp2p	DEAD-box protein 2
DCL	Dicer-like ribonuclease (s)
DDX	DEAD-box RNA helicase
DEAD	Asp-Glu-Ala-Asp
DEAH	Asp-Glu-Ala-His
DED1	DEAD-box helicase 1
Ded1p	<i>DED1</i> -encoded protein

DENV	<i>Dengue virus</i>
DIC	differential interference contrast
DMSO	dimethyl sulfoxide
DNA	deoxyribonucleic acid
DNase	deoxyribonuclease
DO	dropout
dpi	days post inoculation/infiltration
DRB	dsRNA-binding protein
dRBFC	dsRNA-binding dependent fluorescence complementation
dsRNA	double-stranded RNA
EDTA	ethylenediaminetetraacetic acid
eEF1A	eukaryotic elongation factor 1A
eIF	eukaryotic translation initiation factor(s)
eIF4A	eukaryotic translation initiation factor 4A
eIF4B	eukaryotic translation initiation factor 4B
eIF4E	eukaryotic translation initiation factor 4E
eIF(iso)4E	eukaryotic translation initiation factor isoform 4E
eIF4F	eukaryotic translation initiation factor 4F
eIF4G	eukaryotic translation initiation factor 4G
eIF(iso)4G1	eukaryotic translation initiation factor isoform 4G1
eIF(iso)4G2	eukaryotic translation initiation factor isoform 4G2
eIF4H	eukaryotic translation initiation factor 4H
ELISA	enzyme-linked immunosorbent assay
ER	endoplasmic reticulum
ETI	effector-triggered immunity
ETS	effector-triggered susceptibility
FAL1	Translation initiation factor 4AIII-like protein 1
FHV	<i>Flock house virus</i>
FRET	fluorescence resonance energy transfer
g	gram (s)
GFP	green fluorescent protein
GUS	$\beta$ -glucuronidase
h	hour (s)
HBV	<i>Hepatitis B virus</i>
HC-Pro	the helper component protease
HCV	<i>Hepatitis C virus</i>
His	histidine
HIV-1	<i>Human immunodeficiency virus type 1</i>
HM	homozygous
HR	hypersensitive response
Hsc70	heat shock cognate 70 kDa protein
IBV	<i>Infectious bronchitis virus</i>
IMPA	importin $\alpha$
ISE	increased size exclusion limit
iso	isoform
JAX1	jacalin-type lectin required for Potexvirus resistance 1

6K1	the first 6 kDa protein
6K2	the second 6 kDa protein (also referred to as 6K)
kb	kilobase (s)
kDa	kilodalton (s)
kV	kilovolt (s)
l	litre
LB	Luria Bertani
LB	T-DNA left border
Leu	leucine
LiAc	lithium acetate
LMV	<i>Lettuce mosaic virus</i>
LOS4	<i>Arabidopsis</i> osmotically responsive genes 4
LP	left genomic primer
LRR	leucine-rich repeat
µg	microgram
µl	microlitre
µM	micromolar
MAMP	microbe-associated molecular pattern
MARV	<i>Marburg virus</i>
MES	2-N-morpholino-ethanesulfonic acid
mg	milligram
min	minute
miRNA	microRNA
ml	millilitre
mM	millimolar
mRNA	messenger RNA
MW	molecular weight
ng	nanogram
nm	nanometer
nt	nucleotide(s)
NB	nucleotide binding
NCBI	National Center for Biotechnology Information
NIa	the nuclear inclusion a protein
NIa-Pro	the nuclear inclusion a protease
NIb	the nuclear inclusion b protein
NLS	nuclear localization signal
NLoS	nucleolar localization signal
NPC	nuclear pore complex
N-P-K	nitrogen (N)-phosphorus (P)-potassium (K)
N-terminal	amino-terminal
OD	optical density (absorbance)
ORF	open reading frame
OsBIRH1	<i>Oryza sativa</i> BTH-induced RNA helicase 1
P1	the first protein
P1b	the second copy of P1
P3	the third protein

P3N-PIPO	pipo as a translational fusion with the N-terminus of P3
PABP	poly(A)-binding protein
PAMP	pathogen-associated molecular pattern
PCaP1	plasma membrane associated cation-binding protein 1
PCD	programmed cell death
PCR	polymerase chain reaction
PD	plasmodesmata
PDS	phytoene desaturase
PEG	polyethylene glycol
PIPO	pretty interesting <i>Potyviridae</i> ORF
PIAMV	<i>Plantago asiatica mosaic virus</i>
PLRV	<i>Potato leaf roll virus</i>
PMH1	Putative Mitochondrial RNA Helicase1
Poly(A)	polyadenylate
PpDDXL	<i>Prunus persica</i> DDX-like
PPV	<i>Plum pox virus</i>
PRR	pattern recognition receptor
Pro	protease
PSbMV	<i>Pea seed-borne mosaic virus</i>
PTI	PAMP-triggered immunity
PVA	<i>Potato virus A</i>
PVIP	potyvirus VPg-interacting protein
PVX	<i>Potato virus X</i>
PVY	<i>Potato virus Y</i>
qRT-PCR	real-time quantitative RT-PCR
<i>R</i> gene	resistance gene
RecA	recombinase A
REN	RNA replication enhancer
Rev	HIV-1 regulator of virion expression
RDR	RNA-dependent RNA polymerase (plant)
RdRp	RNA-dependent RNA polymerase (virus)
RH	RNA helicase
RISC	RNA-induced silencing complex
RNA	ribonucleic acid
(+) RNA	(viral) positive-sense RNA
(-) RNA	(viral) negative-sense RNA
RNase	ribonuclease
RNP	ribonucleoprotein
RP	right genomic primer
rpm	revolutions per minute
RT-PCR	reverse transcription polymerase chain reaction
RTM	restricted TEV movement
RubisCO	ribulose-1,5-bisphosphate carboxylase/oxygenase
Rx	PVX resistance gene
SA	salicylic acid
SAR	systemic acquired resistance

SARS	severe acute respiratory syndrome
SARS-CoV	SARS-associated coronavirus
SCE1	SUMO conjugation enzyme 1
SD	synthetic defined
SF	superfamily
siRNA	small interfering RNA
SMV	<i>Soybean mosaic virus</i>
sRNA	small RNA
ssRNA	single-stranded RNA
(+) ssRNA	positive-sense single-stranded RNA
STRS1	Stress Response Suppressor 1
STRS2	Stress Response Suppressor 2
SUMO	small ubiquitin-related modifier
TAIR	The Arabidopsis Information Resource
TAS-ELISA	triple-antibody sandwich enzyme-linked immunosorbent assay
TBSV	<i>Tomato bushy stunt virus</i>
TCV	<i>Turnip crinkle virus</i>
T-DNA	transfer DNA
TEV	<i>Tobacco etch virus</i>
TMV	<i>Tobacco mosaic virus</i>
ToMV	<i>Tomato mosaic virus</i>
Tris	tris-hydroxymethyl aminomethane
Trp	tryptophan
TRV	<i>Tobacco rattle virus</i>
TuMV	<i>Turnip mosaic virus</i>
TVMV	<i>Tobacco vein mottling virus</i>
UTR	untranslated region
UWO	The University of Western Ontario
VIGS	virus-induced gene silencing
VPg	the viral genome-linked protein
VPg-Pro	VPg fused to a protease domain at the C terminus
VRC	viral replication complex
WCIMV	<i>White clover mosaic virus</i>
WNV	<i>West Nile virus</i>
WT	wild-type
Y2H	yeast two-hybrid
YC	C-terminal fragment of the YFP protein
YFP	yellow fluorescent protein
YN	N-terminal fragment of the YFP protein
YPD	yeast extract-peptone-dextrose
YPDA	YPD medium supplemented with adenine hemisulfate



## Chapter 1: Introduction

### 1.1 An overview of plant viruses

In the late 19<sup>th</sup> Century, a tiny infectious agent was found to cause a mosaic disease on tobacco plants, which was proven to be irrelevant to bacteria. Unlike bacteria, the infectious agent was in fact filterable. Subsequently, the term “virus”, the Latin word meaning “slimy liquid” or “poison” was coined to indicate the non-bacterial nature of this plant disease and *Tobacco mosaic virus* (TMV) was shown to be the culprit of the tobacco mosaic disease (Beijerinck, 1898). From then on, the concept of a virus as a distinct infectious entity has been established, and a lot of plant diseases that have caused substantial economic losses in the agriculture community have been found to be associated with viruses. Along with the breakthroughs of new biotechnology, numerous viral pathogens have been identified.

In essence, viruses can be regarded as the ultimate and prototypical paradigm of "selfish genes". Like all cellular life forms, viruses carry genetic information constructed by either deoxyribonucleic acid (DNA) or ribonucleic acid (RNA) in a single-stranded or double-stranded form (Astier *et al.*, 2001). However, the genetic code carried by viruses, which must be decoded by the molecular machinery of the host cell that it infects (Wagner *et al.*, 1999), is directed towards only for virus own replication. Besides the genetic materials, all viruses have coat proteins (CPs) that function as a shell to protect the viral genome from degradation, and some are wrapped by an outer membrane envelop that surrounds them during their time outside a cell. The coordinated interactions between CPs and viral nucleic acid are essential to regulate virion assembly and disassembly (Callaway *et al.*, 2001).

All viruses are obligate parasites since they can be maintained only inside living cells. Most of RNA viruses have a small genome ranging from 4 to 15 kilobases (kb) in length and have a very limited coding capacity, encoding a set of proteins that vary from 3 to 10-15 of the upper limit (Matthews and Hull, 2002). Therefore, viruses have to largely depend upon their hosts to complete almost all major steps of their infection process (Whitham and Wang, 2004).

As for a plant virus, a successful infection begins with the efficient penetration of the viral particle into plant cells such as epidermal or mesophyll cells. Then, the viral particle undergoes disassembly for translation and replication in the initially infected cell. Subsequently, the newly assembled viral particle traffics into the adjacent healthy cells via plasmodesmata (PD). Finally, the virus enters the vascular tissue to reach remote sites, thus infecting the whole plant (Schoelz *et al.*, 2011) (Figure 1).

Viruses replicate, evolve and are adapted to the host cells they infect. Viruses are known to be able to infect all types of living organisms including eukaryotes (vertebrates, invertebrates, plants and fungi) and prokaryotes (bacteria and archaea) (Carter and Saunders, 2007). This could be attributed to the fact that viruses themselves are extremely adaptable, using different replication strategies and are highly mutable to generate genetic variation through mutation and recombination in response to various environmental pressures.

In an infected cell, viruses can cause extensive remodeling of the intracellular environment in favor of the replication process (Laliberté and Sanfaçon, 2010). For instance, some plant viruses induce the proliferation of endoplasmic reticulum (ER) membranes for the formation of membranous vesicles to facilitate the assembly of viral replication complexes (Salonen *et al.*, 2005), whereas others may reshape cellular organelles such as chloroplasts, mitochondria, or peroxisomes (Wei *et al.*, 2010).

Plant pathogenic viruses often rely on insect, nematode and/or fungal vectors to gain entry into host plants, move from plant to plant and move over distant regions (Thresh, 2006). In addition, viruses can also be transmitted by human activities such as propagation of infected vegetative materials, grafting of infected materials, as well as through pollen and seed produced by the infected plants (Andret-Link and Fuchs, 2005).

As one of the main threats to agricultural production, viruses cause many important plant diseases, and are responsible for losses in crop yield and quality all over the world. Therefore, a great deal of effort is needed to develop a better comprehension of plant virology and the interplay between plants and viruses, in order to develop more potent strategies against virus infection.

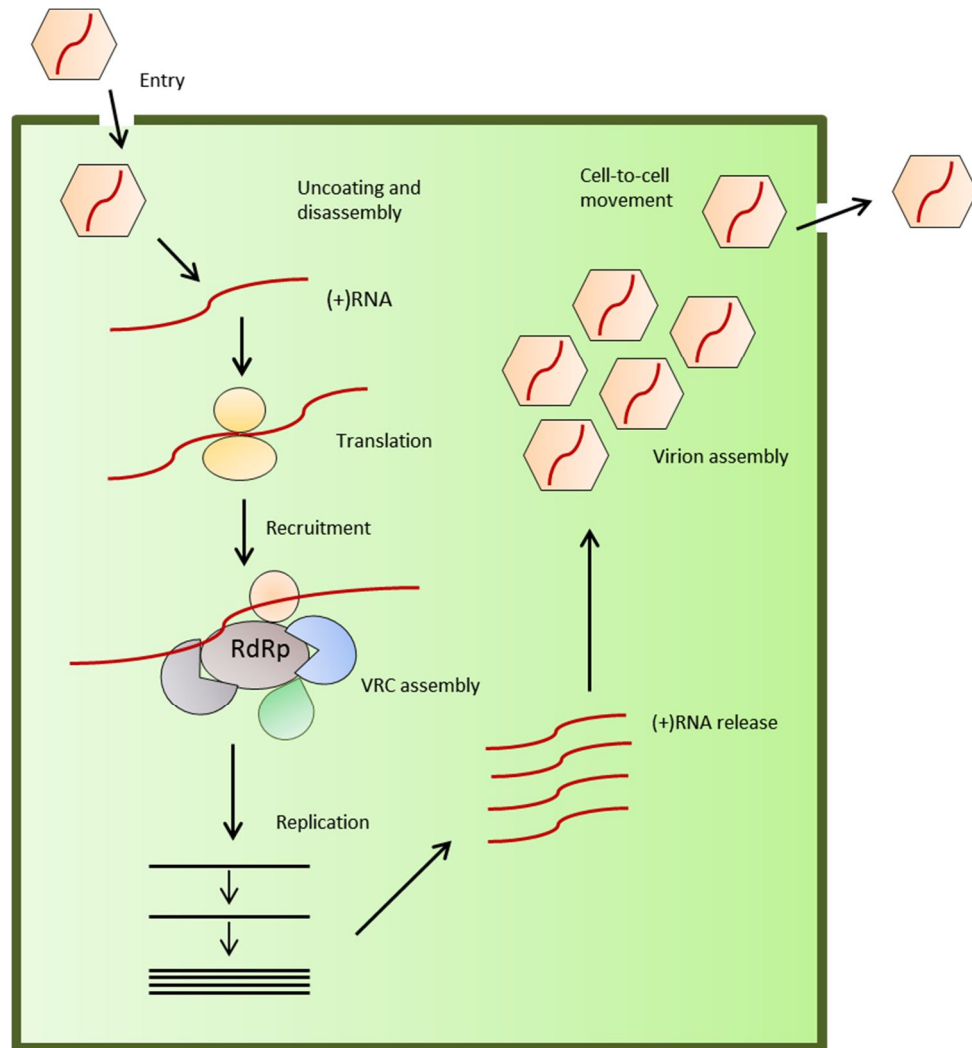


**Figure 1 Schematic depiction of potyvirus infection cycle.**

After viral entry into the cell, the virion is disassembled and viral positive-sense RNA ((+)RNA) is released into the cytoplasm for translation. Newly translated viral proteins such as RNA-dependent RNA polymerase (RdRp) and helicase direct the assembly of viral replication complex (VRC) and recruit the viral RNA to the VRC for replication. Viral negative-sense RNA ((-)RNA) is synthesized and serves as template for amplification of viral (+)RNA progeny. The new viral (+)RNA is released from the VRC and starts a new cycle of translation and replication or is encapsidated into new progeny virions and transport to the adjacent cells. Modified from (Nagy and Pogany, 2011).

### 1.1.1 Replication of positive-sense RNA viruses

The majority of known plant viruses have positive-sense RNA genomes and most viral RNA genomes are made of single-stranded RNA (van Regenmortel *et al.*, 2000). Upon entry into the host cell, the viral positive-sense RNA readily serves as a messenger RNA (mRNA) to direct biosynthesis of viral proteins for viral genome replication (Khan and Dijkstra, 2006). This type of viruses includes many important human and animal viruses, such as *Hepatitis C virus* (HCV), *West Nile virus* (WNV), *Dengue virus* (DENV) and severe acute respiratory syndrome coronavirus (SARS CoV) (Nagy and Pogany, 2011). For plant viruses, the vast majority characterized to date are positive-sense RNA viruses as well, and only the viruses classified into the *Caulimoviridae*, *Geminiviridae* and *Nanoviridae* families store their genetic information in DNA genomes (Astier *et al.*, 2001).

Viral genome replication generally refers to the cellular process by which viral genomic nucleic acid is multiplied. As for a positive-sense RNA virus, the first step of viral genome replication is to synthesize the viral proteins required for viral replication. These viral proteins include viral RdRp, helicase and other essential viral replicase components, and are mainly involved in membrane targeting, template recruitment and amplification as well as RNA capping (Novak and Kirkegaard, 1994; Ivanov and Mäkinen, 2012). However, since viruses do not encode translation factors or ribosomes, they have to hijack the host translational machinery to complete protein synthesis and genome replication (Patarroyo *et al.*, 2012).

Assembly of the viral replication complex (VRC) is a prerequisite for viral genome replication, and provides an environment in which viral RNA can be synthesized and sheltered from the cytoplasmic environment of the cell to avoid antiviral RNA silencing (Laliberté and Sanfaçon, 2010). A growing body of evidence suggests that for all positive-sense RNA viruses, viral genome replication occurs on different types of intracellular membranes (Belov *et al.*, 2007). Hence, VRCs that contain both viral and host components are anchored in a virus-induced membrane compartment. In plants, VRCs have been found to target different subcellular organelles, varying considerably

among viruses, such as the ER, chloroplast, vacuole, peroxisome, Golgi and mitochondria (Salonen *et al.*, 2005). In addition, specific cellular membranes can also be modified by different viruses to facilitate their RNA replication. The requirement for membrane rearrangements and modifications during viral genome replication indicates that the host membranes are essential and functional components of VRCs. Moreover, many viruses encode integral membrane proteins that associate with particular intracellular membranes and act as anchors for the formation of VRCs (Sanfaçon, 2012). In addition, these integral membrane proteins may play a vital role in recruiting other viral proteins and host components into VRCs.

Within VRCs, viral RdRp and helicase are the two most critical components. These two proteins are associated with other viral proteins as well as host cellular factors for viral genome replication. As noted, all the positive-sense RNA viruses encode viral polymerase proteins, which are responsible for catalyzing synthesis of progeny viral RNA genomes from the parental viral RNA genome. A complementary negative-sense RNA is synthesized by the viral RdRp using the positive-sense RNA as a template. As for viral helicase, it functions as a necessary component to help unwind local double-stranded RNA regions during replication. With its assistance, the newly generated negative-sense RNA serves as a template for the synthesis of the progeny positive-sense RNA. It is worth mentioning that not all RNA viruses have a helicase function, as only those with genomes that exceed 6 kb contain genes encoding helicases (Gorbalenya and Koonin, 1993). The progeny positive-sense RNA is synthesized 10 to 100 fold faster than the negative-sense RNA, indicating that viruses have evolved sophisticated mechanisms for temporal and spatial control of RdRp during negative-sense and positive-sense RNA synthesis (Sanfaçon, 2005).

Importantly, the fact that viral genomes of positive-sense RNA viruses serve both as the mRNA for translation and the template for replication raises the possibility that the replication process is tightly coupled to translation. Ribosomes travel from 5' to the 3' end of the viral RNA during protein translation while viral RdRp travels from the 3' to the 5' end of the viral RNA for replication (Ahlquist *et al.*, 2003). As a consequence, successful

viral infection depends on the precise execution of regulatory mechanisms to control the switch from the translation mode to the replication mode (Sanfaçon, 2005) .

### 1.1.2 Picorna-like plant viruses, *Potyviridae*

Potyriviruses represent the largest group of known plant viruses. They are members of the genus *Potyvirus* in the family *Potyviridae*. The family contains seven additional genera: *Brambyvirus*, *Bymovirus*, *Ipomovirus*, *Macluravirus*, *Poacevirus*, *Rymovirus*, and *Tritimovirus*. Among 176 species in the family, 146 species belong to the *Potyvirus* genus (Fauquet *et al.*, 2005; King *et al.*, 2012). Viruses of the family *Potyviridae* share similarities in genome organization and replication strategies with members of the family *Picornaviridae* of human/animal viruses. Therefore, together with plant bipartite comoviruses and nepoviruses in the sub-family *Comovirinae*, viruses in the family *Potyviridae* and picornaviruses are classified into the *Picornavirales* (Goldbach, 1987).

Many of potyriviruses are economically important pathogens of agricultural crops. They have a broad geographical distribution and can infect a wide range of hosts including mono- and dicotyledonous plant species and lead to significant losses in crop yield and economy worldwide each year. For example, as the most devastating viral pathogen of stone fruit crops, *Plum pox virus* (PPV) can infect a variety of fruit species including peaches, apricots, plums, cherries and almonds, leading to a dramatic reduction of fruit yields (Sochor *et al.*, 2012; García *et al.*, 2014). *Potato virus Y* (PVY), as the type species of *Potyvirus*, is a destructive virus that can cause significant damage to potato, tobacco and pepper production. Together with *Potato virus A* (PVA; genus *Potyvirus*) and *Potato leaf roll virus* (PLRV; genus *Polerovirus*), they are three major plant viruses that can pose the biggest threat to potato production worldwide. Due to their high biological and economic importance, PPV and PVY are considered among the top 10 most important plant viruses (Scholthof *et al.*, 2011).

Most of potyriviruses are spread in a non-persistent manner by aphids or via grafting and wounding during agricultural practices and some are also seed-transmitted. Potyriviruses produce non-enveloped, flexuous filamentous particles, about 680-900 nm in length and 11-13 nm in diameter. Each encapsidated genome contains a positive-sense single-

stranded RNA of approximately 10,000 nucleotides (Gibbs and Ohshima, 2010). Due to their diverse transmission modes and wide host range, it is very difficult to control and prevent potyvirus infection in agriculture (Gibbs *et al.*, 2008).

### 1.1.3 Genome organization of potyviruses

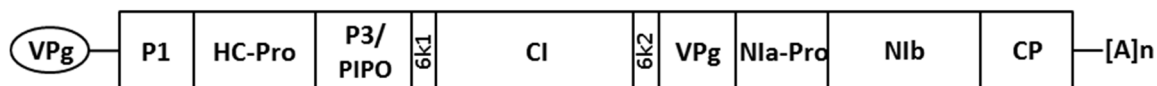
The potyviral genome is a positive-sense, single-stranded RNA with a virus-encoded protein VPg covalently linked to the 5' end, and a polyadenylated [poly(A)] tail at its 3' end. The viral genome contains a single open reading frame (ORF) that is translated into a long polyprotein of about 350 kDa. This large polyprotein is ultimately cleaved by three different virus-encoded proteases into at least ten multifunctional proteins (from N- to C-terminus): P1, helper component protease (HC-Pro), P3, 6K1, cylindrical inclusion (CI) protein, 6K2, viral genome-linked protein (VPg), nuclear inclusion a (NIa), nuclear inclusion b (NIb), and capsid protein (CP) (Urcuqui-Inchima *et al.*, 2001). In addition to the large polyprotein, there is a small ORF called “pretty interesting *Potyviridae* ORF” (PIPO) embedded in the P3 cistron (Chung *et al.*, 2008). PIPO results from a ribosomal frameshift during translation and is produced as a translational fusion with the N-terminus of P3 coding region. The resulting fusion protein is about ~25 kDa, termed P3N-PIPO (Wei *et al.*, 2010; Vijayapalani *et al.*, 2012) (Figure 2).

Unlike many other plant viruses, the *Potyviridae* family do not regulate expression of specific viral genes quantitatively and temporally through synthesis of subgenomic RNAs (Sztuba-Solińska *et al.*, 2011). As the result of translational frameshift at P3, three viral proteins P1, HC-Pro and P3N-PIPO are theoretically produced more than other eight viral proteins, dependent on the frameshift efficiency. However, viral proteins within each of these two groups are translated in an equimolar ratio. It is therefore important for potyviruses to employ different strategies to dynamically regulate viral protein expression during their infection cycle (Ivanov *et al.*, 2014).

### 1.1.4 Functions of potyviral proteins

P1, which is the first protein that is translated, is the most variable potyviral protein. It is located at the beginning of the viral genome of potyviruses, as a serine protease which is

A.



B.

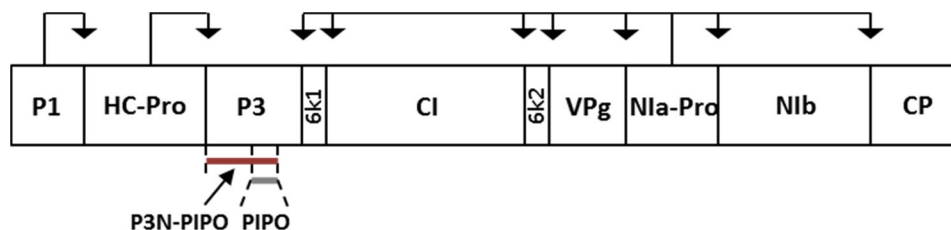


**Figure 2 Potyviral genome organization and polyprotein processing strategy.**

(A) Genome organization of the genus *Potyvirus*. The genome of potyvirus is the (+)ssRNA molecule covalently linked to VPg at the 5' end and poly(A) at the 3' end. The VPg is shown in cycle. The poly(A) tail is shown in [A]n. The viral open reading frame is depicted as a large box in which individual viral proteins are delineated by vertical lines. 5' and 3' untranslated regions are indicated as two short horizontal lines, respectively. Modified from (Ivanov *et al.*, 2014).

(B) Schematic representation of potyviral polyprotein processing strategy. The potyviral genome is translated into a single polyprotein which is then processed by three virus-encoded proteases into individual mature proteins. Proteolytic sites are marked with arrows. P1 protease is responsible for P1/HC-Pro cleavage site. HC-Pro protease is responsible for HC-Pro/P3 cleavage site. NIa-Pro protease is responsible for all other cleavage sites. PIPO derived from a frameshift in the P3 cistron is indicated as a short grey bar. PIPO fused with the N-terminal portion of P3, termed P3N-PIPO is indicated as a red bar. Modified from (Wei *et al.*, 2010).



responsible for *cis*-cleavage of the polyprotein between P1 and HC-Pro (Rohožková and Navrátil, 2011). Although it has been well known that the cleavage is carried out by a serine protease domain within the C-terminus of P1, no other conserved functional domains in P1 have been discovered so far. This is likely due to the fact that P1 is the most divergent potyviral protein in terms of both length and amino acid sequence (Verchot *et al.*, 1991). Swapping experiments between P1 proteins from PPV and *Tobacco vein mottling virus* (TVMV) suggest that P1 may play a critical role in host compatibility and pathogenicity (Salvador *et al.*, 2008). Recently, it has been shown that an amino-acid substitution in the P1 cistron could overcome eIF4E-mediated recessive resistance against *Clover yellow vein virus* (CIYVV) in pea (Nakahara *et al.*, 2010). In addition, although it has long been known that P1 cleavage is required for viral infectivity, the functions of P1 during the virus life cycle remained largely unknown. Over the last decade, accumulated evidence suggests that P1 might be able to play a vital role in effectively counteracting the antiviral defense mediated by RNA silencing. This notion was subsequently strengthened by the findings obtained in *Cucumber vein yellowing virus* (CVYV), a member of the genus *Ipomovirus*, the fourth monopartite genus of the *Potyviridae* family. Unlike the viruses from the genus *Potyvirus*, CVYV does not contain a sequence coding for HC-Pro in its genome, but has two P1 copies organized in tandem. It was revealed that P1 can enhance the activity of HC-Pro in members of the genus *Potyvirus*, and, moreover, the second copy (P1b) in CVYV is able to suppress RNA silencing in a manner similar to that of HC-Pro from the genus *Potyvirus*, suggesting that P1b is replacing HC-Pro in this function (Valli *et al.*, 2006). From an evolutionary angle, this finding may suggest that viruses have evolved to counteract RNA silencing by similar mechanisms using very different proteins within the *Potyviridae* family.

Potyviral HC-Pro is a multifunctional protein that is directly involved in diverse aspects of the potyvirus infection process. It is initially known to act as the helper component for aphid-mediated plant-to-plant transmission (Govier and Kassanis, 1974). In addition, HC-Pro has a cysteine protease activity that autocatalytically cleaves at its own C-terminus, between HC-Pro and P3. Notably, HC-Pro functions as an RNA-silencing suppressor of host antiviral defense mechanism by specifically binding viral 21-nucleotides (nt) small RNAs (Shiboleth *et al.*, 2007; Hasiów-Jaroszewska *et al.*, 2014).

P3, the third protein, is similar to the P1 in its variability among different potyviruses. The roles of P3 involved in symptom development and as a pathogenicity determinant are supported by independent studies from several laboratories (Sáenz *et al.*, 2000; Jenner *et al.*, 2003; Suehiro *et al.*, 2004; Chowda-Reddy *et al.*, 2011; Wen *et al.*, 2011). Recently, a yeast two-hybrid (Y2H) study has provided the evidence that potyviral P3 interacts with the subunit of host ribulose-1,5-bisphosphate carboxylase/oxygenase (RubisCO) protein and the interaction may contribute to the potyvirus symptom development (Lin *et al.*, 2011). In addition, subcellular localization studies of *Tobacco etch virus* (TEV) P3 have revealed that P3 localizes to the ER membrane and forms punctate inclusions associated with the Golgi apparatus. Moreover, the P3 punctate structure could traffic along the actin filaments and colocalize with the replication vesicles, suggesting that the function of P3 may be related to viral replication as well (Cui *et al.*, 2010).

Recent research on P3N-PIPO has indicated that it is essential for potyviral cell-to-cell movement (Wei *et al.*, 2010; Wen and Hajimorad, 2010). This capability was attributed to the role of P3N-PIPO that modulates targeting of CI to form the conical structure at PD. Using a Y2H screen, a host plasma membrane associated cation-binding protein (PCaP1) was found to interact with P3N-PIPO. Knockout of *PCaP1* in *Arabidopsis* could confer enhanced resistance against *Turnip mosaic virus* (TuMV) (Vijayapalani *et al.*, 2012), suggesting PCaP1 may affect viral intercellular transport through regulation of P3N-PIPO function.

6K1 is a short polypeptide whose function is poorly understood. The analysis of *Pea seed-borne mosaic virus* (PSbMV) 6K1 has suggested that the P3-6k1 region may function as a host-specific pathogenicity determinant (Johansen *et al.*, 2001). Recent study of one isolate of *Soybean mosaic virus* (SMV) has provided evidence that 6K1 protein is likely to play a role in the cell-to-cell movement during potyvirus infection (Hong *et al.*, 2007).

CI is a versatile protein that forms pinwheel-shaped cylindrical cytoplasmic inclusions in infected cells. CI processes NTPase and RNA helicase activities, which are involved in unfolding of structured RNA duplexes during viral genome replication. Potyviral CI may

also contribute to symptom determination and elicitation of dominant resistance responses (Zhang *et al.*; Seo *et al.*, 2009). Additionally, interactions between CI protein and host proteins originating from the ER and chloroplast have been pointed out, suggesting the presence of CI in virus-induced vesicles (Jiménez *et al.*, 2006). The role of CI in potyvirus cell-to-cell movement through PD has been demonstrated by analyzing TEV CI-mutants (Carrington *et al.*, 1998). Intriguingly, CI protein that expressed transiently in TuMV-infected cells is further targeted to PD, accumulating as spike-like structures in proximity to the viral vesicles, in addition to structures penetrating the cell wall (Wei *et al.*, 2010). The targeting of CI to PD is mediated by P3N-PIPO (Wei *et al.*, 2010). Taken together, CI protein acts as an RNA helicase involved in viral genome replication inside viral vesicles, and also exhibits different functions, such as facilitating virus transport to adjacent cells (Sorel *et al.*, 2014).

6K2, the second 6 kDa polypeptide, is a putative membrane-anchor protein that plays a critical role in anchoring the potyviral VRCs to intracellular membrane structures through its highly hydrophobic domain (Restrepo-Hartwig and Carrington, 1992). 6K2 is also responsible for membrane modifications and rearrangements of the early secretory pathway in infected cells. It can induce the formation of viral vesicles from ER membranes in the host cell, leading to the formation of the VRCs that contain all components required for viral genome replication (Schaad *et al.*, 1997). Recently, 6K2 was also found to be involved in intracellular movement of viral vesicles along actin microfilaments (Grangeon *et al.*, 2013). In addition, a variety of intermediate polyprotein precursors containing the domain for the 6K2 protein, including CI-6K2 and 6K2-NIa, have been identified in infected cells through an alternative cleavage of the large viral polyprotein.

Potyviral NIa localizes to the nucleus where nuclear inclusions are induced. NIa is processed to yield two viral proteins, VPg and NIa-Pro by its C-terminal protease domain. NIa has recently been observed to interact with fibrillain in the nucleus and this interaction may play a role in suppression of antiviral gene silencing (Rajamäki and Valkonen, 2009).

VPg is a virus-encoded protein that is covalently linked to the 5' end of viral genome and serves as a protein primer for viral genome replication and a functional equivalent to the eukaryotic mRNA cap structure for protection of the viral RNA genome and translational initiation (Wittmann *et al.*, 1997). Accordingly, VPg is a versatile protein that controls many processes leading to viral proliferation. Various precursor forms of VPg have been detected in infected cells resulting from the cleavage of polyprotein and maturation of viral proteins. For example, VPg-Pro (NIa) is detected in the cytoplasm and nucleus of infected cells (Léonard *et al.*, 2004). 6K2-VPg-Pro is found to be associated with intracellular membranes and within vesicular structures derived from the ER (Jiang and Laliberté, 2011). VPg is suggested to be a hub protein, interacting with host proteins as well as viral proteins during the potyvirus life cycle (Jiang and Laliberté, 2011). VPg can bind eukaryotic translation initiation factor 4E (eIF4E) and its isoform eIF(iso)4E (Wittmann *et al.*, 1997; Leonard *et al.*, 2000). Knockout of *eIF(iso)4E* can lead to resistance to potyvirus in *Arabidopsis* (Lellis *et al.*, 2002). Other host factors interacting with VPg include a cysteine-rich protein termed potyvirus VPg-interacting protein (PVIP) (Dunoyer *et al.*, 2004), AtRH8, an *Arabidopsis* DEAD-box RNA helicase-like protein (Huang *et al.*, 2010), eukaryotic elongation factor eEF1A (Thivierge *et al.*, 2008) and poly(A)-binding proteins (PABP) (Dufresne *et al.*, 2008).

NIa-Pro is located at the C-terminal region of the NIa protein and is responsible for cleavage of at least six cleavage sites in the potyviral polyprotein. As a cysteine protease, NIa-Pro shares structural similarity with cellular serine protease (Adams *et al.*, 2005). The nuclear distribution of NIa-Pro is manifested as a formation of inclusion bodies and observed in the late stage of viral infection (Schaad *et al.*, 1996). Since NIa-Pro has non-substrate-specific DNase activity, it is likely that NIa-Pro may play a role in degradation of the host DNA (Anindya and Savithri, 2004). The ability of interacting with viral RdRp (NIb) and non-specific binding of RNA suggests that NIa-Pro is involved in the viral genome replication process (Li *et al.*, 1997; Guo *et al.*, 2001). A recent study has shown that overexpression of NIa-Pro can attract aphid vectors and increase their reproduction in order to promote virus transmission (Casteel *et al.*, 2014).

Potyviral NIb acts as a viral RdRp and interacts with VPg and NIa-Pro. During viral infection, NIb functions in combination with other viral and host factors to catalyze synthesis of new viral progeny genomes (Hong and Hunt, 1996). It has been shown that the interaction of NIb with 6K2-VPg-Pro is required for the recruitment of NIb into the virus-induced membrane-bound vesicles that house VRC (Li *et al.*, 1997). Additionally, uridylylation of VPg protein by NIb plays a pivotal role in regulation of viral RNA synthesis (Puustinen and Mäkinen, 2004). More recently, SUMOylation of NIb by *Arabidopsis* SCE1 has been demonstrated to be essential for viral infection. It has also been proposed that the SUMOylation may directly regulate the function(s) of NIb involved in viral replication. Considering that NIb from not only TuMV but also TEV and SMV can interact with SCE1, the SUMOylation of NIb within the host cell is most likely conserved in the potyvirus replication process (Xiong and Wang, 2013).

Potyviral CP forms the capsid that mainly functions to encapsidate the potyviral RNA. The functions of CP have been related to viral translation, replication and transmission (Dolja *et al.*, 1994). Moreover, accumulating evidence indicates that CP can bind HC-Pro, and the interaction is essential for efficient virus transmission mediated by aphid (Blanc *et al.*, 1997). In addition, based on the similarity of CPs among different potyviruses, the amino acid sequence of CP has been used for determination of relationship within potyviruses. CP has also been suggested to participate in potyvirus intercellular movement, together with HC-Pro, CI and P3N-PIPO (Lucas, 2006; Hofius *et al.*, 2007; Wei *et al.*, 2010).

#### 1.1.5 *Turnip mosaic virus* (TuMV)

TuMV is a member of the genus *Potyvirus*. Historically, TuMV was first reported in the USA on *Brassica rapa* in 1921 (Gardner and Kendrick, 1921), but is now known to occur in many regions of the world including the temperate and tropical climate areas of Africa, Asia, Europe, Oceania and the Americas (Ohshima *et al.*, 2002). As one of the most prevalent viral pathogens, TuMV infects a wide range of plant species, mostly (although not exclusively) in the family *Brassicaceae* (Sánchez *et al.*, 2003). Other non-brassica crops (radish, lettuce, endive, escarole, horseradish, peas, and rhubarb) and ornamentals

were also found to be naturally susceptible to TuMV infection. By 1991, TuMV had been found to infect over 318 species in 156 genera of 43 plant families (Edwardson and Christie, 1991). As it causes significant economic losses in many infected vegetable and horticultural crops, TuMV was ranked second after *Cucumber mosaic virus* (CMV, genus *Cucumovirus*) amongst the most damaging plant viruses worldwide (Tomlinson, 1987). Given the fact that TuMV is able to infect the model plants *Arabidopsis thaliana* (*Arabidopsis*) and *Nicotiana benthamiana* (*N. benthamiana*), it makes TuMV an ideal model to study plant-virus interactions from both plant and virus perspectives (Walsh and Jenner, 2002).

Like other potyviruses, TuMV is transmitted by phloem-feeding insects, such as aphids, in a non-persistent manner (Edwardson and Christie, 1986). It has been reported that at least 89 species of aphids are able to transport TuMV virions to a healthy plant after feeding on the diseased plants (Shukla *et al.*, 1994).

In general, disease symptoms caused by TuMV infection appear on virtually all parts of the infected plants, including leaves, stems, roots, fruits, flowers and seeds. The characteristic symptoms of TuMV infection include mosaic, mottling, chlorotic rings on leaves or color break on flowers, fruits, and stems. In severe cases, infected plants are stunted with leaf distortion and necrosis, fruit and stem malformations, as well as fruit drop (Shukla *et al.*, 1994). Basically, symptoms that develop on plants in response to TuMV infection are usually regarded as harmful effects on the infected plants.

## **1.2 Host factors required for viral infection**

### **1.2.1 Host factors**

Plant viruses have small and compact genomes whose coding capacity is not sufficient to fulfil the viral life cycle. However, as successful pathogens, plant viruses can replicate efficiently within host cells. It is very clear that they have evolved with the ability to hijack host proteins and reprogram host metabolites to support the infection process (Nagy and Pogany, 2011).

Many efforts have been made towards understanding the role of host factors and recent progress has led to the identification and characterization of a number of important host factors recruited for plant virus replication. Different approaches have been employed, such as genome-wide screening and proteome-wide screening (Nagy and Pogany, 2010). In *Saccharomyces cerevisiae* (*S. cerevisiae*), several genome-wide screenings have identified approximately 130 genes that affect *Tomato bushy stunt virus* (TBSV, genus *Tombusvirus*, family *Tombusviridae*) replication (Panavas *et al.*, 2005; Jiang *et al.*, 2006). In the case of *Brome mosaic virus* (BMV, genus *Bromovirus*, family *Bromoviridae*), around 100 yeast genes have also been shown to play a role in viral replication (Kushner *et al.*, 2003; Gancarz *et al.*, 2011).

Diverse approaches have also been used to identify host factors from plants required for viral infections by several plant viruses including potyviruses (Dufresne *et al.*, 2008; Hafrén *et al.*, 2010), *Tomato mosaic virus* (ToMV, genus *Tobamovirus*) (Nishikiori *et al.*, 2006) and TBSV (Serva and Nagy, 2006). An emerging picture from these studies is that host factors play versatile roles during plant RNA virus replication, including: 1) assistance in the proper assembly of VRCs and cellular membrane remodelling; 2) recruitment of viral proteins and template RNA to the VRC; 3) regulation of the switch from viral genome translation to replication; 4) participation in the intracellular transport of viral proteins and viral RNA; and 5) facilitating folding of viral proteins as protein chaperones (Nagy and Pogany, 2011; Hyodo and Okuno, 2014).

For instance, the potyviral replication factory is associated with intracellular membranous structures derived from the ER (Wei *et al.*, 2010) and where a number of host proteins are recruited to form the VRC for viral replication (Wang, 2013). These host factors include eukaryotic translation initiation factors (eIFs) (Wittmann *et al.*, 1997; Schaad *et al.*, 2000), a cysteine-rich protein PVIP (Dunoyer *et al.*, 2004), Heat shock cognate 70-3 (Hsc70-3) (Dufresne *et al.*, 2008), PABP (Dufresne *et al.*, 2008), eEF1A (Thivierge *et al.*, 2008), DEAD-box RNA helicase (Huang *et al.*, 2010) and DNA-binding protein phosphatase 1 (DBP1) (Castelló *et al.*, 2010). Among them, eIFs and DEAD-box RNA helicases are relatively well characterized.

### 1.2.2 Eukaryotic translation initiation factors (eIFs)

Translation of the viral genome is fully dependent on the host translation machinery. Translation initiation is the highly-regulated and rate-limiting step of protein synthesis (Sonenberg and Hinnebusch, 2009). It is initiated by the recruitment of the eIF4F complex to the viral RNA (Bushell and Sarnow, 2002). The eIF4F complex is composed of factors eIF4E, eIF4G and eIF4A. eIF4E is a cap binding protein that binds to the 5' cap structure of mRNA or the viral protein linked to the 5' end of the viral genomic RNA. eIF4E is associated with eIF4G, a scaffold protein that interacts with other components of the eIF4F complex (Sonenberg and Hinnebusch, 2009; Jackson *et al.*, 2010). eIF4A is responsible for recruiting ternary 40S ribosomal complexes and unwinding double-stranded RNA structures (Rogers *et al.*, 1999).

Previous studies have shown that potyviruses selectively recruit one of eIF4E and eIF4G or their corresponding isoforms for their infection (Nicaise *et al.*, 2007). The recruitment of these translation initiation factors occurs through their physical interactions with the viral protein VPg or its precursor NIa. Mutations or knockout of *eIF4E* or *eIF4G* or their isoforms *eIF(iso)4E* and *eIF(iso)4G1* or *eIF(iso)4G2*, could confer resistance against certain potyvirus infection without compromising regular plant growth and development (see section 1.4.2) (Gallois *et al.*, 2010).

### 1.2.3 Eukaryotic translation initiation factor 4A, eIF4A

Among eIFs, eIF4A is the prototype of DEAD-box RNA helicases (Rogers *et al.*, 1999). It was first characterized through its requirement in translation and was further identified as a component of eIF4F complex (Grifo *et al.*, 1982). Together with the central scaffolding protein eIF4G and the cap-binding protein eIF4E, eIF4A forms the eIF4F complex accompanied by accessory proteins eIF4B and eIF4H (Jackson *et al.*, 2010). The eIF4F complex is essential for the translation of most cellular mRNAs and is an important target for regulation (Jackson *et al.*, 2010).

eIF4A possesses both ATP-dependent RNA helicase activity and RNA remodelling activity. It is suggested that eIF4A is responsible for unwinding RNA secondary



structures in the 5' UTR which would inhibit ribosome scanning (Svitkin *et al.*, 2001). eIF4A also facilitates viral translation initiation by exhibiting RNA helicase activities (Robaglia and Caranta, 2006). RNA helicase activities of eIF4A are largely dependent on stimulation from other translation initiation factors. In the eIF4F complex, the helicase activities of eIF4A are increased which suggests that the helicase activity requires the recruitment of eIF4A to a specific mRNA, preventing the unwinding of RNA structures not targeted by the binding partners (Lu *et al.*, 2014). Hence, the research on eIF4A, as one of the first DEAD-box RNA helicases that have been studied extensively, has led to the discovery of the fundamental principles underlying the functions of DEAD-box RNA helicases (Andreou and Klostermeier, 2013).

### 1.3 DEAD-box RNA helicase

RNA helicases, which function as highly conserved enzymes, can utilize ATP to catalyze the separation of RNA duplexes and the structural rearrangement of RNA and RNA/protein complexes (ribonucleoprotein (RNP) complexes) in all aspects of RNA metabolism, from transcription, mRNA splicing and translation, RNA modification and transport, ribosome biogenesis, RNP complex assembly to mRNA degradation (Cordin *et al.*, 2006; Pyle, 2008). RNA helicases are present in all eukaryotic cells and many bacteria and some viruses also encode one or more helicase proteins (Hilbert *et al.*, 2009).

Based on sequence and structural features, RNA helicases are classified into five main groups, namely superfamily (SF) 1 to SF5 (Gorbalenya and Koonin, 1993). DEAD-box RNA helicases belong to the helicase superfamily 2 (SF2), together with DEAH, DExH and DExD families, which are commonly referred to as the DExD/H helicase family (Fairman-Williams *et al.*, 2010).

#### 1.3.1 Structure and functions

DEAD-box RNA helicases represent a large family of proteins which have been shown to be involved in almost every step of RNA metabolism (Cordin *et al.*, 2006). The name of the family was derived from the highly conserved amino acid sequence D-E-A-D (Asp–Glu–Ala–Asp) of its motif II (Linder and Jankowsky, 2011).

It has been suggested that some DEAD-box RNA helicases may act as RNA chaperones, promoting the formation of optimal RNA structures through local RNA unwinding, or as RNPs by mediating RNA-protein association/dissociation (Fuller-Pace, 2006). DEAD-box RNA helicases play essential roles in regulating cellular RNA metabolism. For example, they function as part of the spliceosome complexes and/or the eukaryotic translation initiation machinery (Rocak and Linder, 2004).

DEAD-box RNA helicases are characterized by a set of conserved motifs, namely Q, I, Ia, Ib, Ic, II, III, IV, IVa, V, Va, and VI, which contribute to ATP binding and hydrolysis, RNA binding and duplex unwinding (Cordin *et al.*, 2006). Motifs Ia, Ib, Ic, IV, IVa and V participate in RNA binding, whereas motifs Q, I, II and VI have been implicated in ATP binding and hydrolysis (Rocak and Linder, 2004). The motifs III and Va are responsible for coupling ATPase and duplex separation (Tanner *et al.*, 2003). These characteristic sequence motifs are located within a conserved spatial arrangement in the helicase core, which is formed by two recombinase A (RecA)-like domains with flexible central regions (Singleton *et al.*, 2007; Linder and Jankowsky, 2011).

Although DEAD-box RNA helicases share the highly conserved structure of the helicase core, they have been associated with a variety of ATP-dependent cellular functions (Rocak and Linder, 2004). RNA unwinding activity is the main function performed by DEAD-box RNA helicases, and involves ATP-dependent binding and RNA or RNP structure remodelling (Pyle, 2008). DEAD-box RNA helicases load directly onto the duplex region and then separate the strands apart in an ATP-dependent manner instead of translocation on the RNA. This evident unwinding style is termed local strand separation (Yang *et al.*, 2007). The highly targeted unwinding process prevents large-scale unravelling of exquisite-assembled RNA or RNP structures. Each RNA unwinding event utilizes one single ATP molecule through ATP binding and hydrolysis (Chen *et al.*, 2008). In addition to ATP-dependent RNA unwinding, DEAD-box RNA helicases may also participate in export of mRNA from the nucleus to the cytoplasm. For example, the DEAD-box protein Dbp5 has been shown to mediate mRNA export to the cytoplasm (Tran *et al.*, 2007).

### 1.3.2 Association with abiotic stress

Plants are immobile organisms and are subject to a wide range of environmental insults, including biotic and abiotic stresses. Abiotic stresses, such as low temperatures, high salinity and drought, have an adverse influence on the plant growth, development and productivity (Knight and Knight, 2001). Plants respond to abiotic stresses in different ways and have evolved a complex variety of strategies to increase their tolerance to environmental stresses through physical adaptation and molecular and cellular changes (Takken *et al.*, 2006). As part of plant stress responses, plants regulate gene expression in order to activate and integrate various tolerance mechanisms. The targeted genes encode proteins involved in different biological functions, including nucleic acid metabolism (Chinnusamy *et al.*, 2004; Zhu *et al.*, 2007).

Recent studies have revealed that RNA helicases play a critical role in plant stress responses (Owtrim, 2006; Vashisht and Tuteja, 2006). Notably, when exposed to low temperatures, RNA molecules form stable non-functional secondary structures, and hence require RNA chaperones to perform the proper functions (Lorsch, 2002). It is possible that DEAD-box RNA helicases, which can operate as RNA chaperones, are able to unwind misfolded RNA structures using energy derived from ATP hydrolysis, thereby ensuring correct RNA folding (Vashisht and Tuteja, 2006).

An *Arabidopsis* osmotically responsive gene, *LOS4* encoding a DEAD-box RNA helicase (AtRH38), which has been reported to be crucial for expression of cold-responsive genes under conditions of low temperatures. *LOS4* functions in cold tolerance through regulating mRNA export from the nucleus to the cytoplasm (Gong *et al.*, 2002; Gong *et al.*, 2005). Moreover, two *Arabidopsis* DEAD-box RNA helicase genes, *Stress Response Suppressor 1 (STRS1)* and *2 (STRS2)* have been identified to suppress responses to abiotic stresses (Kant *et al.*, 2007). Mutations of either *STRS1* or *STRS2* in *Arabidopsis* led to an increased tolerance to salt, osmotic, and heat stresses, and thus both *STRS1* and *STRS2* appear to play critical roles in response to abiotic stresses by attenuating expression of upstream stress signaling components (Kant *et al.*, 2007). Interestingly, in a similar study to characterize functional roles of DEAD-box RNA helicases in response to

abiotic stresses, *AtRH25* (*STRS2*) was shown to be up-regulated in response to low temperature treatment and contribute to enhanced cold tolerance in *Arabidopsis* by exerting RNA chaperone activity (Kim *et al.*, 2008).

In addition to the functional roles in abiotic stress response, some DEAD-box RNA helicases also participate in modulating defence against biotic stresses. For instance, a rice gene *Oryza sativa* BTH-induced RNA helicase 1 (*OsBIRHI*), encoding a DEAD-box RNA helicase, has been implicated in stress response to oxidative stress. Overexpression of *OsBIRHI* confers enhanced disease resistance against fungal pathogen infection in *Arabidopsis* (Li *et al.*, 2008).

### 1.3.3 Association with viral infection

During the past decade, accumulating evidence suggests that RNA helicases likely play several essential roles during viral infection including (i) facilitating viral genomic RNA translation, (ii) recruiting viral RNA for replication, (iii) coordinating viral RNA template for translation or replication, and (iv) regulating viral RNA stability or degradation (Huang *et al.*, 2010). However, detailed studies towards understanding the functions of RNA helicases in positive-sense RNA virus life cycle are very limited.

In a seminal work, Noueiry and colleagues showed that the yeast gene *DED1*, encoding a DEAD-box RNA helicase is required for the translation of BMV, a bromovirus. A point-mutation in *DED1* inhibits BMV RNA replication via disrupting expression of viral-encoded polymerase protein 2a but not affect yeast growth (Noueiry *et al.*, 2000). Coincidentally, through a genome-wide screening of yeast genes, *DED1* has also been identified as a host gene required for replication of TBSV, a tombusvirus. Down-regulation of *DED1* affects TBSV viral infection by inhibiting the accumulation of virus-encoded replication proteins (Jiang *et al.*, 2006). Recently, it has been shown that *DED1*-encoded protein Ded1p is required for viral replication of TBSV and *Flock house virus* (FHV, genus *Alphanodavirus*) by binding to the negative-sense viral RNA and promoting positive-sense viral RNA synthesis. Ded1p is recruited to TBSV VCR as an important host component, and ATPase-defective Ded1p mutant fails to initiate TBSV replication, suggesting that helicase activity is required for TBSV replication (Kovalev *et al.*, 2012).

Similar to Ded1p, another RNA helicase Dbp2p (the homolog of the human p68 protein) also binds to the 3' end of the viral negative-sense RNA of TBSV and unwinds the local secondary structure to promote positive-sense RNA replication in yeast (Kovalev *et al.*, 2012). AtRH20, an RNA helicase in *Arabidopsis* sharing high sequence similarity with DED1, can stimulate TBSV positive-sense RNA synthesis, suggesting RNA helicases in plants may assist viral replication in a similar manner (Kovalev *et al.*, 2012). More recently, two additional cellular RNA helicases, e.g., the eIF4AIII-like yeast FAL1 and the DDX5-like Dbp3 and their orthologs in *Arabidopsis*, AtRH2 and AtRH5, have been shown to be present in the tombusvirus VRCs (Kovalev and Nagy, 2014). They bind to the 5' proximal RIII (-) replication enhancer (REN) element in the TBSV negative-sense RNA and unwind the dsRNA structure within the RIII(-) REN region (Kovalev and Nagy, 2014). Coordinated unwinding of the dsRNA at the 5' region by this group of RNA helicases and the secondary structure at the 3' terminal region by the DED1/AtRH20 would bring the 5' and 3' terminal sequence of the negative-sense RNA in close vicinity via long-range RNA-RNA base pairing and facilitate asymmetrical viral replication by recycling the viral replicase proteins for multiple rounds of positive-sense viral RNA synthesis (Kovalev and Nagy, 2014). It is also worth to note that an *Arabidopsis* DEAD-box RNA helicase, AtRH8 and a *Prunus persica* DDX-like protein, PpDDXL, have been identified to interact with potyviral VPg. AtRH8 colocalizes with the viral replication vesicles, indicating that AtRH8 is necessary for potyvirus infection by facilitating viral genome translation and replication (Huang *et al.*, 2010).

Interestingly, several lines of evidence obtained in recent years indicate that DEAD-box RNA helicases play critical roles in human virus replication. It has been demonstrated that DEAD-box RNA helicase 1 (DDX1) functions as a Rev cellular co-factor supporting *Human immunodeficiency virus type 1* (HIV-1) replication. HIV-1 Rev protein is responsible for the transport of viral RNA from the nucleus to cytoplasm by remodeling VRC and is required for HIV-1 virion assembly (Fang *et al.*, 2004; Fang *et al.*, 2005). In addition to DDX1, DEAD-box RNA helicase 3 (DDX3) has also been reported to be required for HIV-1 replication. Functioning as a nucleo-cytoplasmic shuttling protein, DDX3 is responsible for restructuring viral RNAs and facilitating the translocation through the nuclear pore complex. Knockdown of *DDX3* suppressed the export of HIV-1

viral RNAs from the nucleus (Yedavalli *et al.*, 2004). Intriguingly, HCV also recruits DDX3 for viral RNA replication. DDX3 might be associated with HCV assembly and the lack of DDX3 would cause a significant decrease of HCV viral RNA accumulation by 95% (Ariumi *et al.*, 2007). A very recent study revealed that DDX3 can also interact with the viral polymerase of *Hepatitis B virus* (HBV), a DNA virus whose replication is dependent on reverse transcription of the viral genome. DDX3 restricts HBV genome replication by inhibition of its reverse transcription (Wang *et al.*, 2009). More recently, DEAD-box RNA helicase 56 (DDX56), a nucleolar helicase has been found to interact with WNV capsid protein. This observation suggests that DDX56 is required for assembly of WNV viral particles. Mutations of DEAD motif of DDX56 would impair the function in packaging viral RNA into virions (Xu *et al.*, 2011; Xu and Hobman, 2012).

Taken together, these studies reinforce the idea that DEAD-box RNA helicases play an essential role in viral infection but the functional mechanisms may differ from helicase to helicase and from virus to virus.

## **1.4 Plant defense responses against viral pathogens**

### 1.4.1 Dominant resistance

Plants are constantly exposed to invasion by a multitude of pathogenic microbes, including viruses. Over the course of evolution, there has always been an "arms race" between plants and plant viruses, in which the viruses evolve mechanisms to survive by invading plants to acquire biosynthetic products and energy, while plants evolve ways to prevent the invasion. Since plants lack mobile defender cells and an adaptive immune system like animals, they rely on an elaborate innate immune system to defend themselves against the viral intruders. There are two general types of antiviral strategies that plants employ to combat viral infections. The better-characterized mechanism is the one mediated by resistance (*R*) genes (Mandadi and Scholthof, 2013). The other is an antiviral RNA silencing pathway, which is triggered by double-stranded RNA, leading to the cellular defense against foreign nucleic acids (Soosaar *et al.*, 2005).

*R*-gene mediated resistance pathways are often associated with the hypersensitive response (HR) which usually induces programmed cell death (PCD) surrounding the infection site. The phenotype of HR is the appearance of necrotic lesions at the site of local infection. The HR functions to limit viral proliferation, thus the virus is constrained to the lesions and unable to spread to adjacent healthy tissues (Ross, 1961; Moffett, 2009). Following HR in the local infection area, *R*-gene mediated resistance responses could also lead to systemic acquired resistance (SAR) in tissues distant from local infected area and result in an enhanced resistance to later pathogen attack (Ross, 1961). SAR is considered to be a broad-spectrum, long-lasting resistance through the whole plant (Ryals *et al.*, 1996). This response is activated by the induction of expression of a set of pathogenesis-related genes which encode antimicrobial compounds (Durrant and Dong, 2004; Kang *et al.*, 2005) and results in the generation of the immune signal molecule salicylic acid (SA) (Gaffney *et al.*, 1993).

*R*-gene mediated resistance is known to be triggered when a pathogen-encoded avirulence factor (Avr) is recognized by a dominant *R*-gene encoded product in the plant (Bent and Mackey, 2007; Moffett, 2009). The classic model of the "gene-for-gene" resistance is that the *N* gene of tobacco plants could confer resistance to TMV (genus *Tobamovirus*) and most tobamoviruses (Erickson *et al.*, 1999). It was first reported by F.O. Holmes in 1938 (Holmes, 1938). The *N* gene product from *Nicotiana glutinosa* specifically recognizes the helicase domain of the TMV replicase protein and triggers the HR (Abbink *et al.*, 1998).

The pathogen is recognized through its conserved structures or proteins associated with the pathogen by plant pattern recognition receptors (PRRs), termed pathogen associated molecular patterns (PAMPs) or microbe-associated molecular patterns (MAMPs). The induced immunity responses are noted as PAMP-triggered immunity (PTI) response (Boller and Felix, 2009). After successful invasion, pathogens deliver specific effector molecules into the plant cell to enhance pathogen virulence and impair host defense signaling cascade. The effectors employed by the pathogen could interfere with PTI response, leading to effector-triggered susceptibility (ETS) (Bent and Mackey, 2007). To contribute defense against the pathogen effectors, plant *R* genes encode a class of

nucleotide binding (NB) and leucine rich repeat (LRR) domain (NB-LRR)-containing proteins which can directly or indirectly recognize the specific effectors to induce effector-triggered immunity (ETI) response (Collier and Moffett, 2009). NB-LRR proteins represent the major class of plant *R* gene products (R proteins) (Moffett, 2009). Compared with PTI response, ETI occurs faster and acts as a stronger response usually associated with HR at the infection site (Jones and Dangl, 2006; Dodds and Rathjen, 2010).

To date, several dominant *R* genes against plant viruses have been identified. For example, an *Arabidopsis* jacalin-type lectin, restricted TEV movement1 (*RTM1*), has been shown to prevent the systemic spread of several potyviruses (Chisholm *et al.*, 2000). In addition to *RTM1*, *RTM2* and *RTM3* physically interact with *RTM1* and also contribute to viral resistance responses (Chisholm *et al.*, 2001; Mandadi and Scholthof, 2013). Lately, another jacalin-type lectin, *JAX1*, was shown to confer broad resistance against multiple potexviruses including *Potato virus X* (PVX), *Plantago asiatica mosaic virus* (PIAMV), *White clover mosaic virus* (WCIMV), and *Asparagus virus 3* (AV-3), suggesting lectins play an important role in plant antiviral immunity (Yamaji *et al.*, 2012). *JAX1*-mediated resistance against PIAMV occurs via inhibition of viral replication whereas *RTM1* impedes viral movement by interference with viral movement-associated proteins (Yamaji *et al.*, 2012). Moreover, tomato (*S. hirsutum*) resistance gene *Tm-1*-encoded protein can bind to the replication protein of ToMV which confers resistance to ToMV by inhibiting viral RNA replication (Ishibashi *et al.*, 2007). Potato (*Solanum tuberosum*) resistance genes *Rx1* and *Rx2* both impart resistance to PVX through recognition and interaction with the PVX CP and are required to block virus replication (Bendahmane *et al.*, 1999; Bendahmane *et al.*, 2000).

#### 1.4.2 Recessive resistance

As discussed above, plant viruses recruit many host factors to complete their life cycle. The inability to recruit an essential host component may result in resistance against viruses, termed recessive resistance. Genes encoding dysfunctional host factors are referred to as recessive resistance genes (Fraser and Van Loon, 1986).



Recessive resistance is prevalently found to confer resistance to potyviruses (Kang *et al.*, 2005). More than half of the recessive resistance genes reported so far are effective against potyviruses (Diaz-Pendon *et al.*, 2004). The recessive genes involved in the potyvirus-related resistance mainly encode eIF4E and eIF4G or their isoforms (Truniger and Aranda, 2009) and are related to the binding capabilities between potyvirus VPg and eIF4E/eIF4G and their isoforms (Wittmann *et al.*, 1997; Leonard *et al.*, 2000; Schaad *et al.*, 2000).

eIF4E is a crucial component of the eukaryotic translation initiation machinery that binds to 5' cap structure of mRNA to initiate mRNA translation (Sonenberg and Hinnebusch, 2009). Potyviruses encode the VPg which is covalently linked to the 5' end of the viral genomic RNA and allows the translation of viral RNA in a cap-independent manner. Potyviral VPg is found to physically associate with eIF4E/eIF4G and their isoforms (Wang and Krishnaswamy, 2012). Disrupting or eliminating the interactions between VPg and eIF4E/eIF4G proves to be sufficient to prevent potyvirus infection *in planta* (Leonard *et al.*, 2000). In all cases, the resistance phenotypes result from a few amino acid changes in the eIF4E or eIF(iso)4E proteins, which are grouped in two regions of the eIF4E structure located near the cap binding pocket and at the surface of the protein (Robaglia and Caranta, 2006). Different potyviruses may selectively recruit eIF4E or the respective isoforms for their replication. Moreover, the same potyvirus may utilize different eIF4E or its isoforms for successful infection of different host plants. For example, *Arabidopsis eif(iso)4e* knockout mutants are resistant to TuMV, *Lettuce mosaic virus* (LMV), TEV and PPV, while *Arabidopsis* eIF4E is required for successful infection of CIYVV (Duprat *et al.*, 2002; Lellis *et al.*, 2002; Sato *et al.*, 2005; Decroocq *et al.*, 2006). In addition, mutations in eIF4G could impart recessive resistance to CMV (genus *Cucumovirus*) and *Turnip crinkle virus* (TCV, genus *Carmovirus*) in *Arabidopsis* (Yoshii *et al.*, 2004). Altogether, these data provide the evidence of a conserved relationship between plant RNA viruses and the host translation initiation machinery during viral life cycle.

### 1.4.3 RNA silencing and its suppression

Upon viral infection, in addition to the aforementioned dominant *R* gene- or recessive gene-mediated resistance, RNA silencing plays a pivotal role in directing antiviral immunity in plants. RNA silencing machinery is a complicated system that recruits unique genetic components to perform their functions. There are four conserved classes of proteins involved in RNA-based antiviral defense, which include Dicer-like ribonucleases (DCLs), Argonaute proteins (AGOs), dsRNA-binding proteins (DRBs), and RNA-dependent RNA polymerases (RDRs) (Vaucheret, 2006).

The RNA silencing pathway is largely mediated by a variety of small RNAs (sRNAs) (Rana, 2007). sRNAs are 18 to 25-nt- long noncoding RNA molecules that can regulate gene expression either transcriptionally or post-transcriptionally (Ruiz-Ferrer and Voinnet, 2009; Katiyar-Agarwal and Jin, 2010). Pathogen-regulated, host endogenous microRNAs (miRNAs) and small interfering RNAs (siRNAs) are the most important sRNA regulators regarding plant-pathogen interaction (Jin, 2008). RNA silencing is considered to be highly specific since it targets mRNA transcripts based on sequence complementarity between the sRNAs and its target RNA (Baulcombe, 2004).

Antiviral RNA silencing is an innate immune response triggered by viral dsRNA, which is derived from viral replication intermediates or secondary RNA folding structures. Antiviral RNA silencing begins with the activity of DCLs that target viral dsRNA and results in the generation of 21-24-nt viral siRNAs, the central components of the RNA silencing pathway (Ding and Voinnet, 2007). Processed viral siRNA duplexes are unwound and recruited by AGOs, which are the catalytic component of RNA-induced silencing complexes (RISCs). RISCs can bind the viral genome and transcripts, and direct the cleavage of homologous mRNAs to achieve post-transcriptional silencing (Ding, 2010). DRBs have been found to modulate the function of DCLs, while RDRs are encoded by the host plant to produce viral secondary siRNAs or some of the dsRNA precursors that serve as templates for DCLs (Brodersen and Voinnet, 2006).

The viral siRNAs involved in the RNA silencing pathway share similar features with host siRNAs and miRNAs (Sharma *et al.*, 2013). They are classified into two groups. One

group, the primary siRNAs, is processed from DCL-mediated cleavage of the initial invading viral RNA. The other type of siRNAs, the secondary siRNAs, recruits host RDRs for their biogenesis (Ruiz-Ferrer and Voinnet, 2009). The amplification of secondary siRNAs has been linked to the long-distance spread of the RNA silencing signals, which allows viral siRNAs move from cell-to-cell for effective RNA silencing responses to viral infection (Hamilton *et al.*, 2002; Himber *et al.*, 2003).

The RNA silencing pathways in *Arabidopsis* have been well characterized and comprise four DCLs, six RDRs, ten AGOs and six DRBs that participate in at least four different endogenous RNA silencing pathways (Vaucheret, 2006). These components have distinct but partially overlapping functions in different RNA silencing pathways. It has been reported that all four DCLs perform the antiviral defense activity in plants (Blevins *et al.*, 2006). Among them, DCL2 and DCL4 are two primary regulators while DCL3 plays a minor role and DCL1 acts negatively as it down-regulates DCL2 and DCL4 functions (Garcia-Ruiz *et al.*, 2010). *Arabidopsis* RDRs play an essential role in RNA silencing defense by amplifying the majority of viral secondary siRNAs. Disease susceptibility to plant RNA viruses was dramatically enhanced in RDR-defective *Arabidopsis* mutant plants (Qu *et al.*, 2005). Accumulating evidence suggests that AGOs which associate with siRNAs to guide sequence-specific silencing, are regulated by DNA methylation (Mallory and Vaucheret, 2010). AGO1 and AGO2 are the key components of the RNA silencing pathways and are recruited for efficient cleavage of viral RNA and processing viral secondary siRNAs in a cooperative manner (Cao *et al.*, 2014). RDR2 is required for the biogenesis of endogenous 24-nt siRNAs that directs DNA methylation in plants (Xie *et al.*, 2004). Moreover, extensive studies have shown that viral siRNA biogenesis is facilitated by RDR1, RDR2 and RDR6 (Qi *et al.*, 2009). Compared to the rapid *R* gene-mediated defense responses, which can constrain further virus spread within 3-4 days, antiviral RNA silencing is a relatively slow process and could not lead to complete clearance of viral infection (Ding, 2010).

Plant viruses have evolved a variety of effective counter-defense strategies to overcome the antiviral RNA silencing of the host. One of the best-characterized strategies plant viruses employ is to encode RNA silencing suppressors, which are viral proteins that can

interfere with the components of RNA silencing pathways and inhibit the effectiveness of plant defense (Qu and Morris, 2005). Virus-encoded silencing suppressors from different virus families are diverse in sequences and structures. They are able to target different steps of RNA silencing pathways and utilize various strategies to obstruct host antiviral defense (Burguán and Havelda, 2011). The functions of silencing suppressors can partially or completely disable the activities of silencing components but the mechanism of the viral suppressors remains to be determined (Levy *et al.*, 2008). There are five possible models to describe how viral suppressors of RNA silencing may work: 1) inhibition of the biogenesis of viral siRNAs; 2) blocking loading of viral siRNAs into the RISC by sequestration of viral siRNAs; 3) manipulation of the formation of components of the RISC; 4) inhibition of the AGO-mediated cleavage of viral RNA; and 5) blocking silencing by interacting with plant components which are required for the antiviral silencing machinery (Katiyar-Agarwal and Jin, 2010).

For instance, TBSV encodes the P19 protein, which is recognized as a suppressor of RNA silencing by a variety of different tombusviruses (Qu and Morris, 2002). P19, which targets and directly binds double-stranded siRNAs, preferentially binds 20-22 nt duplexes to prevent them from being incorporated into the RISC (Silhavy *et al.*, 2002). Given the fact that siRNAs is the key indicator of RNA silencing, the affinity of P19 for siRNAs is essential for viral pathogenesis (Hsieh *et al.*, 2009). The protease HC-Pro, encoded by different potyviruses is one of the first viral silencing suppressors to be characterized. The silencing suppressor function of HC-Pro is likely to act by inhibiting the unwinding of siRNA duplexes and RISC assembly (Chapman *et al.*, 2004). As a multifunctional protein, HC-Pro is also involved in aphid transmission, viral polyprotein processing, and long distance movement (Kasschau *et al.*, 1997). Mutations in HC-Pro that abolish its suppressor function could cause the virus to lose the ability to replicate the viral genome and move from cell to cell (Kasschau and Carrington, 2001). The 2b protein of cucumoviruses is another example of well-studied viral silencing suppressor. It has been demonstrated that CMV 2b protein can enhance viral long distance movement and interfere with systemic spread of RNA silencing signals (Guo and Ding, 2002). P25 of PVX, which was previously shown to be required for cell-to-cell movement of PVX, can suppress RNA silencing by blocking the silencing signals from moving systemically

between the cells (Azevedo *et al.*, 2010). TCV encodes the P38 protein, which has been reported to have the silencing-suppressing function. P38 binds dsRNA of variable lengths and competes with DCL4 to prevent from binding viral dsRNA (Deleris *et al.*, 2006). The suppressor activity of P38 is further supported by the observed interaction between P38 and AGO1, which leads to blocking the RNA silencing pathways (Voinnet *et al.*, 2000). Since many viral silencing suppressors can bind short dsRNA, it is suggested that binding viral siRNAs duplexes might represent an effective silencing suppression strategy employed by plant viruses (Méraï *et al.*, 2006).

### 1.5 Research objectives and goals

It is well known that plant viruses pose a major threat to a broad range of plant species in agriculture. Genetic resistance is the practical approach to the control of viral diseases. Unfortunately, natural genetic resistance is rare. To develop novel genetic resistance, it is essential to better understand the viral infection process. Virus infection in plants is a complicated process that requires specific interactions between viral and host proteins. Due to the complexity of plant genomes and the diversity of plant viruses, identification of the host proteins in these interactions has been limited. Towards the development of novel viral disease resistance in crops, which is the long term goal of this research, my thesis focuses on the molecular isolation of host factors required for viral infection and functional characterization of their working mechanisms in viral infection.

To isolate host factors required for viral infection, I proposed to screen *Arabidopsis* T-DNA insertion lines using TuMV as a model virus. Since DEAD-box RNA helicases likely play essential and regulatory roles in the viral RNA replication and translation of positive-sense RNA viruses, I further selected *Arabidopsis* T-DNA insertion mutants corresponding to this gene family for analysis. Thus, the central hypotheses of this research are that (1) *Arabidopsis* DEAD-box RNA helicases are involved in TuMV infection, and (2) down-regulation or mutation of one of these host factors will lead to recessive resistance against TuMV infection. The specific objectives of this thesis are:

- (1) To identify *AtRHs* essential for TuMV infection through a reverse genomic approach by screening *Arabidopsis atrh* T-DNA insertion mutant lines;

- (2) To functionally characterize the identified candidate *AtRHs* associated with TuMV infection using the model plants *Arabidopsis* and *N. benthamiana*;
- (3) To identify TuMV proteins interacting with candidate *AtRHs*;
- (4) To identify plant proteins involved in the interaction between *AtRHs* and TuMV proteins;
- (5) To study the involvement of the identified *AtRHs* as host factors required for viral replication and/or translation.

## Chapter 2: Materials and Methods

### 2.1 Plant materials and growth conditions

*Arabidopsis* (*Arabidopsis thaliana*) ecotype Col-0 and *Nicotiana benthamiana* (*N. benthamiana*) were used in this study. *Arabidopsis* and wild-type *N. benthamiana* plants were maintained in a growth chamber under constant conditions of 60% relative humidity and a day/night regime of 16 h in the light at 22°C followed by 8 h at 18°C in the dark. Plants were watered daily as needed and fertilized (20-8-20 [N-P-K], 0.5g/l) weekly. Seeds for *Arabidopsis* T-DNA insertion mutant lines were obtained from the Arabidopsis Biological Resource Center (ABRC) at Ohio State University, Columbus, Ohio, USA. T-DNA insertion information was obtained from the Salk Institute Genomic Analysis Laboratory website (<http://signal.salk.edu/>).

### 2.2 Virus materials

The pCambiaTunos/GFP plasmid (TuMV-GFP) containing the full-length cDNA of the TuMV genome and pCambiaTunos/6KmCherry (TuMV::6K-mCherry) having an additional copy of the 6K2-coding sequence tagged with fluorescent protein mCherry between P1 and HC-Pro were obtained from Dr. Jean-François Laliberté at the Institut Armand-Frappier, Institut National de la Recherche Scientifique, Laval, Québec, Canada (Cotton *et al.*, 2009). The recombinant TuMV infectious clone carrying an additional copy of the 6K2-coding sequence fused to yellow fluorescent protein (YFP) at the junction of P1 and HC-Pro (TuMV::6K-YFP) was described previously (Huang *et al.*, 2010).

### 2.3 Bacterial strains and growth conditions

*Escherichia coli* (*E. coli*) strain DH10B was used for DNA plasmid propagation and isolation. *E. coli* DH10B was grown in Luria-Bertani (LB) liquid medium (tryptone 1%, yeast extract 0.5%, NaCl 1%) or on LB solid medium supplemented with 1.5% w/v agar at 37°C. Ampicillin (100 µg/ml) or kanamycin (100 µg/ml) was added to LB liquid and agar medium based on the selectable markers of the plasmids used. *Agrobacterium*

*tumefaciens* (*A. tumefaciens*) strain GV3101 was employed for plant transformation. *Agrobacterium* strain GV3101 was grown in LB medium containing 100 µg/ml of kanamycin, 50 µg/ml of rifamycin and 25 µg/ml of gentamicin at 28°C.

#### **2.4 Yeast strains and cell culture**

Yeast strain AH109 was used for Y2H assay. Yeast cells were grown at 30°C in rich YPD medium supplemented with adenine hemisulfate (YPDA) or in minimal synthetic defined (SD) base medium (0.17% yeast nitrogen base without amino acids, 2% glucose) combined with appropriate dropout (DO) supplement. For SD solid medium, minimal SD base medium was supplemented with 1.5% w/v agar. Selective medium for yeast transformants was a combination of minimal SD base with -Ade (Adenine)/-His (Histidine)/-Leu (Leucine)/-Trp (Tryptophan) DO supplement.

#### **2.5 Plasmid construction**

Gateway technology (Invitrogen, Burlington, Ontario, Canada) was used to generate all the plasmid constructs used in this study except where otherwise stated. Gene sequences were amplified by polymerase chain reaction (PCR) using Phusion<sup>®</sup> High-Fidelity DNA Polymerase (New England Biolabs, Pickering, Ontario, Canada) for cloning purposes. GoTaq<sup>®</sup> Flexi DNA Polymerase (Promega, Madison, WI, USA) was employed for genotyping and other analysis.

The full-length P1, HC-Pro, P3, 6K1, CI, 6K2, VPg, NIa-Pro, NIB and CP coding regions of TuMV (GenBank accession NC\_002509) were obtained by PCR amplification from the pCambiaTunos/GFP infectious clone (Cotton *et al.*, 2009) using the primer sets indicated (Table 1). *Arabidopsis AtRH9* (AT3G22310), *AtRH26* (AT5G08610), *PRH75* (AT5G62190), *IMPA1* (AT3G06720), *IMPA2* (AT4G16143), *eIF(iso)4E* (AT5G35620), and *fibrillar* (AT5G52470) coding sequences were generated using the primer pairs listed (Table 2) from cDNA derived from *Arabidopsis* leaves. The resulting DNA fragments were purified and transferred into the entry vector pDONR221 (Invitrogen) by recombination using BP Clonase<sup>®</sup> (Invitrogen) following the standard conditions and procedures recommended by the supplier (Karimi *et al.*, 2002). Insertions in the resulting



**Table 1 Primers used for plasmid construction to express TuMV viral proteins in plants.** The *attB* recognition site is underlined.

<b>Primer Name</b>	<b>Primer sequence (5'-3')</b>
P1-Gate-F	<u>GGGGACAAGTTTGTACAAAAAAGCAGGCTTC</u> ATGATGGCAGCAGTTACATTTCGCAT
P1-Gate-R	<u>GGGGACCACTTTGTACAAGAAAGCTGGGTCT</u> ACTAAAGTGCACAATCTTGTGAC
HC-Pro-Gate-F	<u>GGGGACAAGTTTGTACAAAAAAGCAGGCTTC</u> ATGGCAGGTGCAGCGGGAGCC
HC-Pro-Gate-R	<u>GGGGACCACTTTGTACAAGAAAGCTGGGTCT</u> CCAACGCGGTAGTGTTC AAG
P3-Gate-F	<u>GGGGACAAGTTTGTACAAAAAAGCAGGCTTC</u> ATGGGAACAGAATGGGAGGACT
P3-Gate-R	<u>GGGACCACTTTGTACAAGAAAGCTGGGTCT</u> TGATGAACCACCGCCTTTTCT
6K1-Gate-F	<u>GGGGACAAGTTTGTACAAAAAAGCAGGCTTC</u> ATGGCGAAGAGACAATCCGAGCAA
6K1-Gate-R	<u>GGGGACCACTTTGTACAAGAAAGCTGGGTCT</u> CTGATGGTAGACTGTAGGTTCC
CI-Gate-F	<u>GGGGACAAGTTTGTACAAAAAAGCAGGCTTC</u> ATGACTCTCAATGATATAGAGGATGAC
CI-Gate-R	<u>GGGGACCACTTTGTACAAGAAAGCTGGGTCT</u> TGATGGTGAAGTGCCTCAAGA
6K2-Gate-F	<u>GGGGACAAGTTTGTACAAAAAAGCAGGCTTC</u> ATGAACACCAGCGACATGAGCAAATT
6K2-Gate-R	<u>GGGGACCACTTTGTACAAGAAAGCTGGGTCT</u> CGCTTCATGGGTTACGGGTTCCG
VPg-Gate-F	<u>GGGGACAAGTTTGTACAAAAAAGCAGGCTTC</u> ATGGCGAAAGGTAAGAGGCAAAGG
VPg-Gate-R	<u>GGGGACCACTTTGTACAAGAAAGCTGGGTCT</u> CTCGTGGTCCACTGGGACG
NIa-Pro-Gate-F	<u>GGGGACAAGTTTGTACAAAAAAGCAGGCTTC</u> ATGAGTAACTCCATGTTTCAGAGGGT
NIa-Pro-Gate-R	<u>GGGGACCACTTTGTACAAGAAAGCTGGGTCT</u> TTGTGCGTAGACTGCCGTGC
NIb-Gate-F	<u>GGGGACAAGTTTGTACAAAAAAGCAGGCTTC</u> ATGACCCAGCAGAATCGGTGGATG
NIb-Gate-R	<u>GGGGACCACTTTGTACAAGAAAGCTGGGTCT</u> CTGGTGATAAACACAAGCCTCA
CP-Gate-F	<u>GGGGACAAGTTTGTACAAAAAAGCAGGCTTC</u> ATGCAGGTGAAACGCTTGATGCA
CP-Gate-R	<u>GGGGACCACTTTGTACAAGAAAGCTGGGTCT</u> CAACCCCTGAACGCCAGTA

**Table 2 Primers used for construction of plasmids to express *Arabidopsis* proteins.**

The *attB* recognition site is underlined.

<b>Primer Name</b>	<b>Primer sequence (5'-3')</b>
AtRH9-Gate-F	<u>GGGGACAAGTTTGTACAAAAAAGCAGGCTTC</u> ATGATTAGCACAGTACTTCGCCGAT
AtRH9-Gate-R	<u>GGGGACCACTTTGTACAAGAAAGCTGGGTC</u> GTAAGATCTTTTACCATCGTTTGAT
AtRH26-Gate-F	<u>GGGGACAAGTTTGTACAAAAAAGCAGGCTTC</u> ATGTCCTCGAAGTTCCTCTCGGT
AtRH26-Gate-R	<u>GGGGACCACTTTGTACAAGAAAGCTGGGTC</u> CCTGGTTCTAAGACCAGGAACG
PRH75-Gate-F	<u>GGGGACAAGTTTGTACAAAAAAGCAGGCTTC</u> ATGCCTTCCCTAATGTTATCTGA
PRH75-Gate-R	<u>GGGGACCACTTTGTACAAGAAAGCTGGGTC</u> ATATCTCTGGCCTCTACCACCA
IMPA1-Gate-F	<u>GGGGACAAGTTTGTACAAAAAAGCAGGCTTC</u> ATGTCACTGAGACCCAACGCTAAG
IMPA1-Gate-R	<u>GGGGACCACTTTGTACAAGAAAGCTGGGTC</u> GCTGAAGTTGAATCCTCCGGATG
IMPA2-Gate-F	<u>GGGGACAAGTTTGTACAAAAAAGCAGGCTTC</u> ATGTCTTTGAGACCTAACGCTAAG
IMPA2-Gate-R	<u>GGGGACCACTTTGTACAAGAAAGCTGGGTC</u> CCTGGAAGTTGAATCCACCTG
eIF(iso)4E-Gate-F	<u>GGGGACAAGTTTGTACAAAAAAGCAGGCTTC</u> ATGGCGACCGATGATGTGAACG
eIF(iso)4E-Gate-R	<u>GGGGACCACTTTGTACAAGAAAGCTGGGTC</u> GACAGTGAACCGGCTTCTTC
fibrillarin-Gate-F	<u>GGGGACAAGTTTGTACAAAAAAGCAGGCTTC</u> ATGAGACCCCCAGTTACAGG
fibrillarin-Gate-R	<u>GGGGACCACTTTGTACAAGAAAGCTGGGTC</u> TGAGGCTGGGGTCTTTT

pDONR221 clones were verified by DNA sequencing.

Forward primers PRH75-F, PRH75-115F, PRH75-356F and PRH75-451F (Table 3) were designed to amplify regions of *Arabidopsis* PRH75 starting at amino acids 1, 115, 356 and 451, respectively. Reverse primers PRH75-R, PRH75-114R, PRH75-355R and PRH75-450R were designed to amplify regions of PRH75 ending at amino acids 114, 355, 450 and 671, respectively.

To construct vectors for the targeted Y2H assay, inserts of the resulting intermediate pDONR221 clones were further transferred into modified Gateway-compatible vectors pGADT7-DEST (prey) or pGBKT7-DEST (bait) (Lu *et al.*, 2010) by recombination using LR Clonase<sup>®</sup> (Invitrogen) to yield pGAD-NIb, pGAD-NIa-Pro, pGAD-VPg, pGAD-CI, pGAD-IMPA1, pGAD-IMPA2 and pGBK-eIF(iso)4E, pGBK-PRH75, pGBK-IMPA1, pGBK-IMPA2, respectively.

For bimolecular fluorescence complementation (BiFC) assay, the coding sequences of TuMV NIb, VPg, NIa-Pro, CI and 6K2 cistrons and the full-length coding sequences of *Arabidopsis AtRH9*, *PRH75*, *IMPA1* and *IMPA2* were introduced into the BiFC vectors pEarleyGate201-YN or pEarleyGate201-YC (Lu *et al.*, 2010) to produce NIb-YN, NIb-YC, VPg-YN, VPg-YC, NIa-Pro-YN, NIa-Pro-YC, CI-YN, CI-YC, 6K2-YN, IMPA1-YN, IMPA1-YC, IMPA2-YN, IMPA2-YC, AtRH9-YN, AtRH9-YC, PRH75-YN and PRH75-YC, respectively.

For transient expression analysis in plant cells, the entire NIb, VPg, NIa-Pro and CI coding regions of TuMV, the full-length coding sequences of *Arabidopsis AtRH9*, *AtRH26* and *PRH75*, *Arabidopsis fibrillarin*, *IMPA1*, *IMPA2* and *eIF(iso)4E* were transferred by recombination into the binary destination vectors pEarleyGate101 or pEarleyGate102 (Earley *et al.*, 2006) to generate plant expression vectors for transient expression of AtRH9-YFP, PRH75-YFP, NIb-YFP, NIa-Pro-YFP, VPg-YFP, CI-YFP, IMPA1-YFP, IMPA2-YFP and eIF(iso)4E-YFP; AtRH26-CFP (cyan fluorescent protein), PRH75-CFP and fibrillarin-CFP, respectively.

For nuclear localization signal (NLS) analysis, PRH75<sub>(1-114)</sub>, PRH75<sub>(115-355)</sub>, PRH75<sub>(356-</sub>

**Table 3 Primers used for construction of plasmids for PRH75 domain analysis.** The *attB* recognition site is underlined.

<b>Primer Name</b>	<b>Primer sequence (5'-3')</b>
PRH75-Gate-F	<u>GGGGACAAGTTTGTACAAAAAAGCAGGCTTC</u> ATGCCTTCCCTAATGTTATCTG
PRH75-Gate-R	<u>GGGGACCACTTTGTACAAGAAAGCTGGGTCA</u> TATCTCTGGCCTCTACCA
PRH75-Gate-115F	<u>GGGGACAAGTTTGTACAAAAAAGCAGGCTTC</u> ATGGGTATTGAAGCTCTTTTCCCG
PRH75-Gate-114R	<u>GGGGACCACTTTGTACAAGAAAGCTGGGTCA</u> ATTCGCCTTAAGCTTCTCCCTCA
PRH75-Gate-356F	<u>GGGGACAAGTTTGTACAAAAAAGCAGGCTTC</u> ATGTTGCTGAAACTAAAGTTCAAG
PRH75-Gate-355R	<u>GGGGACCACTTTGTACAAGAAAGCTGGGTCA</u> AATAATAGTTTGGCCTCCACTGC
PRH75-Gate-451F	<u>GGGGACAAGTTTGTACAAAAAAGCAGGCTTC</u> ATGGATTCTAGAAAGTCGAGTGTA
PRH75-Gate-450R	<u>GGGGACCACTTTGTACAAGAAAGCTGGGTCA</u> GTAGAGTGTAACCGCAACT

450), PRH75<sub>(451-671)</sub>, PRH75<sub>(1-355)</sub>, PRH75<sub>(1-450)</sub>, PRH75<sub>(115-450)</sub>, PRH75<sub>(115-671)</sub> and PRH75<sub>(356-671)</sub> were transferred by recombination into the binary destination vectors pEarleyGate101-GUS to generate plant expression vectors for transient expression of PRH75<sub>(1-114)</sub>-GUS-YFP, PRH75<sub>(115-355)</sub>-GUS-YFP, PRH75<sub>(356-450)</sub>-GUS-YFP, PRH75<sub>(451-671)</sub>-GUS-YFP, PRH75<sub>(1-355)</sub>-GUS-YFP, PRH75<sub>(1-450)</sub>-GUS-YFP, PRH75<sub>(115-450)</sub>-GUS-YFP, PRH75<sub>(115-671)</sub>-GUS-YFP and PRH75<sub>(356-671)</sub>-GUS-YFP, respectively. The coding sequence of  $\beta$ -glucuronidase (*GUS*) was obtained by PCR from plasmid pENTR-GUS (Invitrogen) and ligated into AvrII-restricted pEarleyGate101 to yield GUS-YFP (Xiong and Wang, 2013).

For *Tobacco rattle virus* (TRV)-based virus induced gene silencing (VIGS), a 110 base-pair (bp) of *AtRH9* fragment and a 125 bp of *PRH75* fragment were amplified from *Arabidopsis* cDNA with two pairs of primers that contained an EcoRI and BamHI site specific to the 5' and 3' end of the fragments, respectively (*AtRH9*-EcoRI-F/*AtRH9*-BamHI-R and *PRH75*-EcoRI-F/*PRH75*-BamHI-R) (Table 4). The amplified fragment was digested with EcoRI and BamHI, then ligated into the corresponding sites of EcoRI and BamHI-restricted pTRV2 vector (Burch-Smith *et al.*, 2006) to generate the vectors pTRV2-*AtRH9* and pTRV2-*PRH75*, respectively.

## 2.6 Bacterial transformations

### 2.6.1 *E. coli* transformation

*E. coli* strain DH10B competent cells were thawed on ice for 10 min prior to mixing with the plasmid DNA. The mixture of competent cells and the recombinant plasmid was incubated on ice for 30 min and followed by a heat shock at 42°C for 90 seconds and then cooled on ice. LB medium was added and the transformed cells were incubated at 37°C for one hour with agitation to allow expression of antibiotic resistance genes. The resulting culture was then spread on LB agar plates containing the appropriate antibiotics to select for the transformed bacteria. The plates were incubated overnight at 37°C and colonies that were able to form in the presence of antibiotics were counted as successful plasmid DNA transformations after 12-16 h. The colonies were checked by colony PCR to confirm the presence of plasmid/gene.

**Table 4 Primers used to amplify *AtRH9* and *PRH75* DNA fragments that are inserted into the TRV-based vector. The *EcoRI* and *BamHI* sites are underlined.**

<b>Primer Name</b>	<b>Primer sequence (5'-3')</b>
AtRH9-EcoRI-F	CCGGAATTCTGATGTTGCTGCCCGTGGACT
AtRH9-BamHI-R	CGCGGATCCCACGACCAGTTCGCCCCGTT
PRH75-EcoRI-F	CCGGAATTCGCCGAACAGGAAGAGCTGGCA
PRH75-BamHI-R	CGCGGATCCAGGTTGAGGTGCAGCAAGGTGC

### 2.6.2 *Agrobacterium* transformation

*Agrobacterium* transformation of plasmid DNA was carried out using the electroporation following the Bio-Rad *E. coli* Pulser (Bio-Rad) manual. The plasmid DNA from BP/LR reaction or ligation products were mixed with *Agrobacterium* strain GV3101 competent cells on ice for 10 min. The mixture was transferred to a cold 0.1 cm Gene Pulser<sup>®</sup> cuvette (Bio-Rad) and kept on ice for 10 min. A single electric pulse of 1.8 kV voltage was applied using a Bio-Rad MicroPulser. Following electroporation, 200 µl of liquid LB medium was immediately added to the mixture and incubated at 28°C with shaking for 2 h. The resulting culture was spread on LB agar plates containing the appropriate antibiotics. The plates were incubated at 28°C for 48 h and colonies were selected for further analysis.

### 2.7 Plant genomic DNA extraction

*Arabidopsis* leaf tissue (200 mg) was collected and ground in liquid nitrogen. Extraction buffer (500 µl) [10 mM Tris-HCl, 1.4 M NaCl, 20 mM ethylenediaminetetraacetic acid (EDTA), 2% cetyltrimethyl-ammonium bromide (w/v) (CTAB)] (Porebski *et al.*, 1997) was added to each sample, then 500 µl of chloroform:isoamyl alcohol (24:1) was added and mixed well, followed by a centrifugation at 10,000 rpm for 5 min. The upper aqueous phase was transferred to a clean tube and DNA was precipitated by adding 0.7 volume of isopropanol. Samples were incubated at -20°C for 1 h, kept on ice for 10 min and then centrifuged at 10,000 rpm for 20 min to collect the pellets. After two washes with 500 µl 70% ethanol and centrifugation, the pellet was air-dried for 20 min at room temperature and resuspended in 50 µl of milli-Q water.

### 2.8 RNA isolation

Total RNA was isolated from *Arabidopsis* leaf tissue using the RNeasy Plant Mini Kit (Qiagen) following the manufacturer's instructions. DNase I treatment was performed to remove genomic DNA contamination prior to elution in RNase free water (Invitrogen).

The concentration of total RNA was determined by measuring absorbance at 260 nm/280 nm using a spectrophotometer (Nanodrop1000, ABI). Reverse transcription was

performed by synthesizing first-strand cDNA from 1.5 µg of total RNA (pretreated with DNase I) as the template using Superscript III reverse transcriptase (Invitrogen) and an oligo(dT)<sub>12-18</sub> primer (Invitrogen) following the manufacturer's protocols.

## **2.9 Functional analysis of *Arabidopsis* T-DNA insertion lines of *AtRHs***

### **2.9.1 Selection of *Arabidopsis* T-DNA insertion lines of *AtRHs***

Genebank accession numbers were used to select *Arabidopsis* T-DNA insertion lines of *Arabidopsis* DEAD-box RNA helicases (*AtRHs* or *RHs*). So far, approximately 113 sequences from *Arabidopsis* genome have been annotated in the TAIR unigene set as putative RNA helicase genes (Umate *et al.*, 2010). Based on their predicted functions, 42 *AtRH* genes were selected for this study. These genes encode the proteins that are related to eIF4A (Boudet *et al.*, 2001) or have putative functions in stress response regulation. *Arabidopsis* T-DNA insertion mutants were selected for each gene based on their availability and genotype, with a preference for T-DNA insertions in the exon or 5' UTR regions. Seed stocks of 128 *Arabidopsis* T-DNA insertion lines corresponding to these 42 *AtRH* genes were obtained from the Arabidopsis Biological Resource Center (ABRC). Mutant and insertion information was obtained from the Salk Institute Genomic Analysis Laboratory website (<http://signal.salk.edu/>).

### **2.9.2 Screening for homozygous *Arabidopsis* T-DNA insertion lines of *AtRHs***

The genotype of each *Arabidopsis atrh* T-DNA insertion line was confirmed by PCR following the protocols suggested by ABRC (<http://signal.salk.edu/tdnaprimers.2.html>). Two sets of primers were used to amplify the target alleles with two gene specific primers to detect the wild-type allele or with a gene specific primer and a T-DNA left border specific primer (LB) to identify the mutant allele. Primers for genotyping were designed using the T-DNA iSect tool (<http://signal.salk.edu/tdnaprimers.2.html>) and were listed in Table 5. The homozygous lines were used for ELISA analysis and gene expression analysis.



**Table 5 Primers used for PCR-screening of homozygous *Arabidopsis atrh* T-DNA insertion lines.**

<b>Primer Name</b>	<b>Primer sequence (5'-3')</b>
LB (LBb1.3)	ATTTTGCCGATTTTCGGAAC
SALK_035421-LP	TCATAAATGGAAGTGGCGAAG
SALK_035421-RP	TCTTGTTGCAACTGATGTTGC
SALK_060677-LP	TTCTCATCCACGGTCAAGATC
SALK_060677-RP	TGTACAAGAACCCGTTCTTGG
SALK_068401-LP	TTCTAATGTCCTTGCCATTGG
SALK_068401-RP	TTAAGCTTCTCCCTCAAAGGC
SALK_040389-LP	CTACAGGTCTGGTCCAGATGG
SALK_040389-RP	TTAAGCTTCTCCCTCAAAGGC
SALK_106823-LP	TGCGTATGCCTATAGGACCTG
SALK_106823-RP	TGGTGTCCCTGTCTACGTTTC

### 2.9.3 Gene expression analysis of *Arabidopsis* T-DNA insertion lines of *AtRHs*

The expression of *AtRH* gene in different *Arabidopsis* T-DNA insertion lines was verified by RT-PCR with gene specific primers. cDNA was synthesized from total RNA isolated from leaf tissue of *Arabidopsis* T-DNA insertion mutant plants. PCR amplifications were carried out as described below (section 2.10.2).

## 2.10 Polymerase chain reaction (PCR)

### 2.10.1 Polymerase chain reaction (PCR)

PCR reactions were carried out using a thermocycler (Eppendorf) following the program guideline. For a routine PCR using Phusion<sup>®</sup> High-Fidelity DNA Polymerase, a denaturing temperature of 98°C for 30 seconds was followed by an annealing temperature of 55°C for 1 min, and primer extension was achieved at 72°C for 30 seconds per kilobase (kb) of target DNA to be amplified. These three steps were repeated for a total of 30 to 35 cycles, followed by a final extension for 5 min.

### 2.10.2 RT-PCR

To quantify the expression level of *AtRH* gene in different T-DNA insertion lines, total RNA was extracted from leaf tissue of *Arabidopsis* T-DNA insertion mutants and wild-type plants (WT) using the RNeasy Plant Mini Kit (Qiagen) and treated with DNase I following the manufacturer's instructions (Invitrogen). cDNA was synthesized by reverse transcription of RNA samples and used to determine the mRNA expression levels of target genes. Primers were designed within the coding region (Table 6) and target genes were amplified with annealing temperature at 60°C for 30 cycles following the same PCR procedure as section 2.10.1. *Arabidopsis Actin II* (*Actin2*) was used as an internal control.

### 2.10.3 Real-time quantitative RT-PCR (qRT-PCR)

Real-time qRT-PCR was conducted and analyzed with the CFX96 Real-Time PCR Detection System (Bio-Rad) following the manufacturer's instructions. For each primer set, gel electrophoresis and melting curve analysis were carried out to ensure that only a single expected PCR product and melting temperature were generated. Each reaction

**Table 6 Primers for RT-PCR**

---

<b>Primer Name</b>	<b>Primer sequence (5'-3')</b>
AtRH9-F	ATGATTAGCACAGTACTTCGCCGAT
AtRH9-R	TCAGTAAGATCTTTTACCATCGTTTG
PRH75-F	ATGCCTTCCCTAATGTTATCTGA
PRH75-R	TCAATATCTCTGGCCTCTACCA
AtRH26-F	ATGTCCTCGAAGTTCCTCTCGGT
AtRH26-R	CTACTTGGTTCTAAGACCAGGAACG
At-Actin2-F	GCCATCCAAGCTGTTCTCTC
At-Actin2-R	GAACCACCGATCCAGACACT

---

contained 40 ng of cDNA template, 5  $\mu$ M of primer mix, and 1X SsoFast™ EvaGreen® Supermix (Bio-Rad) in a total volume of 10  $\mu$ l of reaction solution. qRT-PCR reactions were carried out following cycling conditions: initial incubation at 95°C for 30 seconds followed by 40 cycles of a denaturing temperature at 95°C for 5 seconds and an annealing temperature at 60°C for 5 seconds. Melting curve was recorded after 40 reaction cycles by heating from 65°C to 95°C with a ramp speed of 0.5°C every 2-5 seconds. Relative transcript abundances were calculated using CFX Manager Software (Bio-Rad). The expression of CP gene of TuMV was detected to reflect viral accumulation level using primer sets TuMV-CP-F and TuMV-CP-R. qRT-PCR analysis was also carried out to detect *AtRH* gene expression of the corresponding *Arabidopsis* T-DNA insertion lines. Gene specific primers were used for gene expression analysis. Expression of *Arabidopsis Actin II* was used as a reference gene to normalize the data and to calculate the relative mRNA abundance levels. For each sample analyzed, three biological replicates were included and for each biological replicate, three technical repeats were carried out. All results are shown as means of biological replicates with corresponding standard errors. The primers used for qRT-PCR were listed in Table 7.

### **2.11 Gateway-based cloning**

The Gateway cloning technology exploits an *in vitro* site-specific recombination system to clone the gene of interest into an entry vector using the BP reaction. Subsequently, the gene of interest from the entry clone was subcloned into various destination vectors using the LR reaction to produce expression clones (Karimi *et al.*, 2002). Gateway protocols rely essentially on the BP and LR Clonase® reactions (Hartley *et al.*, 2000). PCR primers for Gateway cloning system were designed following the manufacturer's instructions (Invitrogen). DNA fragments were amplified from cDNA of *Arabidopsis* leaf tissue as the template and Phusion® High-Fidelity DNA polymerase was used to construct the entry clones. A mixture of 1  $\mu$ l of purified PCR product, 0.5  $\mu$ l pDONR221 vector and 0.5  $\mu$ l BP Clonase® (Invitrogen) was set up for BP reaction. After overnight incubation at 25°C, 2  $\mu$ l of BP reaction product was transferred into 100  $\mu$ l of *E. coli* DH10B competent cells for transformation as described. The entry clones were linearized and the insertion fragments were purified before subcloning into destination vectors.

**Table 7 Primers for real-time quantitative RT-PCR (qRT-PCR)**

<b>Primer Name</b>	<b>Primer sequence (5'-3')</b>
At-Actin2-F	GCCATCCAAGCTGTTCTCTC
At-Actin2-R	GAACCACCGATCCAGACACT
TuMV-CP-F	TGGCTGATTACGAACTGACG
TuMV-CP-R	CTGCCTAAATGTGGGTTTGG
AtRH9-realtime-F	TCGTGCTGGAAAGAAAGGAAGCG
AtRH9-realtime-R	TTCCACAGCAATGCTAGGCAGCTC
PRH75-realtime-F	ATCTGGTGGTATGGAAGCTGCTG
PRH75-realtime-R	AGGAATGCAGGAACCACACTGTC

A mixture of 1 µl of linearized entry clone plasmid, 1 µl destination vector and 0.5 µl LR Clonase<sup>®</sup> (Invitrogen) was set up for LR reaction. After overnight incubation at 25°C, 2 µl of LR reaction product was transferred into *E. coli* DH10B for transformation as described.

### 2.12 Yeast transformation

Yeast cells were transformed following the Yeast Protocols Handbook (Clontech Protocol PT3024-1). A 2 ml rich YPD medium with a yeast colony was grown overnight at 30°C with shaking, then sub-cultured into 30 ml of fresh YPD medium and continued to grow for another 3-4 h until an optical density at 600 nm (OD<sub>600</sub>) reached 0.6. Yeast cells were pelleted by centrifugation, washed in 500 µl distilled H<sub>2</sub>O and resuspended in 100 µl of freshly prepared lithium acetate (LiAc) solution (0.1 M LiAc, 10 mM Tris-HCl [PH 7.5], 1 mM EDTA). Denatured carrier DNA (10 µl) and 0.1 µg of plasmid DNA were added to 100 µl yeast competent cells and mixed well followed by the addition of 600 µl of 40% PEG 4000 (50% polyethylene glycol 4000) in LiAc solution. After incubation at 30°C for 30 min with shaking at 200 rpm, 70 µl of DMSO was added, followed by a 15 min heat shock in a 42°C water bath. Yeast cells were collected by centrifugation and resuspended in 100 µl of TE buffer (10 mM Tris-HCl [PH 7.5], 1 mM EDTA). The resuspended cells were plated on an appropriately supplemented SD medium and the plates were incubated at 30°C until colonies appeared.

### 2.13 Yeast two-hybrid assay

The Y2H assay was performed following the Clontech yeast protocols (Clontech). To perform protein-protein interaction assay, the Gateway-compatible vectors pGBKT7-DEST (bait) and pGADT7-DEST (prey) were used (Lu *et al.*, 2010). The full-length coding regions of NIb, NIa-Pro, VPg and CI from TuMV and the full-length coding sequences of *Arabidopsis* PRH75, IMPA1, IMPA2 and *eIF(iso)4E* were introduced into vectors pGAD and pGBK, respectively. Yeast strain AH109 was co-transformed with bait and prey constructs using the LiAc transformation method (Schiestl and Gietz, 1989).

After the bait and prey constructs (in different combinations) were co-transformed into

yeast strain AH109, the yeast was plated on selection agar medium lacking leucine and tryptophan (SD/-Leu/-Trp) at 30°C for up to 5 days. The selected individual yeast transformants were grown in liquid medium and a series of diluted culture were plated onto a high-stringency selective medium lacking adenine, histidine, leucine and tryptophan (SD/-Ade/-His/-Leu/-Trp) for up to 5 days to assess positive protein-protein interactions. The interaction between TuMV VPg and *Arabidopsis* eIF(iso)4E expressed from pGAD-VPg and pGBK-eIF(iso)4E, respectively was used as a positive control, whereas the empty pGBK and pGAD vectors (no insert) were used in co-transformation as negative controls.

#### **2.14 Transient expression in *N. benthamiana***

For transient expression analysis in *N. benthamiana* leaves, constructs were generated in Gateway-compatible binary vectors and transformed into *Agrobacterium* strain GV3101 via electroporation. Four-week-old *N. benthamiana* plants were used for *Agrobacterium*-mediated transient expression.

For agroinfiltration, *Agrobacterium* cultures were grown overnight in LB medium with appropriate antibiotic selection at 28°C. The *Agrobacterium* cells were harvested by centrifugation, and then resuspended in infiltration buffer (10 mM MgCl<sub>2</sub>, 10 mM MES, and 150 µM acetosyringone). After incubation for 2 h at room temperature, the culture was diluted to 0.5-1.0 at OD600 and agroinfiltrated into leaf epidermal cells under gentle pressure using a syringe barrel (Sparkes *et al.*, 2006). After agroinfiltration, the plants were maintained under normal conditions for observation.

For subcellular localization, target genes were recombined with pEarleyGate101 or pEarleyGate102 to produce transient expression vectors tagged with YFP or CFP, respectively. The corresponding vectors were transformed into *Agrobacterium* GV3101. *Agrobacterium* cultures were agroinfiltrated into *N. benthamiana* leaves at 0.5-1.0 of OD600. For colocalization studies of two proteins, two *Agrobacterium* cultures were mixed with equal volume, and 150 µl of the mixed cultures were agroinfiltrated into *N. benthamiana* leaves.

For BiFC assay, *Agrobacterium* cultures carrying the fusion constructs containing the N-terminal or C-terminal fragment of YFP were co-agroinfiltrated into *N. benthamiana* leaves. The reconstitution of YFP signals was monitored using a confocal microscopy 2-4 days after agroinfiltration as described (Wei *et al.*, 2010). For protein pairs showing the YFP signals, the YFP signal and bright-field were imaged and overlaid.

### **2.15 Confocal microscopy**

Fluorescence was visualized 2-4 days post infiltration using a Leica TCS SP2 inverted confocal microscopy (<http://www.leica.com/>) with an Argon-Krypton laser. Sections from agroinfiltrated leaves were excised and placed between two microscopy cover slides with a drop of water. YFP signals were imaged using a 63× water immersion objective at an excitation wavelength of 514 nm, and emissions were collected between 525 and 575 nm. Images of CFP fluorescence were obtained using the same microscopy at an excitation wavelength of 458 nm and emissions were collected between 470 and 500 nm. GFP signal was excited at 488 nm and the emitted light was captured at 505 to 525 nm. mCherry fluorescence was excited at 543 nm and the emissions were captured at 590-630 nm. Light emitted at 630-680 nm was used to record chlorophyll autofluorescence. Data for the different color channels were collected simultaneously. The samples were scanned at a resolution of 512×512 pixels. Images were collected with a charge-coupled device camera and analyzed by Leica confocal software.

### **2.16 Quantification of Fluorescence Resonance Energy Transfer (FRET) efficiency by acceptor photobleaching**

The full-length coding regions of NlB, NIa-Pro, VPg and CI of TuMV were PCR amplified and recombined into pEarleyGate101 to produce the transient expression vectors of NlB-YFP, NIa-Pro-YFP, VPg-YFP and CI-YFP in plants, respectively. The full length coding sequence of *PRH75* was amplified and cloned into pEarleyGate102 to produce the transient expression vector of PRH75-CFP in plants. To quantify FRET efficiency, PRH75-CFP and one of NlB-YFP, NIa-Pro-YFP, VPg-YFP or CI-YFP were co-agroinfiltrated into four-week-old *N. benthamiana* leaves. Forty-eight hours after infiltration, leaf epidermal cells exhibiting coexpression of YFP- and CFP-tagged



proteins were bleached in the acceptor YFP channel with a 514-nm argon laser. The change in donor CFP fluorescence intensity was quantified by comparing pre-bleach and post-bleach images using a confocal microscopy (TCS SP2, Leica), and FRET efficiency was calculated from the formula as follows:  $E = [(CFP \text{ signal after photobleaching} - CFP \text{ signal before photobleaching}) / CFP \text{ signal after photobleaching}] \times 100$  (Karpova and McNally, 2006; Song *et al.*, 2011). The combination of PRH75-CFP and GUS-YFP was used as a negative control. Error bars represent standard deviations from nine independent FRET analysis in three independent experiments.

### **2.17 dsRNA-binding dependent fluorescence complementation (dRBFC) assay**

The dRBFC assay was performed based on the system developed by our lab (Cheng *et al.*, unpublished data). In detail, the dsRNA-binding domain of B2 of FHV (GenBank accession X77156) and the dsRNA-binding domain of VP35 of *Marburg virus* (MARV) (GenBank accession GQ433353) were cloned and recombined into Gateway-compatible BiFC vectors pEarleyGate201-YN or pEarleyGate201-YC (Lu *et al.*, 2010) to produce B2-YN and VP35-YC, respectively.

For dRBFC assay, *Agrobacterium* cultures carrying B2-YN and VP35-YC constructs were agroinfiltrated into *N. benthamiana* leaves which were infected with TuMV::6K2-mCherry. The YFP signals were monitored 48 h after agroinfiltration to label the dsRNA intermediates during viral replication, highlighting the dsRNA-containing 6K2-mCherry vesicles as described (Wei *et al.*, 2010).

### **2.18 TuMV infection assay**

TuMV infection assay was carried out to test the susceptibility of *Arabidopsis atrh* T-DNA insertion lines to TuMV infection. The seedlings of *Arabidopsis* wild-type plants (WT) and selected homozygous *Arabidopsis* T-DNA insertion mutant plants were inoculated with TuMV either by mechanical inoculation or using agroinfiltration. Plants were inoculated at the five to six leaf stage of development. Virus was applied to the two oldest leaves by mechanical inoculation.

Approximately 1 g TuMV-infected leaf tissue of *N. benthamiana* was harvested as the

source of virus inoculum. The tissue was homogenized using a mortar and pestle in 10 ml inoculation buffer (50 mM potassium phosphate buffer, [pH 7.5]). Carborandum powder was lightly dusted on plant leaves intended to be inoculated. A gentle rubbing of the TuMV-containing inoculum over the leaf surface was performed to facilitate virus entry. The negative control plants were rubbed with inoculation buffer also as mock inoculations. TuMV infection assay was repeated three times for each *Arabidopsis atrh* T-DNA insertion line. Eight plants for each T-DNA insertion line were inoculated with the addition of four plants serving as a mock inoculation treatment. The TuMV infectious clone pCambiaTunos/GFP (TuMV-GFP) was used for agroinfiltration. Leaf tissue from TuMV-infected *Arabidopsis* T-DNA insertion mutants was harvested for ELISA analysis.

### **2.19 Triple-antibody sandwich enzyme-linked immunosorbent assay (TAS-ELISA)**

After mechanical inoculation or agroinfiltration, TAS-ELISA was performed to quantify viral accumulation level of WT plants and *Arabidopsis atrh* T-DNA insertion mutants at the days indicated. The newly-emerged leaves of TuMV-infected mutants and WT plants were harvested for ELISA analysis. Leaf tissue was weighted and ground in ELISA sample extraction buffer, then TAS-ELISA was conducted with an ELISA kit (Agdia) following the manufacturer's instructions. Absorbances were recorded at 405 nm with an iMark microplate reader (Bio-Rad) (Figure 3).

### **2.20 TRV-based virus-induced gene silencing (VIGS)**

To suppress expression of *AtRH9* and *PRH75* in *Arabidopsis* by VIGS, a TRV-based vector was used. To induce silencing, *Agrobacterium* carrying pTRV1 vector and pTRV2-derived vector were combined in a ratio of 1:1(v/v) mixtures and agroinfiltrated into *Arabidopsis* seedlings. For example, pTRV1 and pTRV2-*AtRH9* vectors were separately introduced into *Agrobacterium* and co-agroinfiltrated into *Arabidopsis* at the four leaf stage. Similarly, *Agrobacterium* carrying pTRV1 and pTRV2-*PRH75* were co-agroinfiltrated to silence *PRH75* in *Arabidopsis*. Plants co-agroinfiltrated with pTRV1 and pTRV2 empty vectors or with pTRV1 and pTRV2-PDS were used as controls. Twelve days post-infiltration, treated plants were mechanically inoculated with TuMV.

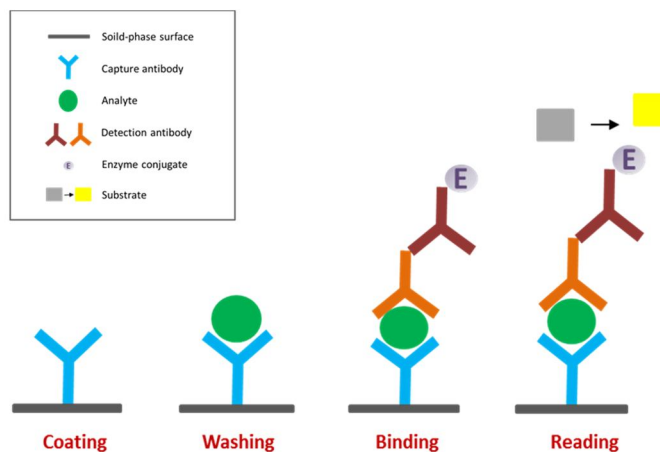


**Figure 3 Methodology of triple-antibody sandwich enzyme-linked immunosorbent assay (TAS-ELISA).**

Immobilized capture antibody is attached to a solid-phase surface. After adding test sample, antibody-analyte binding occurs. Enzyme-labeled analyte-specific detection antibody is added to bind to the analyte, forming the "sandwich". Then substrate is added and will produce a colored product in the presence of enzyme.

### **2.21 Gene structure and multiple sequence alignments**

Identification and analysis of domain organization and conserved motifs of *Arabidopsis* PRH75 were performed using the specialized BLAST program for conserved domain searches at the National Center for Biotechnology Information (NCBI) protein database (<http://www.ncbi.nlm.nih.gov/cdd>). Multiple sequence alignments of PRH75 and DEAD-box RNA helicase (DDX) proteins from other plant species were obtained using ClustalW2 (<http://www.ebi.ac.uk/Tools/clustalw2/index.html>).

### **2.22 Statistical analysis**

ELISA values and relative fold changes of TuMV accumulation were compared between *Arabidopsis atrh* T-DNA insertion mutants and WT plants using the student's t-test. All statistical analysis were performed using Microsoft Excel software. A p-value of 0.05 or less indicates significant difference.

## Chapter 3: Results

### 3.1 Identification of *Arabidopsis* DEAD-box RNA helicase (*AtRH*) genes essential for TuMV infection

#### 3.1.1 Screening for homozygous T-DNA insertion lines of *AtRH* genes in *Arabidopsis*

*Arabidopsis* was used as the model host to study the involvement of *Arabidopsis* DEAD-box RNA helicase genes (*AtRH* or *RH*) in TuMV infection. Previous studies predicted that the *Arabidopsis* genome is composed of 53 *AtRH* genes (Aubourg *et al.*, 1999; Boudet *et al.*, 2001). A recent study has revealed a total of 113 putative helicase genes encoded by the *Arabidopsis* genome (Umate *et al.*, 2010). Based on the presence of the conserved DEAD helicase motif and database annotations, a dataset representing *AtRH* genes in the *Arabidopsis* genome was generated in the Arabidopsis Information Resource (TAIR) database (<http://www.arabidopsis.org/>) (Poole, 2007). The gene dataset was also cross-checked with the NCBI database (<http://www.ncbi.nlm.nih.gov/>) (Appendix I). Although a large number of DEAD-box RNA helicases had been identified as 'computer predicted putative helicases', only a few of them were experimentally confirmed to have helicase activity and their biological functions were not well characterized. To elucidate the role of *AtRH* genes associated with TuMV infection, *Arabidopsis* T-DNA insertion mutants carrying genetic lesions in the corresponding *AtRH* genes were analyzed.

*Arabidopsis* T-DNA insertion lines corresponding to 42 *AtRH* genes were selected from the TAIR database. These genes encode the proteins that are either related to eIF4A or have possible functions in PD formation or stress response regulation. Seed stocks of 128 *Arabidopsis* T-DNA insertion lines corresponding to these *AtRH* genes were ordered and obtained from ABRC (Table 8). PCR-based genotyping was carried out to screen for homozygous lines for the T-DNA insert. Based on the preliminary genotyping result, a total of 53 homozygous *Arabidopsis* T-DNA insertion lines corresponding to 26 *AtRH* genes were identified. Thirty-five *Arabidopsis* T-DNA insertion lines did not contain T-DNA inserts at the reported positions and 40 *Arabidopsis* T-DNA insertion lines were heterozygous lines. For example, only heterozygous progeny plants were recovered for

**Table 8 List of *AtRH* genes and corresponding *Arabidopsis atrh* T-DNA insertion lines.**

Gene Names	Locus	<i>Arabidopsis</i> T-DNA insertion lines
<b>AtRH family (Boudet <i>et al.</i>, 2001)</b>		
RH1	AT4G15850	SALK_049804; SALK_049805; CS839540; SALK_049812; SALK_016796
DRH1	AT3G01540	SALK_063362; CS879140; SALK_073018; SALK_109174
RH2(eIF-4A-III)	AT3G19760	CS808417
RH3	AT5G26742	SALK_005920
RH4(eIF-4A)	AT3G13920	SALK_135778; SALK_038072; CS833761; SALK_072655; SALK_107633; CS849805; SALK_123728; CS877175
RH6	AT2G45810	CS805454; CS837992
RH8	AT4G00660	SALK_016830
RH9	AT3G22310	SALK_035421; SALK_060677; CS807388; SALK_063973
RH10	AT5G60990	SALK_001503; CS854587
RH11	AT3G58510	SALK_122885; SALK_138586; CS381476
RH12	AT3G61240	SALK_016921; SALK_024905; CS811341 SALK_148563
RH16	AT4G34910	SALK_066621; CS843929; CS852120
RH17	AT2G40700	SALK_076414; SALK_027066
RH18	AT5G05450	SALK_027422; SALK_083512; CS801613
RH20	AT1G55150	CS871647; SALK_005956; SALK_114853; SALK_124308
RH21	AT2G33730	SALK_100059; CS839970
RH22	AT1G59990	SALK_065388; SALK_032399; CS856759
RH24	AT2G47330	SALK_087182; SALK_144439; CS831825; SALK_045730; SALK_079711
RH26	AT5G08610	SALK_022561; SALK_106823; CS846644; CS873761; CS836908; SALK_009049 CS832362
RH28	AT4G16630	SALK_012018; SALK_020556; SALK_082807
RH29	AT1G77030	SALK_112020
RH30	AT5G63120	CS848715
RH31	AT5G63630	SALK_090068
RH33	AT2G07750	SALK_119034; SALK_017083
RH34	AT1G51380	CS815277; SALK_068534
RH37	AT2G42520	SALK_099097
RH40	AT3G06480	SALK_056041; SALK_117253; CS857553
RH41	AT3G02065	SALK_020125; CS843411; CS858153
RH46	AT5G14610	SALK_068359; SALK_068406; CS852203; SALK_086013; SALK_116644

RH48	AT1G63250	SALK_013253; SALK_144751; SALK_144971
RH49	AT1G71370	SALK_140258
RH52	AT3G58570	SALK_068712; SALK_116448
RH53	AT3G22330	SALK_056387; SALK_065080
RH57	AT3G09720	SALK_019721; SALK_143440; SALK_020854 SALK_140120; CS823406
RH58	AT5G19210	CS832329
PRH75	AT5G62190	SALK_060686; SALK_068401; SALK_066279; SALK_016729; SALK_040389; SALK_040581; SALK_018195; SALK_062900
<b>Increased Size Exclusion Limit (ISE) (Burch-Smith and Zambryski, 2010)</b>		
ISE1(RH47)	AT1G12770	CS821051; CS807604; CS802911; CS843211
ISE2	AT1G70070	SALK_022088; SALK_117413; CS802933; SALK_137857; CS835737; CS848778; CS814056; CS16227
<b>Stress Response Suppressor (STRS) (Kant <i>et al.</i>, 2007)</b>		
STRS1(RH5)	AT1G31970	CS815216; CS849995; CS851469; SALK_062509
STRS2(RH25)	AT5G08620	SALK_140146; SALK_028850
<b>eIF-4A putative</b>		
eIF-4A-2	AT1G54270	SALK_051038
eIF-4A-3	AT1G72730	SALK_065267

*Arabidopsis* mutants with T-DNA insertion in *eIF4A*, *Increased Size Exclusion Limit (ISE) 1* and *ISE2*. These results were consistent with the reported embryo-defective phenotypes in homozygous *Arabidopsis* lines corresponding to those genes. eIF4A is required for mRNA translation and is essential for plant growth and development. Disruption of eIF4A function would cause deleterious effects in plants and its homozygote is nonviable (Huang *et al.*, 2010). ISE1 and ISE2 are required for PD formation and embryogenesis, and their null mutants are embryo lethal (Kobayashi *et al.*, 2007).

### 3.1.2 Identification of *AtRH* genes associated with TuMV infection

Based on the availability of homozygous T-DNA insertion lines, we further selected 41 T-DNA insertion lines corresponding to 26 *AtRH* genes, with a preference for T-DNA insertions in either an exon or the 5' UTR region. These homozygous mutants and WT plants in parallel were evaluated for their susceptibility to TuMV infection by conducting a TuMV infection assay (Table 9). Selected *Arabidopsis* T-DNA insertion lines and wild-type plants were rub-inoculated with TuMV, followed by observation of disease symptoms. Newly-emerged leaves from systemically TuMV-infected T-DNA mutant plants and wild-type plants (WT) were sampled and assayed for viral CP accumulation at 10 dpi (days post inoculation) by ELISA (Figure 4).

Among these 41 mutant lines, 18 *AtRH* gene mutant lines, i.e., T-DNA insertion lines of *DRH1*, *AtRH11*, *AtRH16*, *AtRH18*, *AtRH20*, *AtRH21*, *AtRH24*, *AtRH30*, *AtRH31*, *AtRH33*, *AtRH37*, *AtRH40*, *AtRH41*, *AtRH46*, *AtRH53*, *AtRH57*, *STRS1*, and *STRS2* displayed higher CP accumulation compared to WT plants and were consistent with the enhanced severity of symptoms caused by TuMV infection. Those mutants exhibited more severe phenotypes, including stunted growth, yellowish and curled leaves, chlorotic and mosaic lesions and abnormal flower morphology. In contrast, TuMV CP accumulation in T-DNA insertion lines of *AtRH9*, *AtRH26* and *PRH75* were significantly lower than the level observed in WT plants. The attenuated symptoms in the systemically-infected plants of those mutant lines indicated that either viral replication or long-distance movement were affected. Intriguingly, ELISA results also revealed that



**Table 9 List of homozygous *Arabidopsis atrh* T-DNA insertion lines for ELISA analysis.**

<b>Gene name</b>	<b>Locus</b>	<b><i>Arabidopsis</i> T-DNA insertion lines</b>
RH1	AT4G15850	SALK_049805; CS839540
DRH1	AT3G01540	SALK_063362; SALK_073018
RH9	AT3G22310	SALK_035421; SALK_060677
RH10	AT5G60990	SALK_001503
RH11	AT3G58510	SALK_122885; SALK_138586
RH12	AT3G61240	SALK_024905; SALK_148563
RH16	AT4G34910	CS852120
RH18	AT5G05450	SALK_083512
RH20	AT1G55150	SALK_124308; SALK_114853
RH21	AT2G33730	SALK_100059; CS839970
RH22	AT1G59990	SALK_032399; SALK_065388
RH24	AT2G47330	SALK_087182; SALK_045730
RH26	AT5G08610	SALK_106823; CS832362
RH28	AT4G16630	SALK_012018; SALK_082807
RH30	AT5G63120	CS848715
RH31	AT5G63630	SALK_090068
RH33	AT2G07750	SALK_017083; SALK_119034
RH37	AT2G42520	SALK_099097
RH40	AT3G06480	SALK_056041
RH41	AT3G02065	SALK_020125; CS843411
RH46	AT5G14610	SALK_068359
RH53	AT3G22330	SALK_056387
RH57	AT3G09720	SALK_019721; SALK_143440
PRH75	AT5G62190	SALK_040389; SALK_068401
STRS1	AT1G31970	SALK_062509
STRS2	AT5G08620	SALK_028850

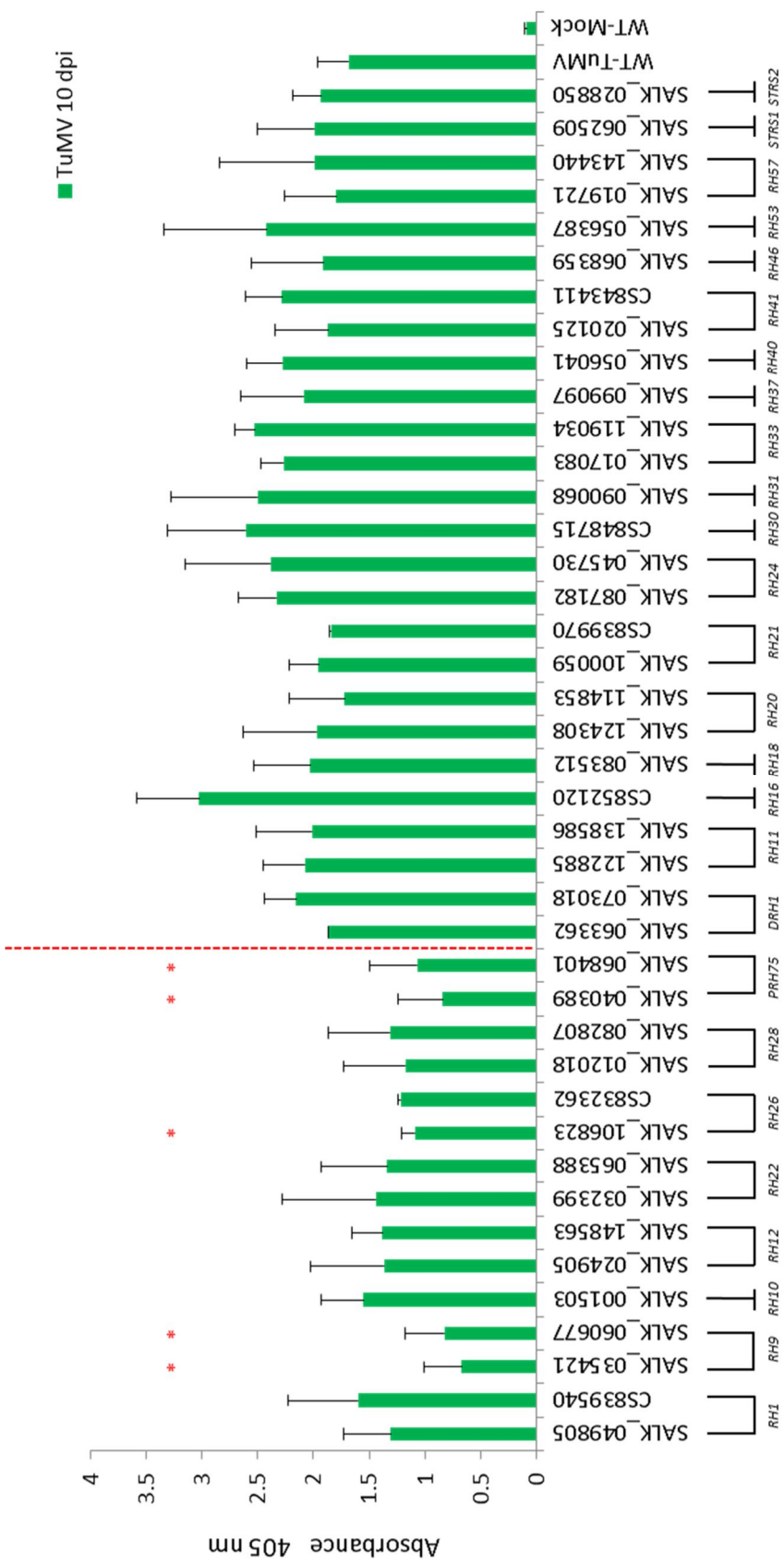


**Figure 4 ELISA analysis of candidate *Arabidopsis atrh* T-DNA mutants.**

A total of 41 homozygous *Arabidopsis* T-DNA insertion mutant lines corresponding to 26 *AtRH* genes were selected for TuMV infection assay. The *Arabidopsis atrh* T-DNA insertion mutants and WT plants were mechanically inoculated with TuMV. ELISA analysis was used to determine the accumulation of TuMV CP in *atrh* T-DNA mutants and WT plants. Extracts from newly-emerged leaves of TuMV-infected individual plants were subjected to ELISA using TuMV CP-specific antibody. The y-axis represents ELISA values at 10 days post inoculation (dpi). Error bars represent standard deviation ( $n \geq 5$ ). Asterisk indicates significant difference from WT plants (student's t test,  $p < 0.05$ ).

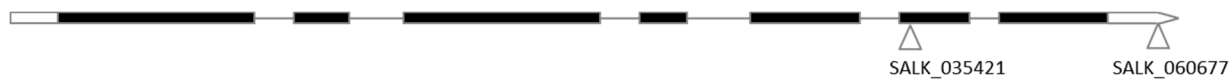
TuMV CP levels were reduced in newly-emerged leaves of T-DNA insertion lines of *AtRH1*, *AtRH10*, *AtRH12*, *AtRH22* and *AtRH28* relative to WT plants. But the reduction did not reach significant levels. TuMV-infected wild-type *Arabidopsis* plants displayed symptoms such as mottle and mosaics, leaf distortion, curled bolts and stunting, leaves at late infection stages developed necrotic lesions. Compared with WT plants, only mild disease symptoms were developed on the *Arabidopsis atrh9*, *atrh26* and *prh75* mutant plants, suggesting these *atrh* mutants conferred partial resistance against TuMV infection. These data also supported the biological relevance of the genes *AtRH9*, *AtRH26* and *PRH75* to TuMV infection. Thus, T-DNA insertion lines of *AtRH9*, *AtRH26* and *PRH75* were selected for further analysis.

### 3.2 Characterization of *Arabidopsis atrh9* T-DNA insertion line

#### 3.2.1 Verification of *Arabidopsis atrh9* T-DNA insertion line

Two *atrh9* T-DNA insertion lines were acquired and analyzed (Figure 5A and 5B). T-DNA insertion line SALK\_035421 contains a T-DNA insertion within Exon 6 of *AtRH9*, which recently has been confirmed to be a true knockout mutant on the basis of a Northern blot analysis (Köhler *et al.*, 2010). At3g22310-encoded protein was previously designated Putative Mitochondrial RNA Helicase1 (PMH1), and SALK\_035421 was named *pmh1-1* (Matthes *et al.*, 2007). In this thesis, SALK\_035421 was designated *atrh9* in consistency of the gene name *AtRH9* in the *AtRH* family (Aubourg *et al.*, 1999). A homozygous insertion in *atrh9* was identified using two gene-specific primers (LP+RP) to detect wild-type genotype and a gene-specific primer (RP) with a T-DNA specific primer (LB) to detect T-DNA insertion genotype (Figure 5C). Loss of transcript in *atrh9* was revealed by reverse transcription (RT)-PCR analysis using *AtRH9*-specific primers (Figure 5D). RT-PCR result was consistent with the published data (Köhler *et al.*, 2010). Another *AtRH9* T-DNA insertion line SALK\_060677 with a T-DNA insertion located in the 3' untranslated region (UTR), was genotyped as a homozygous line for *AtRH9* as well (Figure 5E). This mutant line is named *atrh9-1*. Since the insertion position of the T-DNA in this mutant was mapped to the 3' untranslated region, which suggested a likely knockdown expression, we did not test this mutant further.

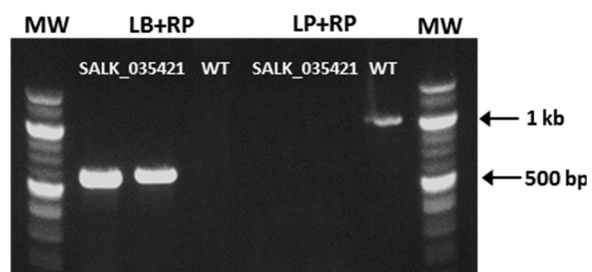
A.

AT3G22310 (*AtRH9*)

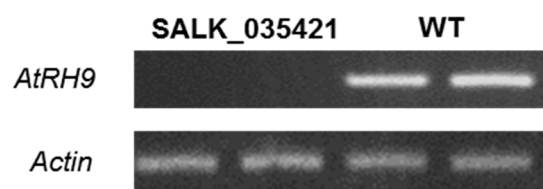
B.

Gene name	Locus	Salk line	T-DNA insertion sites
<i>AtRH9</i>	AT3G22310	SALK_035421.56.00.x SALK_060677.54.50.x	Exon 3' UTR

C.



D.



E.

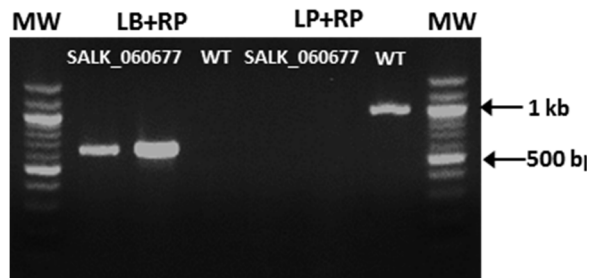


**Figure 5 Genotyping and RT-PCR analysis of *Arabidopsis atrh9* T-DNA insertion lines.**

(A) Schematic characterization of *AtRH9* and T-DNA insertion sites (triangles) in *Arabidopsis* T-DNA insertion mutants. Exons and introns are indicated by boxes and lines respectively. 5' and 3' untranslated regions are shown as open boxes.

(B) A summary of the two *Arabidopsis atrh9* T-DNA insertion lines.

(C) Screening for homozygous *atrh9* T-DNA insertion lines. PCR was conducted using genomic DNA from *atrh9* (SALK\_035421) and WT plants. Two gene-specific primers (LP+RP) were used to detect wild-type genotype. A T-DNA specific primer and a gene-specific primer (LB+RP) were used to amplify a single PCR fragment which represented the pattern of homozygous genotype. WT, wild-type *Arabidopsis*; LP, left genomic primer; RP, right genomic primer; LB, Left border primer of the T-DNA insertion.

(D) RT-PCR analysis of *AtRH9* expression in *atrh9* mutants and WT plants (SALK\_035421). RT-PCR was performed using cDNA derived from leaf tissues of *Arabidopsis atrh9* mutants and WT plants with *AtRH9* specific primers. *Actin2* (*Actin*) gene was used as an internal control.

(E) Screening for homozygous *atrh9-1* T-DNA insertion line, SALK\_060677. A single PCR product was amplified using genomic DNA from the mutant using a T-DNA specific primer and a gene-specific primer (LB+RP).

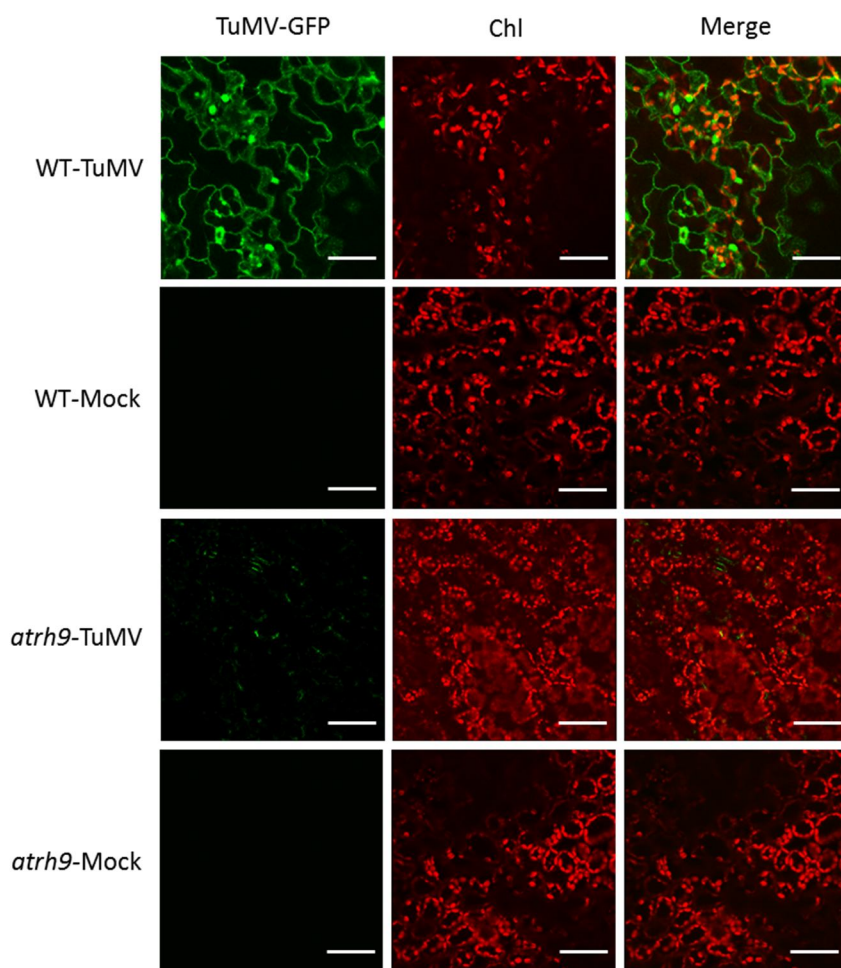
### 3.2.2 The accumulation of TuMV was reduced in *atrh9* mutant plants

Under standard growth conditions, *atrh9* mutant plants displayed no abnormal phenotypes distinguishable from *Arabidopsis* WT plants. To confirm the partial TuMV resistance in the *atrh9* mutant plants, three-week-old *atrh9* mutants and WT plants were agroinfiltrated with a GFP-tagged TuMV infectious clone (TuMV-GFP). To monitor TuMV infection in these plants, confocal microscopy was used to observe GFP fluorescence intensity. Strong signals of GFP fluorescence were observed in the newly-emerged leaves of infected WT plants, whereas only weak and scattered GFP fluorescence was detected in *atrh9* mutant plants at 10 dpi (Figure 6A). Real-time RT-PCR was carried out to quantify TuMV accumulation. In the *atrh9* mutant plants, TuMV viral accumulation showed a substantial decrease by 85% with respect to that in WT plants at 15 dpi (Figure 6B). In contrast to severe TuMV symptoms such as necrosis, chlorotic leaves and dwarfing developed on WT plants, *atrh9* mutant plants displayed very minor symptoms, such as curled bolts (Figure 6C). Taken together, these results suggest that *AtRH9* function is required for successful progression of TuMV infection.

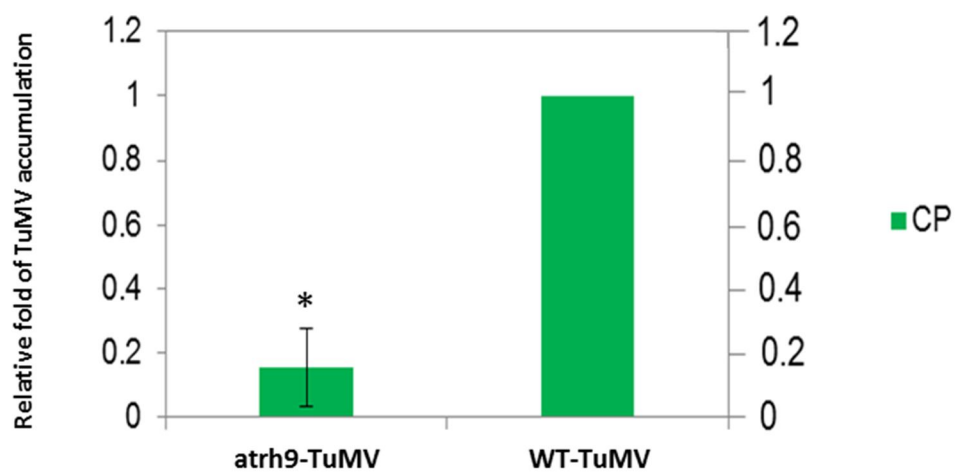
### 3.2.3 Knock down of *AtRH9* expression in *Arabidopsis* by VIGS

To further confirm the involvement of *AtRH9* in TuMV infection, a TRV-based VIGS was used to silence *AtRH9* expression in *Arabidopsis*. A cDNA fragment of *AtRH9* was cloned into a pTRV2-derived vector to produce pTRV2-*AtRH9*. *Arabidopsis* wild-type seedlings were co-agroinfiltrated with the vectors pTRV2-*AtRH9* and pTRV1. At 12 days post agroinfiltration, a bleaching phenotype was observed in control plants co-agroinfiltrated with pTRV2-PDS and pTRV1, indicating VIGS was established. At this time point, the TuMV infection assay was applied on *AtRH9*-downregulated plants (treated with pTRV2-*AtRH9* and pTRV1) as well as WT plants (treated with buffer) and negative control plants (treated with empty pTRV vectors). Real-time RT-PCR was performed to evaluate *AtRH9* expression and TuMV accumulation at 15 dpi (Figure 7A).

A.



B.





C.

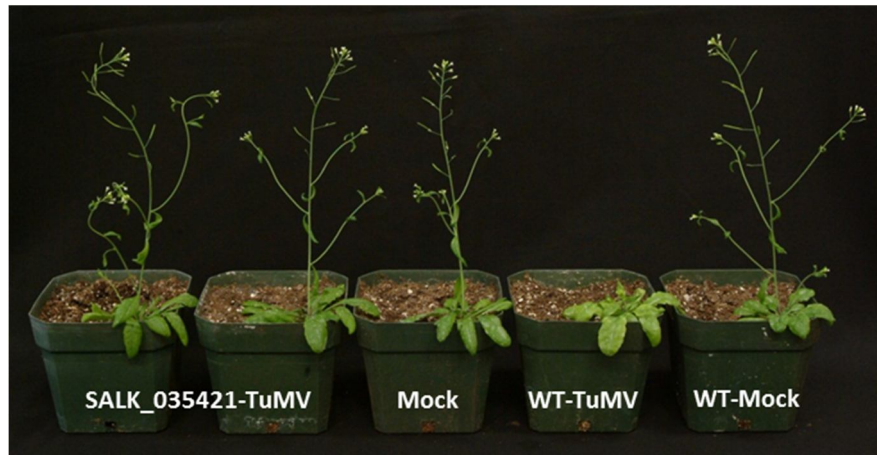


**Figure 6 TuMV accumulation was reduced in *atrh9* mutant plants.**

(A) Three-week-old *Arabidopsis atrh9* mutants (SALK\_035421) and WT plants were agroinfiltrated with TuMV-GFP infectious clone. Newly-emerged leaves were observed by confocal microscopy 10 days post infiltration, and representative images are shown. Mock, *atrh9* mutants and WT plants were agroinfiltrated with buffer. TuMV-GFP, green fluorescence emissions; Chl, chloroplast autofluorescence. Bars, 50  $\mu$ m.

(B) Relative fold changes of TuMV accumulation in *atrh9* mutant plants (SALK\_035421) by real-time RT-PCR at 15 dpi. RNA was extracted from newly-emerged leaves of infected individual plants at 15 dpi. Three independent experiments, each consisting of three biological replicates were carried out for quantification analysis. Each value was normalized against *Actin2* transcripts in the same sample. The values are presented as means of fold change relative to WT. Error bars represent standard deviation (n=9). Asterisk indicated significant difference from WT plants (student's t test,  $p < 0.05$ ).

(C) Phenotypes of TuMV-infected *atrh9* mutants and WT plants. Images were taken at 15 dpi. Mock, inoculated with buffer; TuMV, inoculated with TuMV.

The severely reduced level of the *AtRH9* transcript in *AtRH9*-downregulated plants was coupled with partial resistance to TuMV infection (Figure 7B). Consistent with the results from TuMV infection assays on the *atrh9* mutant plants, these data suggest that downregulation of *AtRH9* effectively inhibits TuMV infection in *Arabidopsis*.

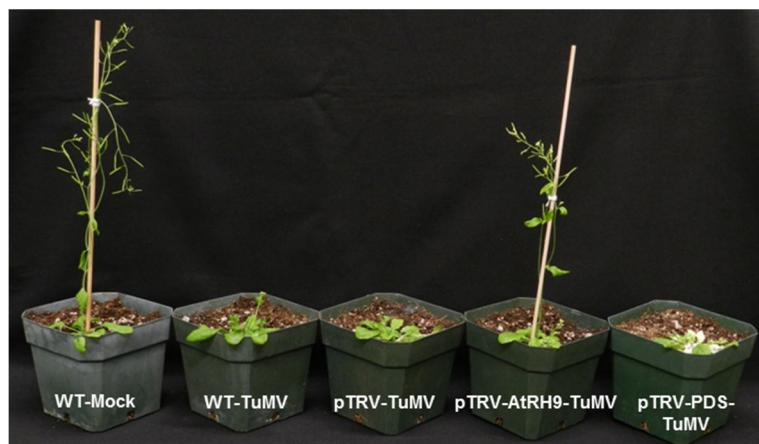
#### 3.2.4 Subcellular localization of Arabidopsis AtRH9

To gain insight into the molecular function of AtRH9 required for TuMV infection, subcellular localization analysis was performed. A translational fusion of AtRH9 with YFP controlled by the CaMV 35S promoter was transiently expressed in *N. benthamiana* leaf epidermal cells via agroinfiltration. Subcellular localizations of fusion proteins were monitored using a Leica TCS SP2 inverted confocal microscopy 48 h post agroinfiltration. Consistent with a previous study (Matthes *et al.*, 2007), AtRH9-YFP was observed mostly in the cytoplasm (Figure 8).

#### 3.2.5 Arabidopsis AtRH9 interacts with TuMV NIa-Pro *in planta*

To investigate if AtRH9 interacts with TuMV viral proteins *in vivo*, the BiFC assay was employed. The *AtRH9* gene and the coding sequence for each of the 11 TuMV viral proteins were introduced into BiFC vectors that contained DNA fragments encoding the N- or C-terminal half of YFP, respectively, and transiently co-expressed into *N. benthamiana* epidermal cells by co-agroinfiltration. The YFP signal would be emitted when split fluorescent protein segments were brought together as a result of positive interaction between two tested proteins. YFP signals were detected only when AtRH9 and NIa-Pro were co-expressed, suggesting AtRH9 interacts with NIa-Pro. The interaction was apparent in both the nucleus and cytoplasm, which was consistent with the known subcellular localization of NIa-Pro (Restrepo *et al.*, 1990). No YFP signal was observed in two negative control experiments (AtRH9-YC and YN, NIa-Pro-YN and YC) (Figure 9).

A.



B.

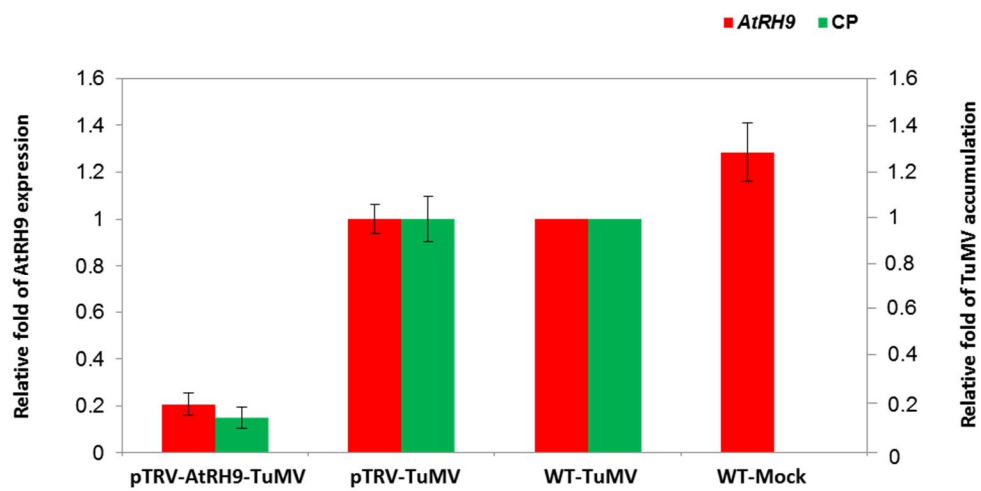


**Figure 7 Knockdown of *AtRH9* expression affects TuMV infection in *Arabidopsis*.**

(A) Phenotypes of TuMV-infected *AtRH9*-knockdown plants, empty VIGS vector-infiltrated plants and *Arabidopsis* WT plants. pTRV-PDS-TuMV, wild-type *Arabidopsis* plants infiltrated with TRV-based VIGS vectors targeting *phytoene desaturase* (*PDS*) to silence and then inoculated with TuMV; pTRV-*AtRH9*-TuMV, WT infiltrated with TRV-based VIGS vectors targeting *AtRH9* followed by inoculation with TuMV; pTRV-TuMV, WT infiltrated with empty TRV-based VIGS vectors and then inoculated with TuMV; WT-Mock, WT infiltrated with buffer and then inoculated with buffer; WT-TuMV, WT inoculated with TuMV. Images were taken 15 days post inoculation. TuMV, inoculated with TuMV. Mock, inoculated with buffer.

(B) Relative fold changes in TuMV accumulation and expression level of *AtRH9* in *AtRH9*-silenced *Arabidopsis* plants and WT plants. RNA was extracted from leaf tissues for real-time RT-PCR analysis at 15 dpi. Three independent experiments, each consisting of three biological replicates were carried out for quantification analysis. Target genes were normalized against *Actin2* transcripts in each sample. The values are presented as means of fold change relative to the WT plants. Error bars represent standard deviations.

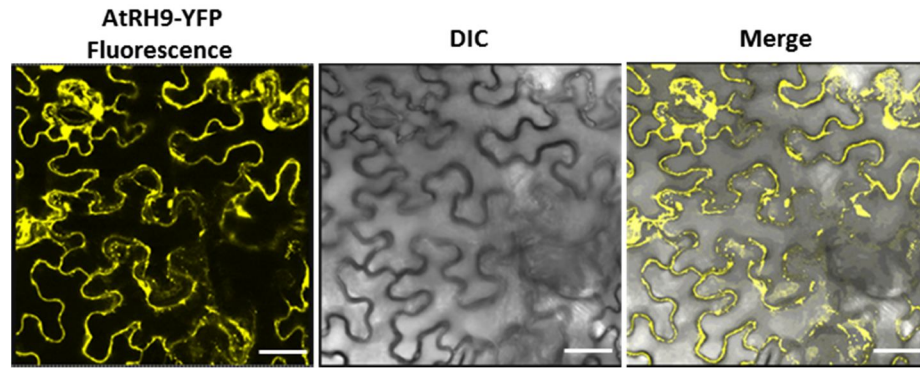


**Figure 8** Subcellular localization of *Arabidopsis* AtRH9.

Transient expression of AtRH9-YFP in *N. benthamiana* leaf epidermal cells. YFP fluorescence was observed using a confocal microscopy 48 h post agroinfiltration. DIC, differential interference contrast. Bars, 30  $\mu\text{m}$ .

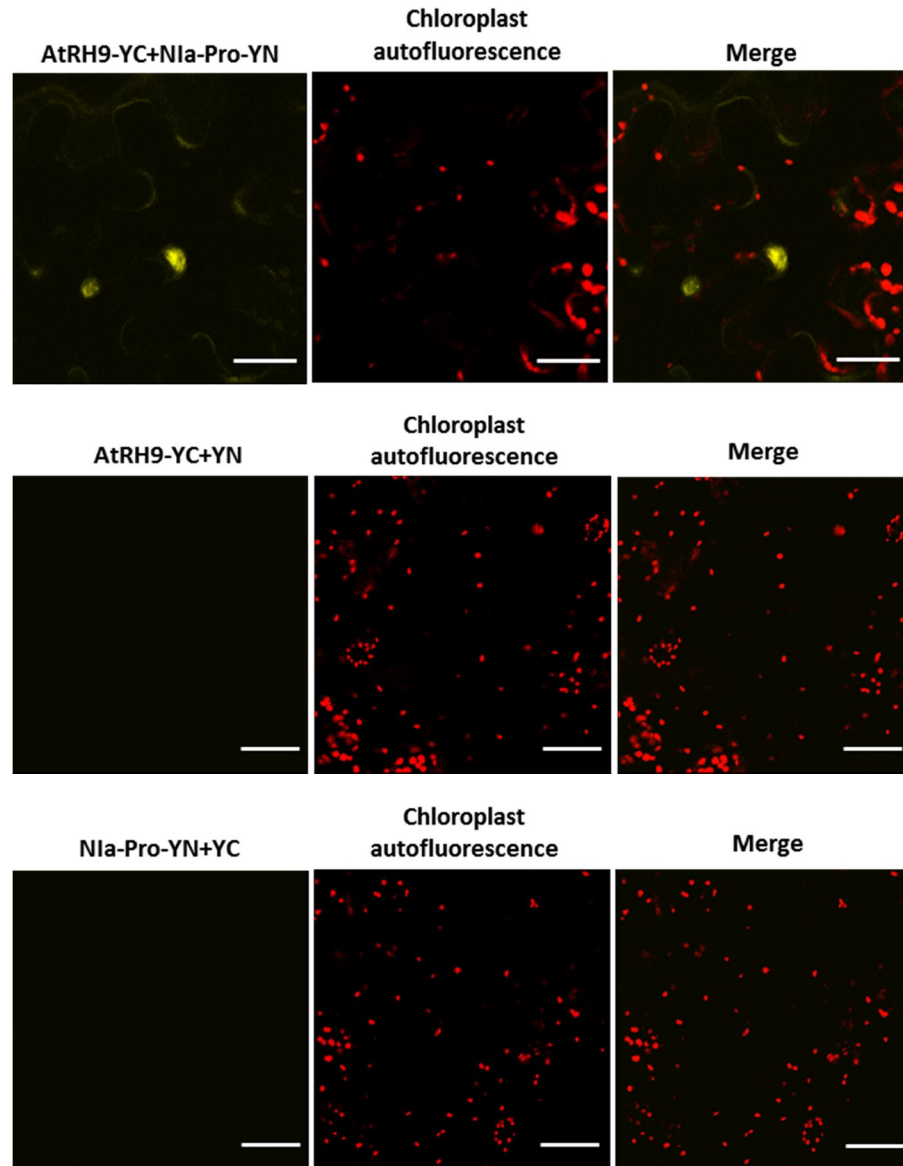


**Figure 9** The BiFC assay for detection of the interaction between AtRH9 and TuMV NIa-Pro *in planta*.

*N. benthamiana* leaves were co-agroinfiltrated with constructs expressing NIa-Pro and AtRH9 fused to the N- and C- terminal half of YFP, respectively. The reconstructed YFP fluorescence was recorded 48 h post agroinfiltration using a confocal microscopy. Leaves coexpressing with AtRH9-YC and YN or NIa-Pro-YN and YC were shown as negative controls. No YFP fluorescence was detected in negative controls. DIC, differential interference contrast. Bars, 35  $\mu$ m.

### 3.3 Characterization of *Arabidopsis atrh26* T-DNA insertion line

#### 3.3.1 Verification of *Arabidopsis atrh26* T-DNA insertion line

To verify the homozygosity of the *atrh26* T-DNA insertion line SALK\_106823, PCR-based genotyping and RT-PCR analysis were carried out. The T-DNA insertion in this mutant line was located in the promoter region of *AtRH26* (Figure 10A). Essentials of

PCR genotyping as described earlier were conducted to identify the T-DNA insertion genotype (Figure 10B). PCR genotyping results were consistent in two generations. Therefore, the mutant obtained was confirmed as a homozygous T-DNA insertion line, and was named *atrh26*. RT-PCR of RNA isolated from *atrh26* leaf tissue failed to amplify the corresponding full-length *AtRH26* mRNA using gene-specific primers. This result further supports that the *atrh26* represents a homozygous knockout mutant line (Figure 10C).

#### 3.3.2 *Arabidopsis AtRH26* is necessary for TuMV infection

*Arabidopsis atrh26* mutant plants exhibited normal growth and development under standard growth conditions (Figure 10D). The involvement of *AtRH26* in TuMV infection was evaluated by analyzing the susceptibility of *Arabidopsis atrh26* mutants to TuMV infection. After inoculation with TuMV, *atrh26* mutant plants showed mild symptoms compared with the TuMV-infected WT plants (Figure 10E).

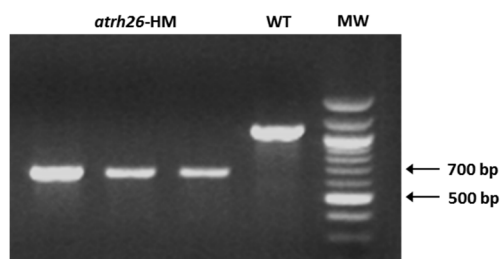
#### 3.3.3 Subcellular localization of *Arabidopsis AtRH26*

To localize *AtRH26*, a plant expression vector containing the coding sequence for *AtRH26* tagged with the CFP controlled by the CaMV 35S promoter was agroinfiltrated into *N. benthamiana* leaf epidermal cells. *AtRH26*-CFP signal was visualized by a confocal microscopy 48 h post agroinfiltration. *AtRH26*-CFP was found in the nucleus and cytoplasm (Figure 11).

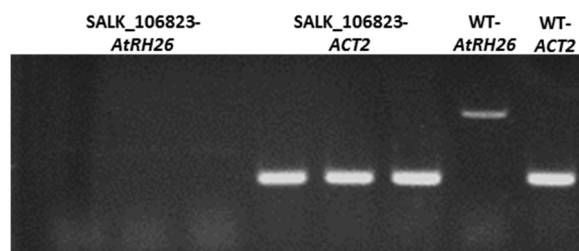
A.

AT5G08610 (*AtRH26*)

B.



C.



D.



E.

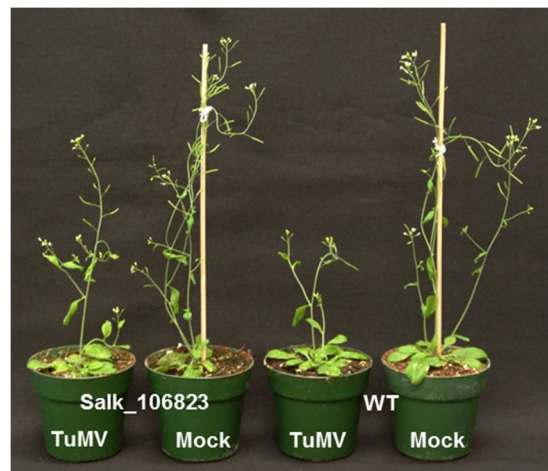




**Figure 10 Characterization of homozygous *Arabidopsis atrh26* T-DNA insertion line.**

(A) Schematic characterization of *AtRH26* and T-DNA insertion sites (triangles) in *Arabidopsis* T-DNA insertion mutants. Exons and introns are indicated by boxes and lines, respectively. 5' and 3' untranslated regions are shown as open boxes.

(B) Genotyping of *Arabidopsis atrh26* T-DNA insertion mutants (SALK\_106823). PCR was conducted using genomic DNA to amplify a single DNA fragment, which corresponds to the homozygous genotype or a single DNA product from WT plant as a control.

(C) RT-PCR analysis of the expression of *Arabidopsis AtRH26* in WT and *atrh26* T-DNA insertion line (SALK\_106823). RT-PCR was performed using cDNA derived from leaf tissues of *atrh26* mutants and WT plants with *AtRH26* gene-specific primers. *Actin2* (*ACT2*) gene was used as an internal control.

(D) Four-week-old of *atrh26* T-DNA insertion mutants and WT plants.

(E) *Arabidopsis atrh26* mutants and WT plants inoculated with TuMV or buffer. TuMV, inoculated with TuMV. Mock, inoculated with buffer. Photos were taken at 10 dpi.

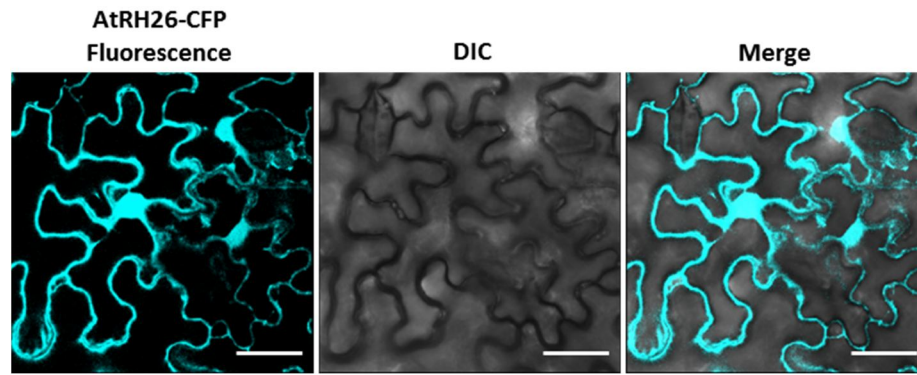


**Figure 11** Subcellular localization of *Arabidopsis* AtRH26.

Transient expression of AtRH26-CFP in *N. benthamiana* leaf epidermal cells. CFP fluorescence was observed using a confocal microscopy 48 h post agroinfiltration. DIC, differential interference contrast. Bars, 30  $\mu\text{m}$ .

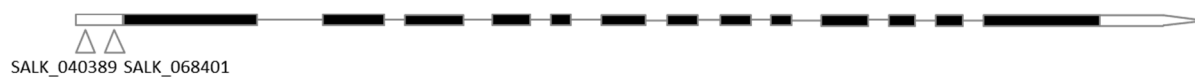
### 3.4 Characterization of *Arabidopsis prh75* T-DNA insertion line

In a recent published report, *PRH75* was shown to be essential for *Arabidopsis* embryo development, implying that there are no knockout T-DNA insertion mutants available for *PRH75* (Nayak *et al.*, 2013). The T-DNA insertion line SALK\_040389 harbors a T-DNA insertion in the 5' UTR region of *PRH75*, 56 bp upstream from the start codon, and was named *prh75* (Figure 12A and 12B). PCR-based genotyping indicated that the mutant line was homozygous (Figure 12C). To determine if this homozygous mutant line is a knockout line, RT-PCR was conducted to examine *PRH75* expression. Although T-DNA insertion did not abolish *PRH75* expression, it indeed remarkably reduced *PRH75* expression when compared with WT plants (Figure 12D). Thus, the T-DNA insertion line *prh75* used in this study is a knockdown mutant line. The down-regulation of *PRH75* expression is likely due to position effect, since T-DNA was inserted in the 5' untranslated region. Knockdown of *PRH75* expression does not result in any apparent change during plant growth and development, and *prh75* mutant plants are morphologically indistinguishable from wild-type plants. Another T-DNA insertion line, SALK\_068401, containing a T-DNA insertion 10 bp upstream of the translation start site of *PRH75* was also included in TuMV infection assay. The homozygous plants were identified by PCR analysis. PCR-based genotyping analysis showed that SALK\_068401 is a homozygous T-DNA insertion line (Figure 12E). RT-PCR analysis revealed that this line is also an expression knockdown mutant line (Figure 12F). This mutant line is named *prh75-1*. The T-DNA insertion in both lines was verified by sequencing analysis of genomic DNA.

#### 3.4.1 *PRH75* was required for TuMV infection

To determine if there is a correlation between the lack of *PRH75* and debilitation of TuMV infection, *Arabidopsis prh75* and WT plants were agroinfiltrated with TuMV-GFP. Confocal microscopy was employed to observe GFP expression levels in order to validate the susceptibility of those mutant plants to TuMV infection. Strong GFP fluorescence was observed in the newly-emerged leaves of infected WT plants whereas only weak GFP fluorescence was detected in *prh75* mutant plants at 10 dpi (Figure 13A).

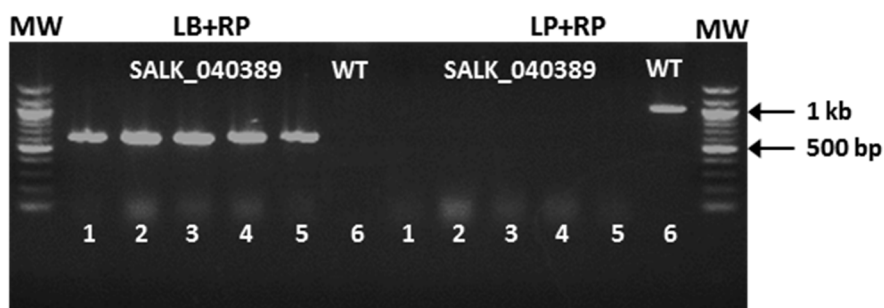
A.

AT5G62190 (*PRH75*)

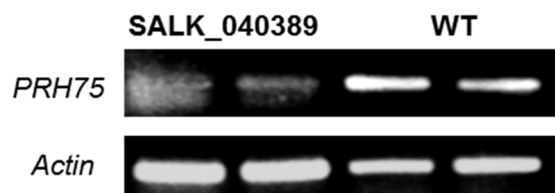
B.

Gene name	Locus	Salk line	T-DNA insertion sites
<i>PRH75</i>	AT5G62190	SALK_040389.55.25	5' UTR
		SALK_068401.35.25.x	5' UTR

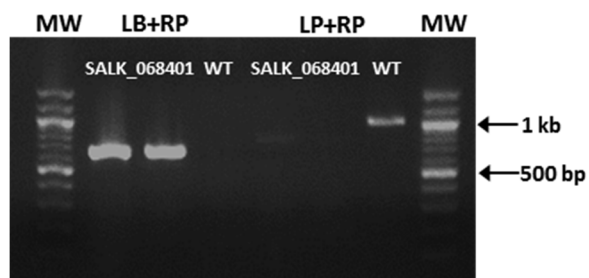
C.



D.



E.



F.

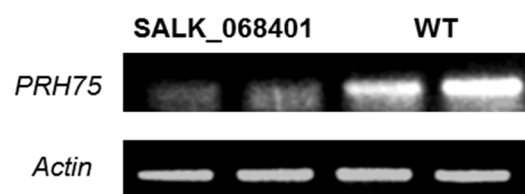


**Figure 12 Genotyping and RT-PCR analysis of *Arabidopsis prh75* T-DNA insertion lines.**

(A) Schematic characterization of *PRH75* and T-DNA insertion sites (triangles) in *Arabidopsis* T-DNA insertion mutants. Exons and introns are indicated by boxes and lines respectively. 5' and 3' untranslated regions are shown as open boxes.

(B) A summary of two *prh75* T-DNA insertion mutant lines used in this study.

(C) Screening for the homozygous *Arabidopsis prh75* T-DNA insertion lines. PCR was conducted using genomic DNA from *prh75* (SALK\_040389) and WT plants. Two gene-specific primers (LP+RP) were used to detect wild-type genotype. A T-DNA specific primer and a gene-specific primer (LB+RP) were used to amplify a single PCR product which represented the pattern of homozygous genotype. WT, wild-type *Arabidopsis*; LP, left genomic primer; RP, right genomic primer; LB, Left border primer of the T-DNA insertion.

(D) RT-PCR analysis of *PRH75* expression in *prh75* mutants (SALK\_040389) and WT plants. RT-PCR was performed using cDNA derived from leaf tissues of *Arabidopsis prh75* mutants and WT plants with *PRH75* specific primers. *Actin2* (*Actin*) was used as an internal control.

(E) Screening for the homozygous *Arabidopsis prh75* T-DNA insertion line, SALK\_068401. A single PCR product was amplified using genomic DNA from leaf tissues using a T-DNA specific primer and a gene-specific primer (LB+RP).

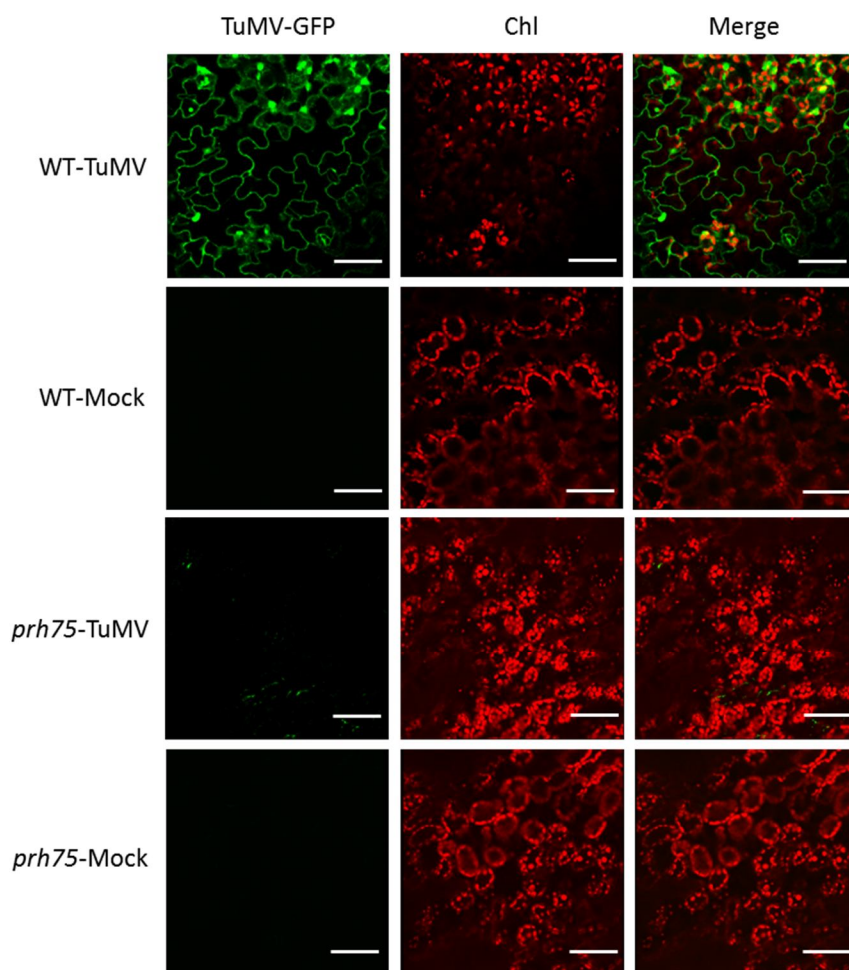
(F) RT-PCR analysis of *PRH75* expression in *prh75-1* mutants (SALK\_068401) and WT plants. RT-PCR was performed using cDNA derived from leaf tissues of *prh75-1* mutants and WT plants with *PRH75* specific primers. *Actin2* (*Actin*) was used as an internal control.

TuMV accumulation in *prh75* mutants and WT plants was monitored by real-time RT-PCR. TuMV viral RNA accumulation decreased significantly in *prh75* mutant plants in comparison with that in WT plants at 15 dpi (Figure 13B). Consistent with the decreased TuMV accumulation, no severe TuMV-induced symptoms developed in *prh75* mutant plants (Figure 13C). Therefore, knockdown of *PRH75* leads to resistance to TuMV infection. Altogether, these data strongly indicate that *PRH75* is essential for TuMV infection in *Arabidopsis*.

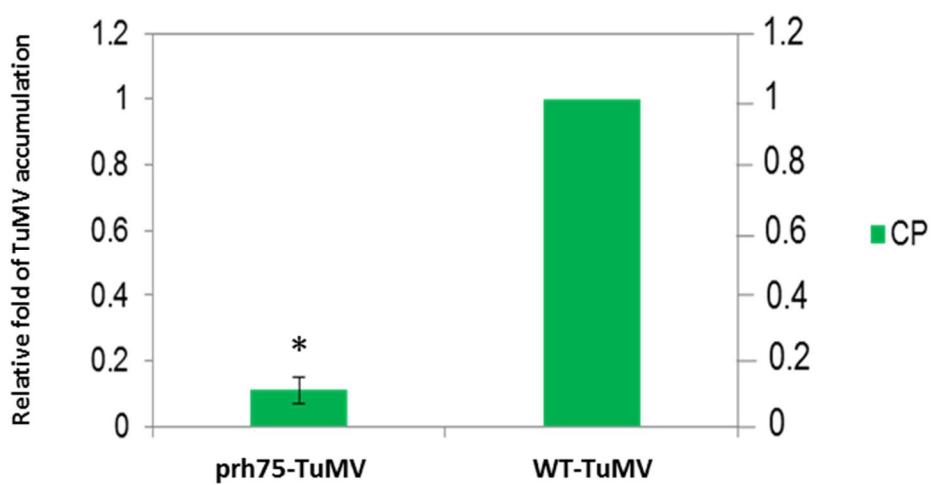
### 3.4.2 Silencing of *PRH75* in *Arabidopsis* by VIGS confers resistance to TuMV

Given that knockout mutants are not available for *PRH75*, VIGS was employed to knock down the expression of *PRH75* in *Arabidopsis* in order to further confirm its requirement for TuMV infection. A cDNA fragment of *PRH75* was cloned into a pTRV2-derived vector, and *Arabidopsis* WT plants were co-agroinfiltrated with the resulting pTRV2-*PRH75* together with pTRV1. After VIGS was established 12 days post agroinfiltration, the infiltrated plants were mechanically inoculated with TuMV. Real-time RT-PCR was performed to detect *PRH75* mRNA abundance and TuMV accumulation at 15 dpi. The amount of *PRH75* mRNA in treated plants was greatly reduced when compared with negative control plants which were co-agroinfiltrated with empty pTRV2 and pTRV1 vectors (Figure 14A). *PRH75*-knockdown *Arabidopsis* plants showed weak TuMV symptoms, such as curled bolts and were slightly shorter in height. In contrast, mock-treated plants (treated with buffer) and negative control plants (treated with empty pTRV vectors) were highly susceptible to TuMV and showed severe typical TuMV infection symptoms such as stunted growth and chlorosis and necrosis (Figure 14B). These data suggest that silencing of *PRH75* confers resistance to TuMV infection, consistent with the results that the *prh75* mutant is resistant to TuMV infection (Figure 13).

A.



B.



C.

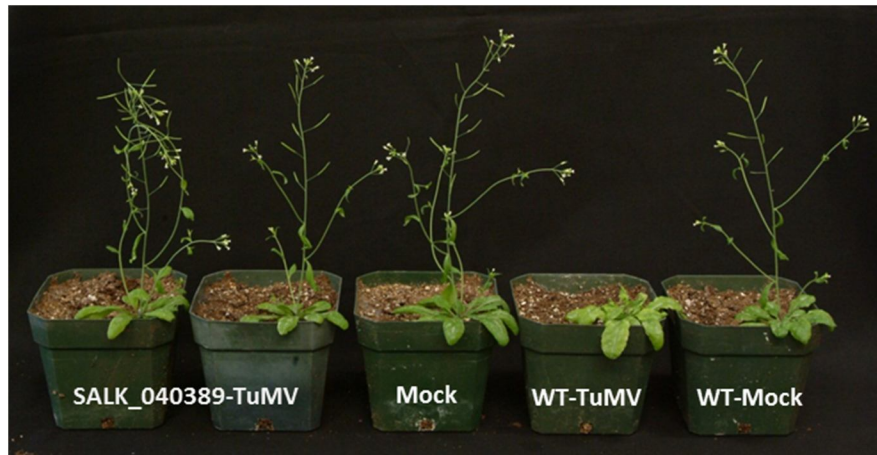


**Figure 13 Relative TuMV accumulation in *prh75* mutant and wild-type plants.**

(A) Confocal images of newly-emerged leaves of TuMV-infiltrated *prh75* mutants and *Arabidopsis* WT plants at 10 days post infiltration. TuMV, *prh75* mutants and WT plants agroinfiltrated with TuMV-GFP. Mock, plants agroinfiltrated with buffer; TuMV-GFP, green fluorescence emissions; Chl, chloroplast autofluorescence. Bars, 50  $\mu$ m.

(B) Real-time RT-PCR of TuMV accumulation in *prh75* mutants and WT plants. RNA was extracted from newly-emerged leaves of infected *prh75* mutants (SALK\_040389) at 15 dpi. Three independent experiments, each consisting of three biological replicates, were carried out for quantification analysis. TuMV accumulation level was normalized against *Actin2* transcripts in the same sample and the means of fold change was calculated relative to the TuMV level in WT plants. Error bars represent standard deviation (n=9). Asterisk indicates significant difference from WT plants (student's t test,  $p < 0.05$ ).

(C) Phenotypes of TuMV-infected *prh75* mutants and WT plants. Images were taken at 15 dpi. Mock, inoculated with buffer; TuMV, inoculated with TuMV.



A.



B.

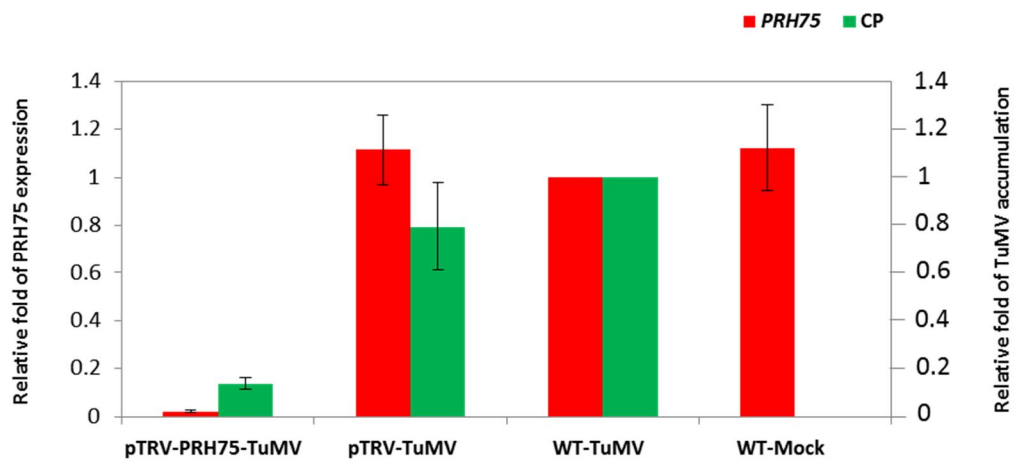


**Figure 14 *PRH75*-silenced plants exhibit partial resistance to TuMV infection.**

(A) Symptoms of TuMV-infected *PRH75*-silenced plants, empty VIGS vector-infiltrated plants and WT plants. pTRV-PDS-TuMV, *Arabidopsis* WT plants infiltrated with TRV-based VIGS vectors targeting *PDS* to silence and then inoculated with TuMV; pTRV-*PRH75*-TuMV, *Arabidopsis* WT plants infiltrated with TRV-based VIGS vectors targeting *PRH75* and then inoculated with TuMV; pTRV-TuMV, *Arabidopsis* WT plants infiltrated with empty TRV-based VIGS vectors and then inoculated with TuMV; WT-Mock, *Arabidopsis* WT plants infiltrated with buffer then inoculated with buffer; WT-TuMV, *Arabidopsis* WT plants inoculated with TuMV. Images were taken at 15 dpi. TuMV, inoculated with TuMV; Mock, inoculated with buffer.

(B) Relative fold changes of TuMV accumulation and *PRH75* expression in *PRH75*-silenced and WT plants. RNA was extracted 15 days post inoculation for real-time RT-PCR analysis. Three independent experiments, each consisting of three biological replicates, were carried out for quantification analysis. Target genes were normalized against *ActinII* transcripts in each sample. The values are presented as means of fold change relative to WT plants. Error bars represent standard deviations.

### 3.5 Molecular characterization of PRH75 and TuMV interactions

#### 3.5.1 The DEAD-box RNA helicase PRH75 is conserved in many plants.

PRH75 is a DEAD-box RNA helicase that has been found in many plant species such as spinach (*Spinacia oleracea*) and mung bean (*Vigna radiate*) (Lorković *et al.*, 1997; Li *et al.*, 2001). BLASTX searches of the NCBI database revealed a number of plant proteins with sequence and structure similarities to PRH75 of *Arabidopsis*. The 12 proteins showing the highest similarity to PRH75 were from the following species: *Capsella rubella*, *Camelina sativa*, *Brassica rapa*, *Eutrema salsugineum*, *Arabis alpine*, *Brassica napus*, *Tarenaya hassleriana*, *Vitis vinifera*, *Jatropha curcas*, *Eucalyptus grandis*, *Cicer arietinum* and *Citrus clementina*. A multi-sequence alignment of corresponding motifs of PRH75 against homologs from different plant species was conducted using the CLUSTAL W program. The alignment result demonstrated that PRH75 shares all the 13 conserved motifs associated with DEAD-box RNA helicases, i.e., motif Q, I, Ia, Ib, Ic, II, III, IV, IVa, V, Va, Vb and VI (Figure 15).

The full-length cDNA of *Arabidopsis PRH75* is 2384 bp in length containing an ORF of 2016 bp which encodes a polypeptide of 671 amino acids (aa), a 94-bp 5' UTR and a 274-bp 3' UTR (Figure 16A). A conserved domain analysis of *Arabidopsis PRH75* using the NCBI structure program (<http://www.ncbi.nlm.nih.gov/Structure/index.shtml>) identified the DEAD-box signature (aa 115 to 304), the helicase conserved domain (aa 376 to 441), and the GUCT domain that is considered as an RNA-binding domain at the C-terminus (aa 530 to 612) (Figure 16B).

Based on structural and functional similarity of conserved motifs, PRH75 motifs Q, I, II and VI are required for ATP binding and hydrolysis, whereas motifs Ia, Ib, Ic, IV, IVa and V are suggested to be responsible for RNA-binding (Rocak and Linder, 2004). Motifs III and Va are assumed to coordinate ATPase and unwinding activities (Tanner *et al.*, 2003) (Figure 16C). Recently, *Arabidopsis PRH75* has been demonstrated to exhibit the capacity for RNA unwinding with RNA duplexes in an ATP-dependent manner (Nayak *et al.*, 2013).

		<b>Q</b>	
CrDDX	LG--AEDVEVD-----NPNASKFRISPLREKLKER	GIEALFPIQ	ATTFFDMVLDGAD 135
CsDDX	LG--IEDVEVD-----NPNVSKFRISAPLREMLKKN	GIEALFPIQ	ATTFFDMVLDGAD 141
PRH75	LG--VEDVEVD-----NPNVSKFRISAPLREKLKAN	GIEALFPIQ	ASTFFDMVLDGAD 135
BrDDX	LS-VVEDVKVVE-----NPNVSKFRISDPLREKLKEK	GIEALFPIQ	ATTFFDMVLDGAD 141
BnDDX	LSSSVEDVKVD-----NPNVSNFRISDPLKAKLKEK	GIEALFPIQ	ATTFFDMVLDGAD 126
EsDDX	LG--VEDVEVD-----NPNVSRFRISAPLREKLKQK	GIEALFPIQ	AMTFDMVLDGAD 148
AaDDX	VG--VEDVVVD-----NPNVSKFRISDPLREQLKKK	GIEALFPIQ	AMTFDMVLDGAD 149
ThDDX	VD---EEEEEE-----NPNVTKFRISTPVVNLKKEK	GIAALFPIQ	AMTFDMVLDGSD 148
VvDDX	EME-EEEGKAE-----ENPNALSNFRISEPLREKLKSK	GIEALFPIQ	AMTFDTILDGSD 158
CcDDX	KVE-PEAGVEEQERGESEHPNAVSRFRISVPLREKLKSK	GIESLFPIQ	AMTFDMVLDGSD 148
EgDDX	DGD-DEVAQEE-----NPNVSNFRISDSLRLKLDNK	IEALFPIQ	AMTFDIVLDGTD 165
JcDDX	KLDEDEEEEGEREVAKAEDPNATSKFRISLPLREKLKSR	GIEALFPIQ	AMTFNDILDGCD 162
CaDDX	KVEDDDDEE-EVAVVKDDPNAVTFNFRISEPLKMKLKEK	GIEALFPIQ	AMTFNTILDGSD 144

	<b>I</b>		<b>Ia</b>	
CrDDX	LVGRARTGQGKTLAFVLP	ILES	LINGPAKSKKNGYGRPPSVLVLI	PTRELAKQVAADF 195
CsDDX	LVGRARTGQGKTLAFVLP	ILES	LINGPAKSKKNGYGRPPSVLVLI	PTRELAKQVNADFE 201
PRH75	LVGRARTGQGKTLAFVLP	ILES	LINGPAKSKRKMGYGRSPSVLVLI	PTRELAKQVAADF 195
BrDDX	LVGRARTGQGKTLAFVLP	ILES	LINGPAKNKRKNGYGRPPSVLVLI	PTRELAKQVFADF 201
BnDDX	LVGRARTGQGKTLAFVLP	ILES	LINGPAKSKRKNYGRPPSVLVLI	PTRELAKQVFADFE 186
EsDDX	LVGRARTGQGKTLAFVLP	ILES	LINGPAQSKRKNYGRPPSVLVLI	PTRELAKQVFADFE 208
AaDDX	LVGRARTGQGKTLAFVLP	ILES	LINGPAKSKRKNYGRPPSVLVLI	PTRELAKQVYSDFE 209
ThDDX	LVGRARTGQGKTLAFVLP	ILES	TNGPSNASRKTGYGRPPSVLVLI	PTRELAKQVFADF 208
VvDDX	LVGRARTGQGKTLAFVLP	ILES	LINGPNRGSRKTGYGRPPCVLVLI	PTRELATQVYADF 218
CcDDX	LVGRARTGQGKTLAFVLP	ILES	TNGPTKASKKTGYGRAPSVLVLI	PTRELAKQVHEDFD 208
EgDDX	LVGRARTGQGKTLAFVLP	LES	TNGPAKTSRKTGYGRPPSVLVLI	PTRELAKQVFSDFE 225
JcDDX	LVGRARTGQGKTLAFVLP	ILES	TNGPAKASRKTGYGRPPSVLVLI	PTRELACQVYDDFK 222
CaDDX	LVGRARTGQGKTLAFVLP	ILES	TNGPAKSVRKTGYGRVPSVLVLI	PTRELANQVYADFE 204

		<b>Ib</b>		<b>Ic</b>		<b>II</b>	
CrDDX	VYGASVGLTSCCLYGG	DSY	TGQEQYKLRGVDIVVG	TPGR	IKDHIERQNIDL	SHLQFRVLD	255
CsDDX	TYGLALGLTSCCVYGG	EGYSFQ	NSLRKGVDIVVG	TPGR	VKDFINTEKID	LSYLQFRVLD	261
PRH75	AYGGSGLLSSCCLYGG	DSYPVQ	EGKLRGVDIVVG	TPGR	IKDHIERQNLD	FSYLQFRVLD	255
BrDDX	AYGGSVGLTSCCVYGG	DPYPPQ	QKLRGVDIVVG	TPGR	IKDHIERQNLD	TYLQFRVLD	261
BnDDX	AYGGAVGLASCCVYGG	DPYAPQ	ERKLRGVDIVVG	TPGR	IKDHIERNLD	TYLQFRVLD	246
EsDDX	AYGGAVGLTSCCVYGG	DPYQPE	YKLRGVDIVVG	TPGR	IKDHIERQNLD	LSYLQFRVLD	268
AaDDX	SYGGSVGLSSCCIYGG	DPYAPQ	EHKLRGVDIVG	TPGR	IKDHLEKGLD	TYLQFRVLD	269
ThDDX	VYGGAVGLSSCCLYGG	DSYQPE	YKLRGVDIVVG	TPGR	IKDHIERGNID	SFLKFRVLD	268
VvDDX	VYGGAIGLTSCCLYGG	APYQAE	IKLRGVDIVVG	TPGR	IKDHIERGNID	FSSLKFRVLD	278
CcDDX	VYGGAVGLTSCCLYGG	APYHAQ	EFLKKGIDVIG	TPGR	IKDHIERGNID	SLLKFRVLD	268
EgDDX	VYGGAVGLTSCCLYGG	APYHAQ	ESHLRRGVDIVIG	TPGR	VKDHIERGNID	LSSLTFRVLD	285
JcDDX	VYGEALGLTTCCLYGG	ASYHPQ	ETSLKRGVDVVG	TPGR	IKDHIERGNID	SLLKFRVLD	282
CaDDX	VYGSSLGLVACAVYGG	APYGAQ	ESKLRRGVDIVIG	TPGR	VKDHIERGNID	SHLKFRVLD	264

	<b>II</b>		<b>III</b>	
CrDDX	EAEMLRMGFVEDVELILGK	VEDATKVQTLLE	SATLPSWVKNISTR	FLKRDQKTIDL VGN 315
CsDDX	EAEMLRMGFVEDVEFILGK	VEDATKVQTLLE	SATLPQWVQSISR	KFLKDLKTIDL VGN 321
PRH75	EAEMLRMGFVEDVELILGK	VEDSTKVQTLLE	SATLPSWVKNISNR	FLKRDQKTIDL VGN 315
BrDDX	EAEMLRMGFVDDVELILGK	VEDPKKVQTLLE	SATLPSWVQNIASR	FLKQDKKTIDL VGN 321
BnDDX	EAEMLRMGFVDDVELILGK	VEDPKKVQTLLE	SATLPSWVQTIAR	FLKQDKKTIDL VGN 306
EsDDX	EAEMLRMGFVDDVELILGK	VEDPKKVQTLLE	SATLPSWVQKIAA	RFLKPEKKTIDL VGN 328
AaDDX	EAEMLRMGFVEEVELILGK	VEDPKKVQTLLE	SATLPTWVKNIAA	KFLKPDRELIDL VGN 329
ThDDX	EAEMLRMGFVEDVELILGK	VQDATKVQTLLE	SATLPDWVKNISSR	FLKPNKKTIDL VGN 328
VvDDX	EAEMLRMGFVEDVELILGK	VEDVSKVQTLLE	SATLPGWVKEISSR	FLKPTLKTADLVGN 338
CcDDX	EAEMLRMGFVEDVELILGK	VEDANKVQTLLE	SATLPSWVKHISTK	FLKSDKKTIDL VGN 328
EgDDX	EAEMLRMGFVEDVELILGK	VKDTSKVQTLLE	SATLPDWVKGISSR	FLKQNKRTIDL VGN 345
JcDDX	EAEMLRMGFVEDVELILGK	VEDVSKVQTLLE	SATLPDWVKHISTR	FLKPSKKTIDL VGN 342
CaDDX	EAEMLRMGFVDDVELILGK	VQVTKVQTLLE	SATLPSWVKQISSK	FLKADKQADLVGN 324

		<b>IV</b>	
CrDDX	DKMKASNSVRHIAIPCNKAAMSRLIPDIIISCYSSGGQTII	FTEK	KKEEASQLSGLLAGSRA 375
CsDDX	DKMKASNSVRHIAIPCNKAAMPRLIPDIIISCYSSGGQTII	FAEK	KKEEANELSGLLAGSRT 381
PRH75	DKMKASNSVRHIAIPCNKAAMARLIPDIIISCYSSGGQTII	FAET	KVQVSELSGLLDGSRA 375
BrDDX	DKMKASNSVRHIALPCSKQAMSRLIPDIIISLYSSGGSTII	FTET	KDQASELSGLLPGARA 381
BnDDX	DKMKASNSVRHIALPCNKQAMSRLIPDIIISLYSSGGSTII	FTET	KDQASELSGLLPGARA 366
EsDDX	DKMKASNSVRHICLPCSKQAMSRLIPDIIISCYSSGGNTII	FTET	KDQASELSGLLPGARP 388
AaDDX	DKMKASNSVRHIALPCSRQAMSRLIPDIIISCYSSAGSTII	FTET	KDHASELSGLLPASRA 389
ThDDX	AKMKASTNVRHIVLPCNKQAMSRLIPDVIRCYSSGGRTII	FTET	KDSASELSGLLPGARA 388
VvDDX	EKMKASTNVRHIVLPCSSARSQVIPDVIRCYSSGGRTII	FTET	KDSASELAGLLPGARA 398
CcDDX	EKMKASTNVRHIVLPCSSARSQVIPDIIRCYSSGGRTII	FTET	KESASQLADLLPGARA 388
EgDDX	EKMKASTNVRHIVIPCTSAARPOLIPDIIIRCYSSGGRTII	FTET	KECASQLSGLLPGARP 405
JcDDX	EKMKASTNVRHIVLPCSASAI SQLIPDIIIRCYSSGGRTII	FTEK	RESANELAGLLHGARA 402
CaDDX	EKMKASTNVRHII LPCNSTARAQLIPDIIIRCYSSGGRTII	FTEK	KESASELAGMLPGARA 384

	<b>IVa</b>	<b>V</b>	<b>Va</b>	<b>Vb</b>	<b>VI</b>	
CrDDX	LHGDIQSSQREVTLAGFRNGKFS	TLVATNVA	ARGLD	INDVQLII	QCEPPREVEAYIHRSG	435
CsDDX	LHGDIQSSQREVTLAGFRKGF	TLVATNVA	ARGLD	INDVQLII	QCEPPRDVESYIHRSG	441
PRH75	LHGEIIPSSQREVTLAGFRNGKFA	TLVATNVA	ARGLD	INDVQLII	QCEPPREVEAYIHRSG	435
BrDDX	LHGDIQSSQREITLAGFRKGF	TLVATNVA	ARGLD	INDVQLII	QCEPPRDVEDYIHRSG	441
BnDDX	LHGDIQSSQREITLAGFRKGF	TLVATNVA	ARGLD	INDVQLII	QCEPPRDVEDYIHRSG	426
EsDDX	LHGDIQSSQREVTLAGFRKGF	TLVATNVA	ARGLD	INDVQLII	QCEPPRDVEDYIHRSG	448
AaDDX	LHGDIQSSQREVTLAGFRKGF	TLVATNVA	ARGLD	INDVQLII	QCEPPRDVEDYIHRSG	449
ThDDX	LHGDIQSSQREVTLAGFRKGF	TLVATNVA	ARGLD	INDVQLII	QCEPPRDVEAYIHRSG	448
VvDDX	LHGDIQSSQREVTLGFRSGKFM	TLVATNVA	ARGLD	INDVQLII	QCEPPRDVEAYIHRSG	458
CcDDX	LHGDIQSSQREVTLGFRSGKFM	TLVATNVA	ARGLD	INDVQLII	QCEPPRDVEAYIHRSG	448
EgDDX	LHGDIQSSQREVTLGFRSGKFM	TLVATNVA	ARGLD	INDVQLII	QCEPPRDVEAYIHRSG	465
JcDDX	LHGEIQSSQREVTLGFRSGKFM	TLVATNVA	ARGLD	INDVQLII	QCEPPRDVEAYIHRSG	462
CaDDX	LHGDIQSSQREITLKGFRSGKFM	TLVATNVA	ARGLD	INDVQLII	QCEPPRDVEAYIHRSG	444

	<b>VI</b>	
CrDDX	RTGRAGNTGVAVTLYDS	452
CsDDX	RTGRAGNTGVAVTLYES	458
PRH75	RTGRAGNTGVAVTLYDS	452
BrDDX	RTGRAGNTGVAVMLYDS	458
BnDDX	RTGRAGNTGVAVMLYDS	443
EsDDX	RTGRAGNTGIAVMLYDS	465
AaDDX	RTGRAGNSGVAVTLYES	466
ThDDX	RTGRAGNTGVAVMLYDS	465
VvDDX	RTGRAGNSGVAVMLFDP	475
CcDDX	RTGRAGNTGVAVMLYDP	465
EgDDX	RTGRAGNTGVAVMLYDP	482
JcDDX	RTGRAGNTGVAVMLYDP	479
CaDDX	RTGRAGNTGVAVMLYDP	461

**Figure 15 Multi-sequence alignment of PRH75 amino acid sequence with corresponding domains from different plant species.**

Multiple sequences were aligned using the CLUSTAL W program. All the 13 conserved motifs of DEAD-box RNA helicase were shown in boxes with the motif acronym and a solid black line above the amino acids representing the motif. The accession numbers of the aligned protein sequences are *Capsella rubella* (CrDDX, XP\_006279587), *Camelina sativa* (CsDDX, XP\_010458375), *Brassica rapa* (BrDDX, XP\_009130201), *Eutrema salsugineum* (EsDDX, XP\_006394423), *Arabis alpina* (AaDDX, KFK27951), *Brassica napus* (BnDDX, CDX87236), *Tarenaya hassleriana* (ThDDX, XP\_010555319), *Vitis vinifera* (VvDDX, XP\_002269873), *Jatropha curcas* (JcDDX, KDP22369), *Eucalyptus grandis* (EgDDX, XP\_010034995), *Cicer arietinum* (CaDDX, XP\_004506292), *Citrus clementina* (CcDDX, XP\_006421777).

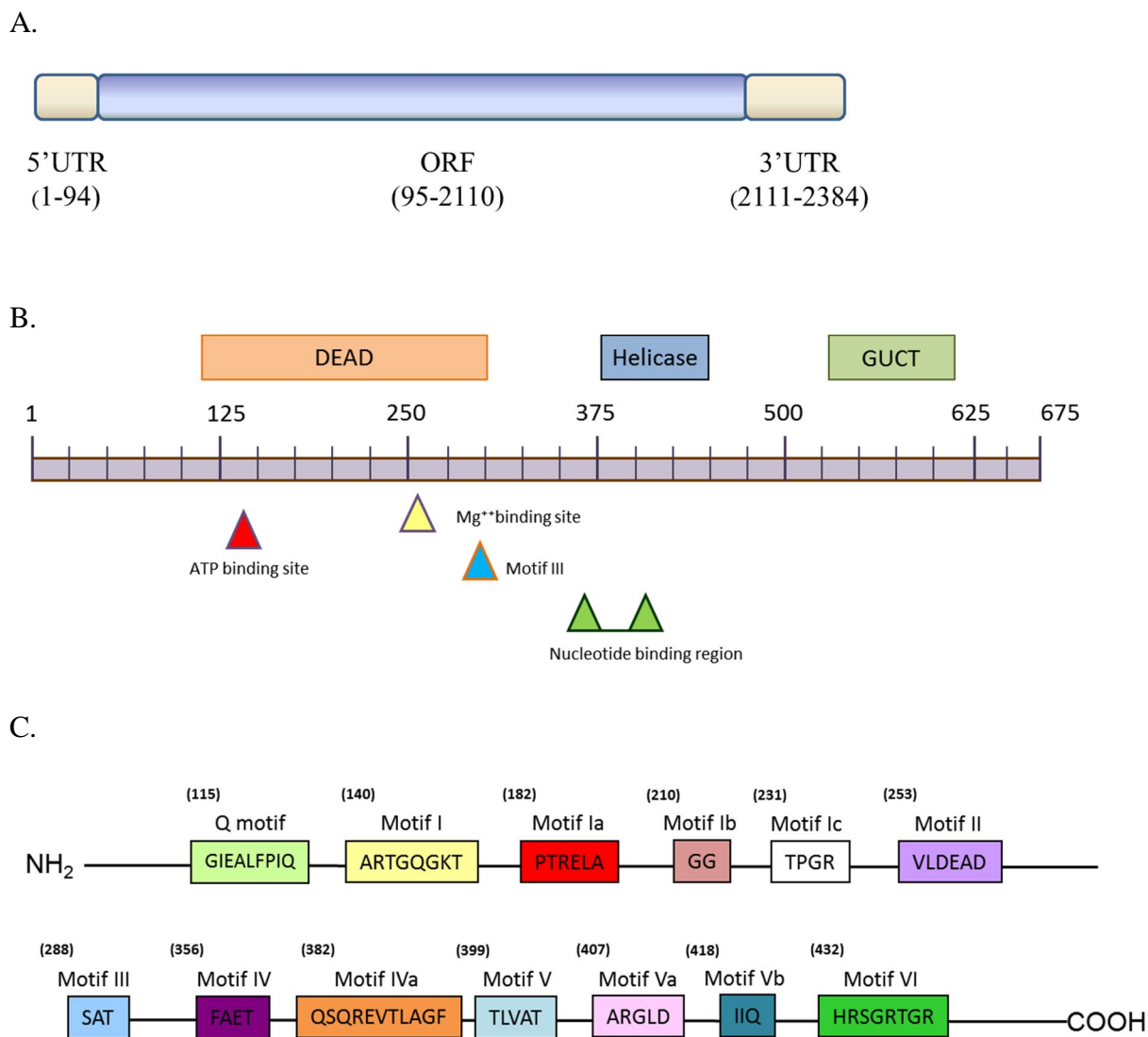


**Figure 16 Characterization of *Arabidopsis* PRH75.**

(A) Schematic representation of *Arabidopsis* PRH75 cDNA.

(B) Schematic representation of *Arabidopsis* PRH75 protein. The functional domains are indicated in boxes. Conserved signatures were obtained based on the NCBI conserved domain database.

(C) Conserved motifs of *Arabidopsis* PRH75. The 13 characteristic motifs of DEAD-box RNA helicase are highlighted in boxes in different colors. The numbers above the boxes indicate the positions of the first amino acid of each motif.

### 3.5.2 PRH75 is a nuclear protein

To explore the role of PRH75 associated with TuMV infection, a transient expression assay was conducted to establish the subcellular localization of PRH75 in plant cells. PRH75 tagged with YFP (PRH75-YFP) was expressed in *N. benthamiana* leaf epidermal cells by agroinfiltration. Consistent with a previous report where PRH75 localization was found in the nucleus using a tobacco protoplast expression system (Lorković *et al.*, 1997), the YFP signal was observed predominantly in the nucleus, particularly in the nucleolar region (Figure 17). This observation indicated that PRH75 is a nuclear protein with preferred localization to the nucleolus. Upon TuMV infection, subcellular localization of PRH75 was altered. This result will be described in section 3.5.6. Distinct from many other AtRHs such as AtRH9 and AtRH26 that are localized to both the nucleus and cytoplasm, the nuclear localization of PRH75 might indicate a specific role of this protein in TuMV infection.

Plasmids containing a series of PRH75 deletion mutants were constructed to determine the region responsible for nuclear targeting. PRH75 was divided into four fragments: N-terminus (corresponding to aa 1-114), DEAD domain (aa 115-355), Helicase domain (aa 356-450) and GUCT domain (aa 451-671) (Figure 18A). The truncated PRH75 derivatives containing one or more of these fragments were fused to a modified pEarleyGate101 vector containing the GUS coding region upstream of YFP. The resulting plasmids were agroinfiltrated into *N. benthamiana* epidermal cells to express PRH75 derivatives fused with GUS-YFP. The localization pattern of truncated PRH75 derivatives indicated that the N-terminal fragment (aa 1-114) was required for nuclear targeting (Figure 18B), which is in agreement with previously published results (Lorković *et al.*, 1997).

### 3.5.3 PRH75 directly interacts with multiple TuMV viral replicase proteins

To examine whether *Arabidopsis* PRH75 interacts with TuMV proteins, I screened the 11 TuMV proteins using the BiFC assay. The full-length coding region for each of the 11 TuMV proteins and PRH75 were fused to N- and C- terminus of YFP, respectively. The functional reconstituted YFP signal was examined under a confocal microscopy when



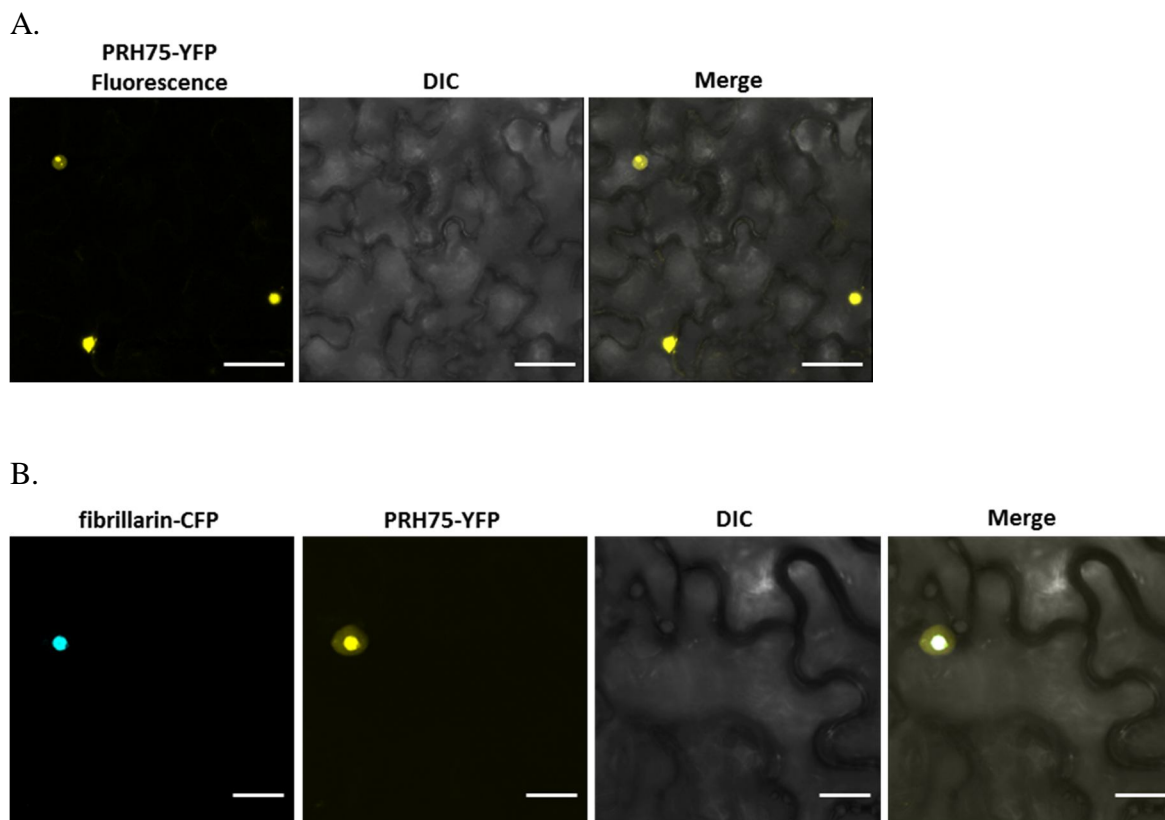
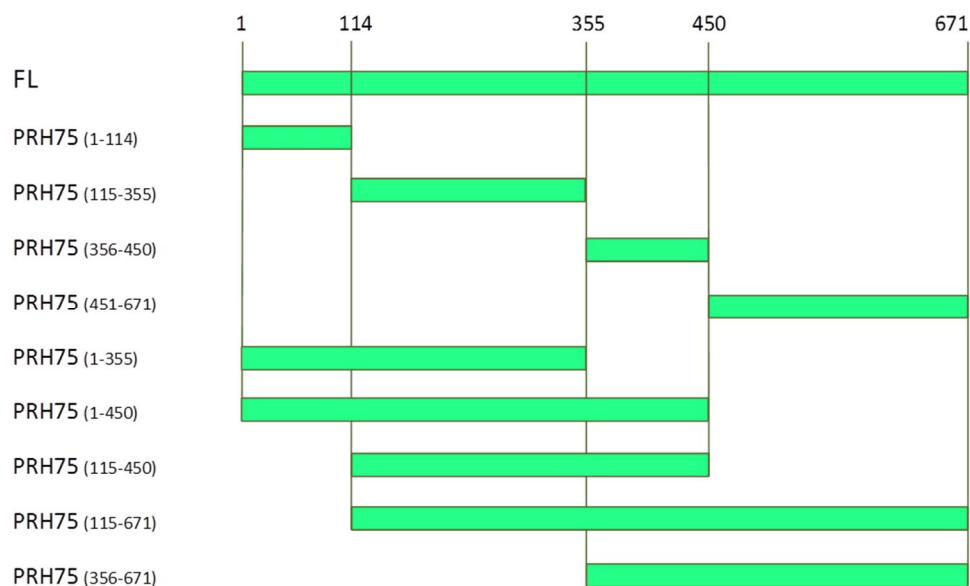


**Figure 17 PRH75 is localized in the nucleus.**

(A) Transient expression of PRH75-YFP in *N. benthamiana* leaf epidermal cells. YFP fluorescence was observed using a confocal microscopy 48 h post agroinfiltration. DIC, differential interference contrast. Bars, 50  $\mu$ m.

(B) Transient expression of PRH75-YFP with fibrillarin-CFP, a nucleolus marker protein in *N. benthamiana* leaf epidermal cells (Koroleva *et al.*, 2009). PRH75-YFP and fibrillarin-CFP were co-expressed in *N. benthamiana* leaves via agroinfiltration. Images were taken using a confocal microscopy 48 h post agroinfiltration. DIC, differential interference contrast. Bars, 15  $\mu$ m.

A.



B.

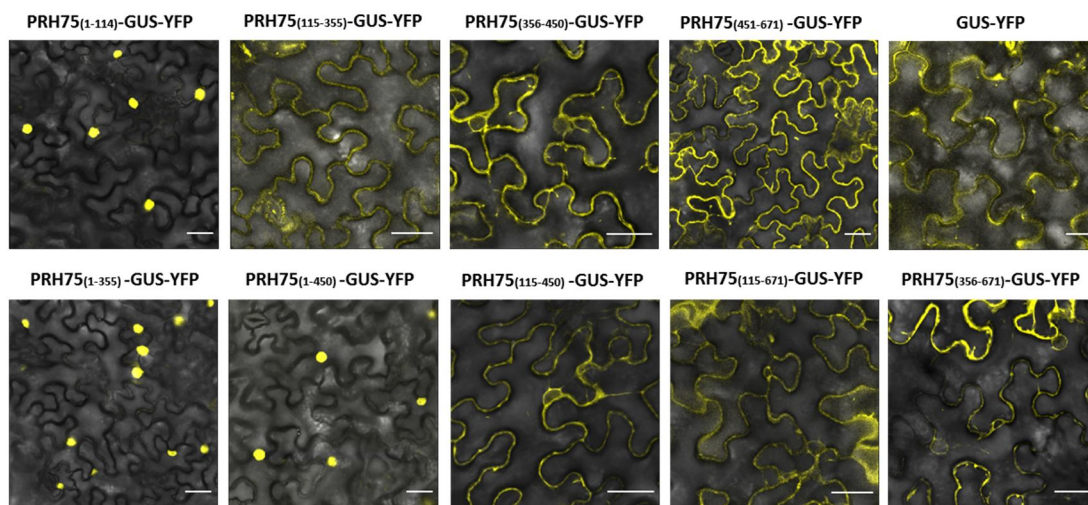


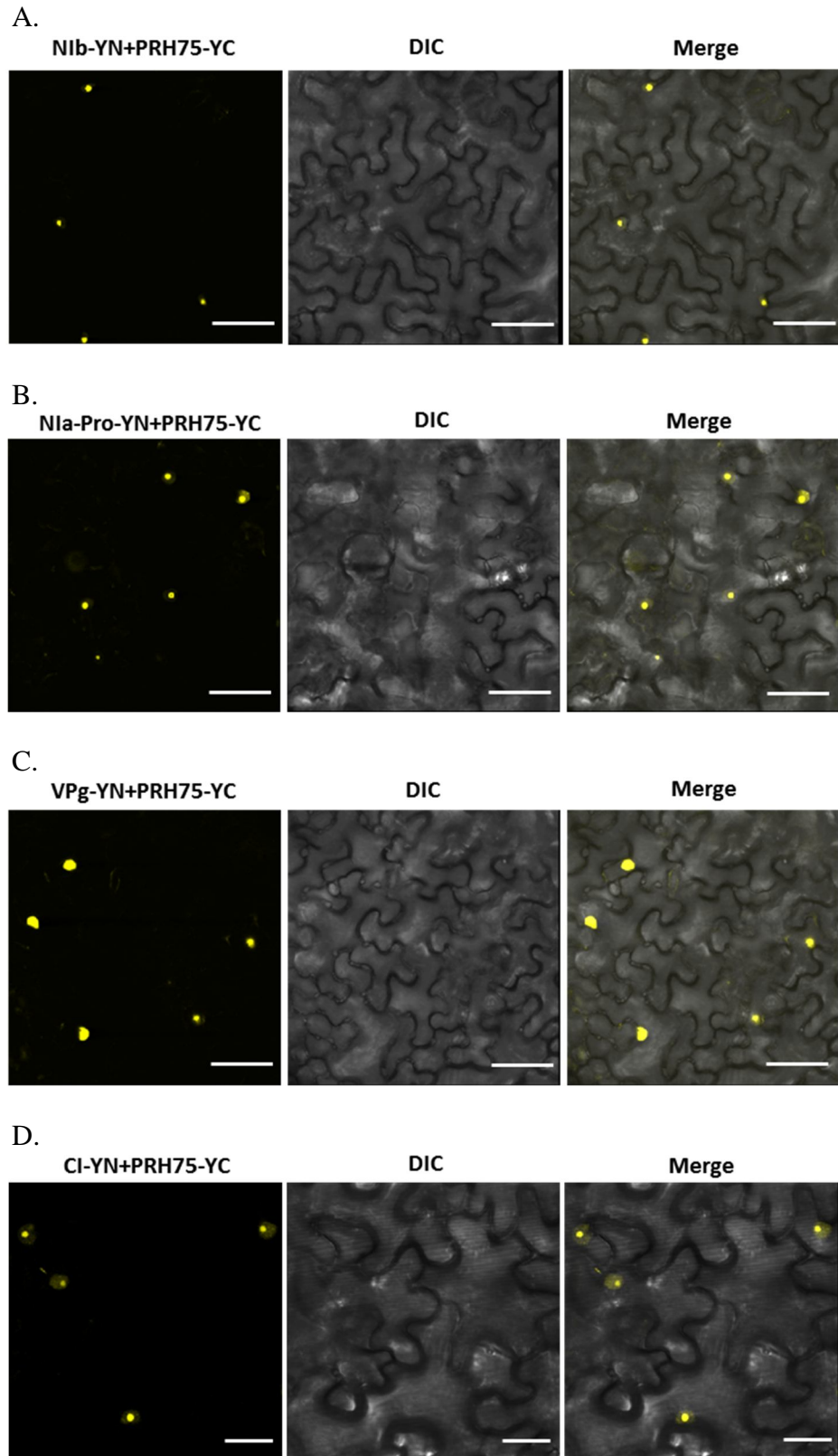
**Figure 18 Analysis of truncated PRH75 proteins.**

(A) Schematic diagram of truncated PRH75 proteins. The positions of the first and last amino acid residues of truncated proteins are indicated in parentheses.

(B) Subcellular localization of truncated PRH75 proteins tagged with GUS-YFP *in planta*. Transient expression of truncated PRH75 proteins tagged with GUS-YFP in *N. benthamiana* leaf epidermal cells. YFP fluorescence was observed using a confocal microscopy 48 h post agroinfiltration. DIC, differential interference contrast. Bars, 30  $\mu$ m.

viral fusion proteins and PRH75 fusion protein were co-expressed in plant cells following the same strategy as described previously. The results showed that PRH75 interacted with viral replicase proteins NIB, NIa-Pro, VPg and CI (Figure 19) but no detectable interactions were found with other viral proteins (Data not shown). For positive interactions, YFP signals were observed predominately in the nucleus with a small amount of signal detected in the cytoplasm. No YFP signal was detected in the negative controls (Appendix II). A targeted Y2H was performed to confirm interactions between PRH75 and TuMV viral proteins. Cotransformants of PRH75 and each viral protein were grown and selected on synthetic defined plates (SD/-Ade/-His/-Leu/-Trp). Yeast colonies co-transformed with PRH75 and each of NIB, VPg and CI, respectively, showed normal growth on the selective plates (SD/-Ade/-His/-Leu/-Trp). Controls, i.e., cotransformants of empty bait and prey vectors, PRH75 and the empty prey vector, or NIB, VPg and CI with bait only, did not grow (Figure 20). Inconsistent with the BiFC data, no positive interaction was found in yeast cells co-transformed with PRH75 and NIa-Pro.

To further confirm the interaction between PRH75 and viral proteins, a fluorescence resonance energy transfer (FRET) assay was conducted. Based on high spatial resolution, FRET analysis provides a powerful tool to detect protein-protein interactions in living cells. Translational fusion of PRH75 tagged with CFP was co-expressed with each of NIB, NIa-Pro, VPg and CI tagged with YFP in *N. benthamiana* leaf epidermal cells. Protein-protein interactions were examined by confocal microscopy. The change in increased intensity of CFP signal after photobleaching of YFP was determined as FRET efficiency, which indicated the positive interaction between two proteins. The results suggested a positive interaction between PRH75 and NIB with a FRET efficiency of 34.98%, as well as between PRH75 and NIa-Pro with a FRET efficiency of 37.49%. The FRET efficiency between PRH75 and VPg was 29.96% whereas between PRH75 and CI was 33.52%, respectively. The FRET efficiency between PRH75-CFP and GUS-YFP, as a negative control, was negligible (Figure 21). Taken together, PRH75 showed positive interactions with TuMV NIB, NIa-Pro, VPg and CI, respectively.



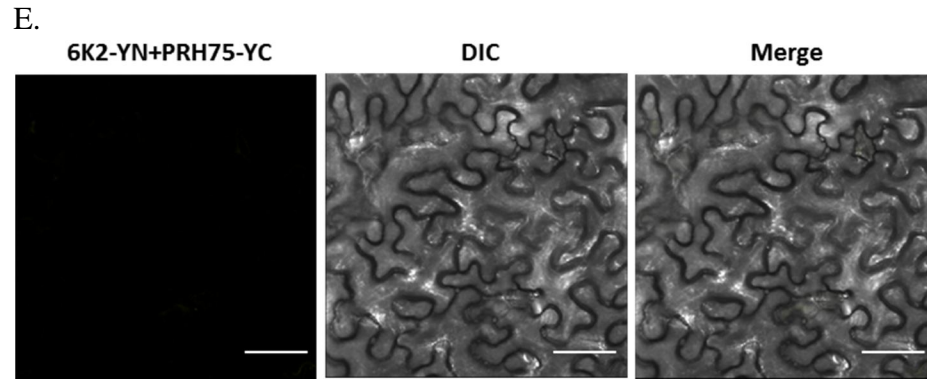


**Figure 19** The BiFC assay for detection of the interactions between PRH75 and TuMV viral proteins *in planta*.

*N. benthamiana* leaves were co-agroinfiltrated with constructs to co-express viral proteins and PRH75: (A) NIb and PRH75 fused with the N- and C- terminal moiety of YFP (YN and YC), respectively, (B) NIa-Pro-YN and PRH75-YC, (C) VPg-YN and PRH75-YC, (D) CI-YN and PRH75-YC, and (E) 6K2-YN and PRH75-YC. The reconstructed YFP fluorescence was recorded 48 h post agroinfiltration using a confocal microscopy. Bars, 50  $\mu$ m.

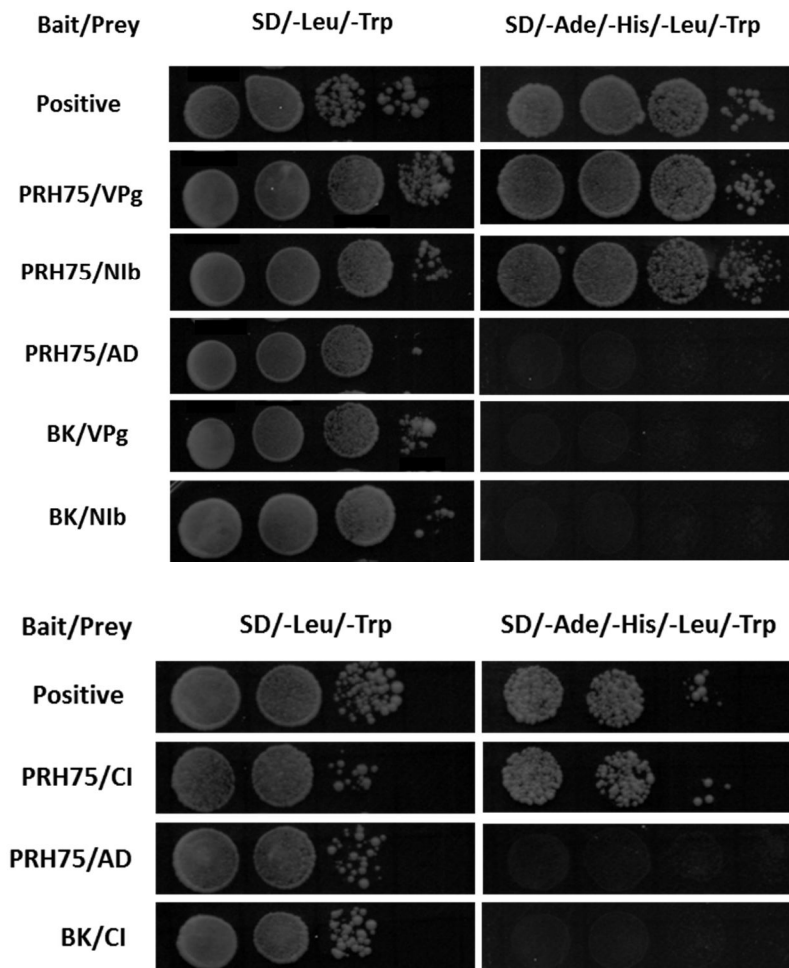
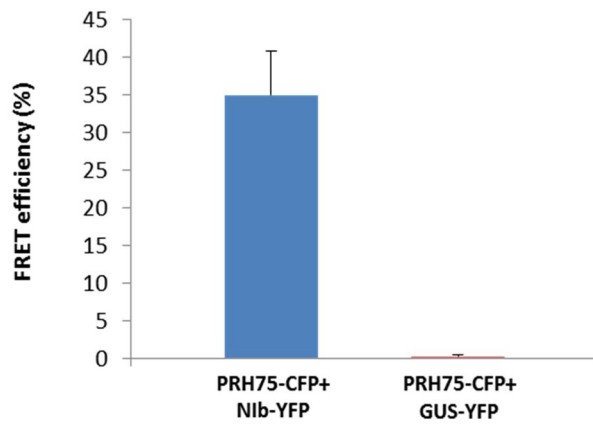


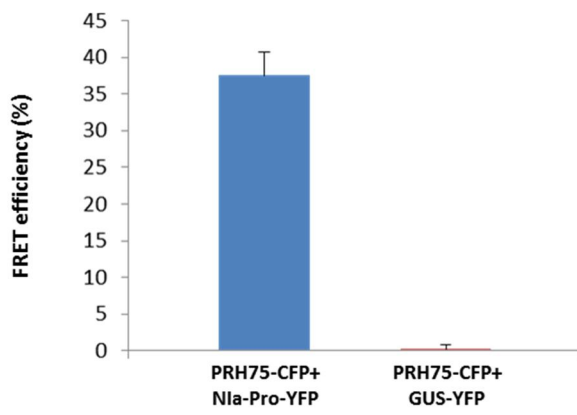
**Figure 20** The yeast two-hybrid assay for detection of the interactions between PRH75 and TuMV viral proteins.

Positive interactions between PRH75 and TuMV Nib, VPg or CI were evident in yeast. A series of 10  $\mu$ l aliquots of 10x yeast dilutions co-transformed with bait and prey were spotted onto synthetic defined (SD) selection plates and incubated for 2- 4 days at 30°C. Yeast cultures were plated on SD/-Leu/-Trp or SD/-Ade/-His/-Leu/-Trp dropout medium to observe yeast growth and to identify positive interactions, respectively. Co-transformation of the pGAD empty vector (prey) with pGBK-PRH75 (bait), and co-transformation of the pGBK empty vectors (bait) with pGAD-VPg (prey), pGAD-Nib (prey) and pGAD-CI (prey), respectively, were used as negative controls, and co-transformation of pGAD-VPg with pGBK-eIF(iso)4E as the positive control. Representative results were obtained in three independent experiments.

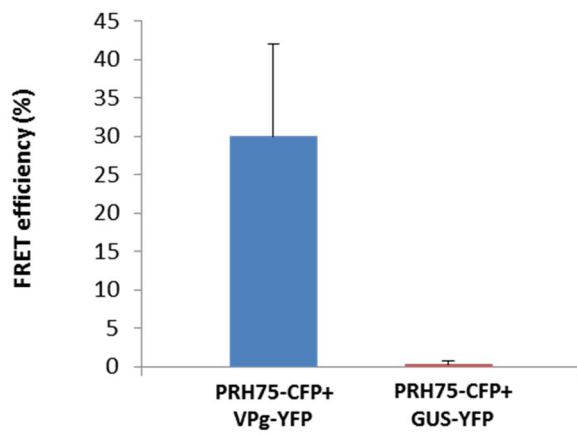
A.



B.



C.



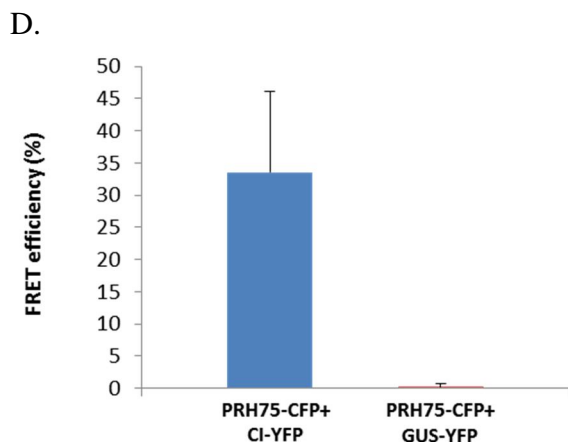


**Figure 21 Quantification of FRET efficiency between PRH75 and TuMV viral proteins.**

FRET efficiencies were calculated using the formula:  $\text{FRET efficiency} = \frac{[(\text{CFP signal after photobleaching} - \text{CFP signal before photobleaching}) / \text{CFP signal after photobleaching}] \times 100$ . Error bars represent standard deviations for nine independent FRET analysis in three independent experiments. (A) FRET efficiency between PRH75-CFP and N1b-YFP, (B) FRET efficiency between PRH75-CFP and N1a-Pro-YFP, (C) FRET efficiency between PRH75-CFP and VPg-YFP, and (D) FRET efficiency between PRH75-CFP and CI-YFP. The combination of PRH75-CFP and GUS-YFP was used as a negative control.



#### 3.5.4 *Arabidopsis* importin $\alpha$ interacts with PRH75 and TuMV viral replicase proteins

The nuclear localization of PRH75 and several potyviral replicase proteins has prompted us to look into the possibility that the nuclear transport of TuMV viral proteins is mediated by *Arabidopsis* importin  $\alpha$ . To investigate whether *Arabidopsis* importin  $\alpha$  is required for nucleocytoplasmic shuttle of these proteins, two isoforms of *Arabidopsis* importin  $\alpha$  (IMPA), IMPA1 and IMPA2, were analyzed. The Y2H and BiFC assays were performed to examine the ability of IMPA1 and IMPA2 to interact with PRH75 and each of these TuMV replicase proteins.

Interactions between PRH75 and IMPA1 and IMPA2 in plant cells were identified using the BiFC assay (Figure 22). YFP fluorescence was observed in the nucleus, which is consistent with the localization pattern of PRH75. The Y2H assay confirmed that PRH75 directly interacts with *Arabidopsis* IMPA1 and IMPA2 (Figure 23).

Positive interactions were also found between IMPA1 and NIB, IMPA1 and NIa-Pro, IMPA1 and VPg, or IMPA1 and CI using the BiFC assay *in planta*. The reconstituted YFP signal was found in the nucleus and cytoplasm of plant cells co-expressing IMPA1 fused to the N-terminus of YFP with NIB, NIa-Pro, VPg and CI fused to the C-terminus of YFP, respectively (Figure 24). The Y2H assay further confirmed that IMPA1 interacted with NIB, NIa-Pro, VPg and CI (Figure 25). Taken together, these data suggest that *Arabidopsis* IMPA1 interacts with TuMV NIB, NIa-Pro, VPg and CI.

Similarly, the BiFC assay indicated the interactions of IMPA2 with NIB, NIa-Pro, VPg and CI, respectively, *in planta*. The YFP fluorescence was observed mostly in the nucleus with partially in the cytoplasm (Figure 26). The interactions between IMPA2 and NIB, NIa-Pro, VPg and CI were further confirmed by the Y2H assay. Altogether, the results showed that *Arabidopsis* IMPA2 also interacts with TuMV NIB, NIa-Pro, VPg and CI (Figure 27).

The tested interactions between PRH75, TuMV viral proteins and *Arabidopsis* IMPA1 and IMPA2 are summarized in Table 10.

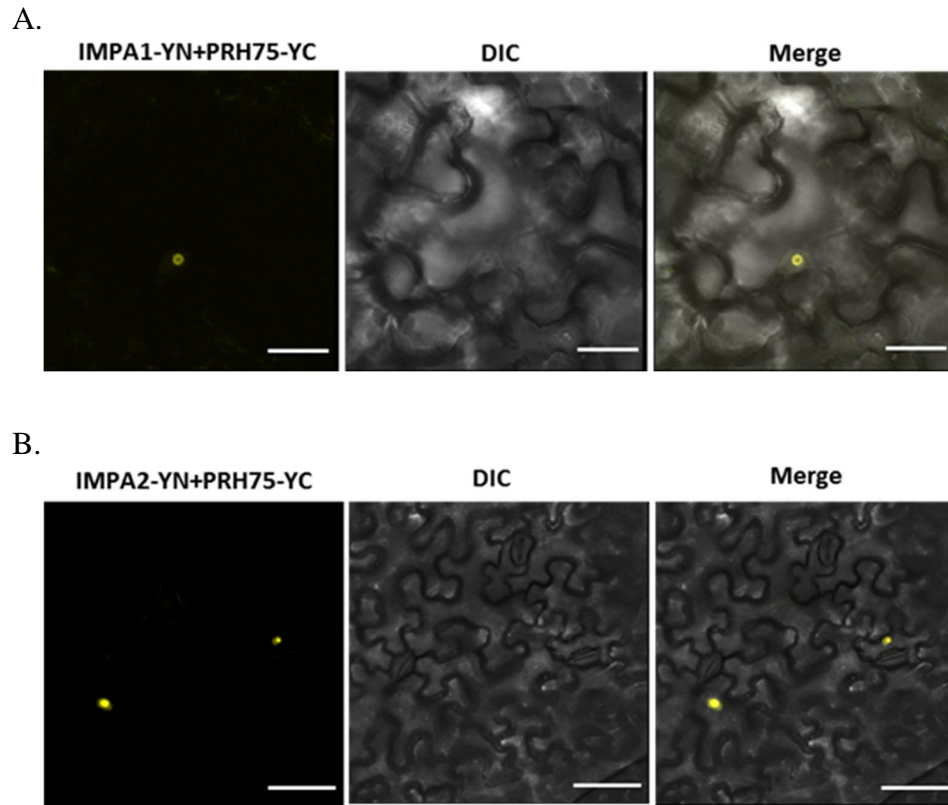


**Figure 22** The BiFC assay for detection of the interactions between PRH75 and *Arabidopsis* IMPA1 and IMPA2 *in planta*.

*N. benthamiana* leaves were co-agroinfiltrated with constructs to co-express (A) IMPA1 and PRH75 fused with the N- and C- terminal half of YFP (YN and YC), respectively, and (B) IMPA2-YN and PRH75-YC. The reconstructed YFP fluorescence was recorded 48 h post agroinfiltration using a confocal microscopy. DIC, differential interference contrast. Bars in (A), 25  $\mu\text{m}$ , and in (B), 50  $\mu\text{m}$ .

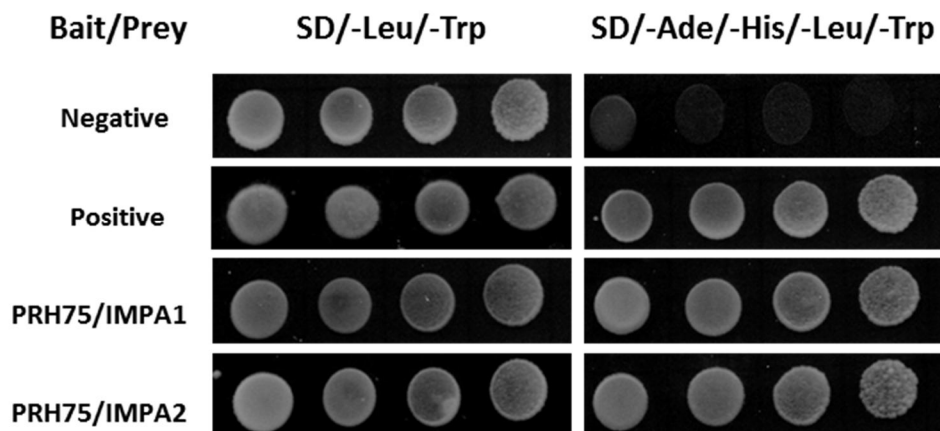


**Figure 23** The yeast two-hybrid assay for detection of the interactions between PRH75 and *Arabidopsis* IMPA1 and IMPA2.

Positive interactions were found between PRH75 and *Arabidopsis* IMPA1 and IMPA2 in yeast. A series of 10  $\mu$ l aliquots of 10x yeast dilutions co-transformed with bait and prey were spotted onto SD selection plates and incubated for 2- 4 days at 30°C. Yeast cultures were plated on SD/-Leu/-Trp or SD/-Ade/-His/-Leu/-Trp dropout medium to observe yeast growth and to identify positive interactions, respectively. Co-transformation of the pGAD empty vector (prey) with the pGBK empty vector (bait) was used as a negative control, and co-transformation of pGAD-VPg with pGBK-eIF(iso)4E as a positive control.

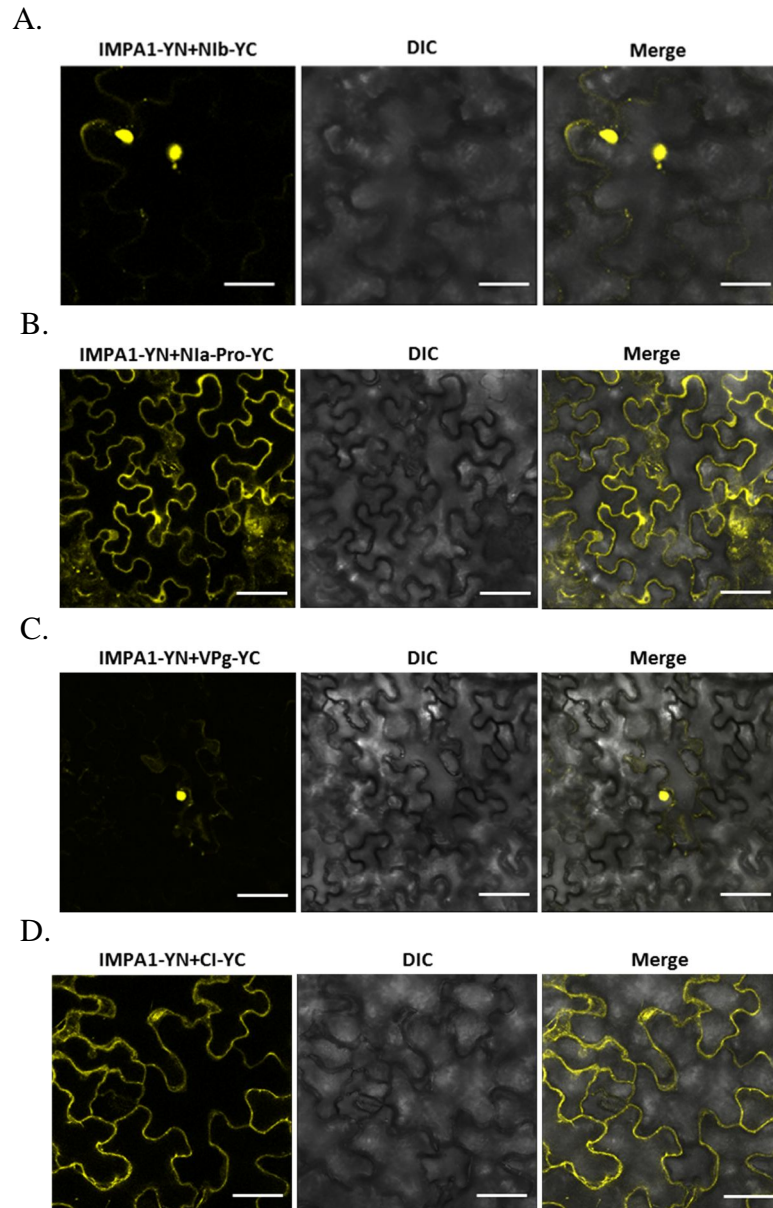


**Figure 24** The BiFC assay for detection of the interactions between IMPA1 and TuMV viral proteins *in planta*.

*N. benthamiana* leaves were co-agroinfiltrated with constructs to co-express (A) IMPA1 and NIB fused with the N- and C- terminal half of YFP (YN and YC), respectively, (B) IMPA1-YN and NIa-Pro-YC, (C) IMPA1-YN and VPg-YC, and (D) IMPA1-YN and CI-YC. The reconstructed YFP fluorescence was recorded 48 h post agroinfiltration using a confocal microscopy. DIC, differential interference contrast. Bars in (A), 20  $\mu\text{m}$ , and in (B, C, D), 50  $\mu\text{m}$ .

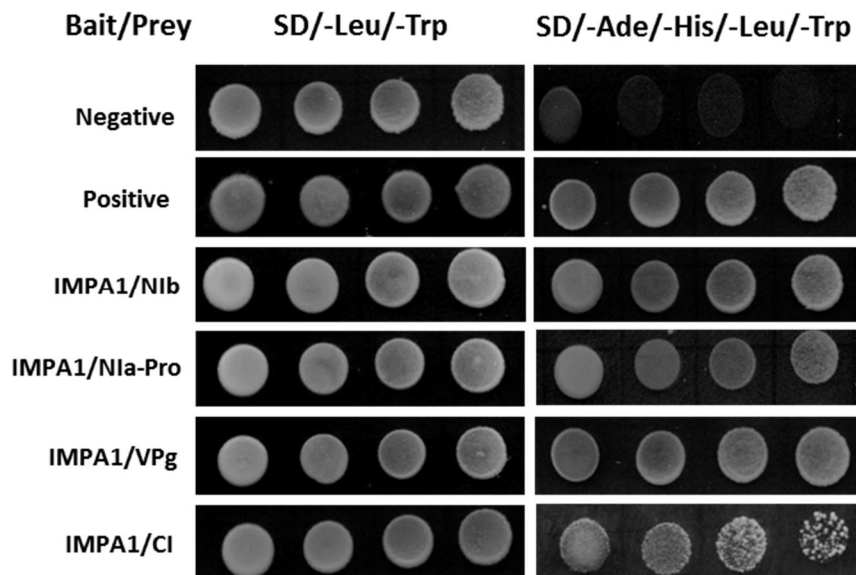


**Figure 25** The yeast two-hybrid assay for detection of the interactions between *Arabidopsis* IMPA1 and TuMV viral proteins.

Positive interactions between *Arabidopsis* IMPA1 and TuMV viral proteins NIb, NIa-Pro, VPg or CI were detected in yeast. A series of 10  $\mu$ l aliquots of 10x yeast dilutions co-transformed with bait and prey were spotted onto synthetic defined (SD) selection plates and incubated for 2-4 days at 30°C. Yeast cultures were plated on SD/-Leu/-Trp or SD/-Ade/-His/-Leu/-Trp dropout medium to observe yeast growth and to identify positive interactions, respectively. Co-transformation of the pGAD empty vector (prey) with the pGBK empty vector (bait) serves as a negative control, and co-transformation of pGAD-VPg and pGBK-eIF(iso)4E as a positive control.

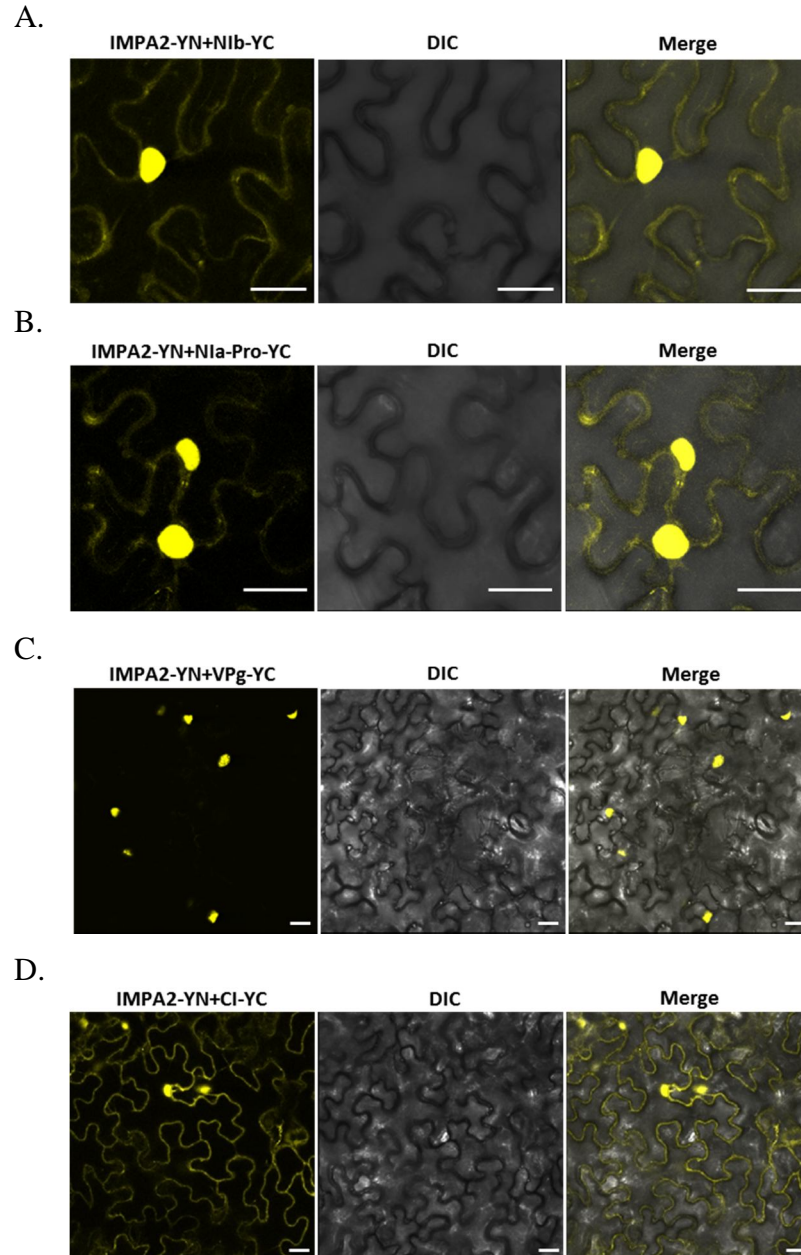


**Figure 26** The BiFC assay for detection of the interactions between IMPA2 and TuMV viral proteins *in planta*.

*N. benthamiana* leaves were co-agroinfiltrated with constructs to co-express (A) IMPA2 and Nib fused with the N- and C- terminal moiety of YFP (YN and YC), respectively, (B) IMPA2-YN and Nla-Pro-YC, (C) IMPA2-YN and VPg-YC, and (D) IMPA2-YN and CI-YC. The reconstructed YFP fluorescence was observed 48 h post agroinfiltration using a confocal microscopy. DIC, differential interference contrast. Bars, 20 μm.

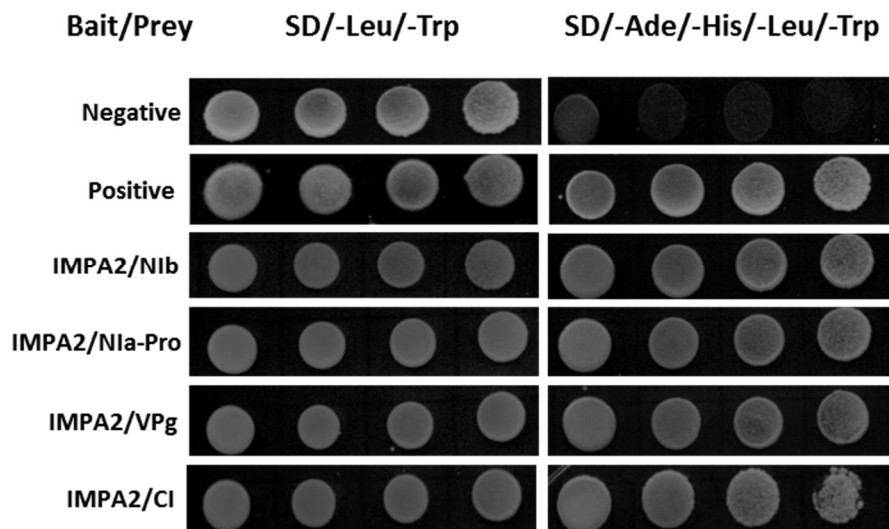


**Figure 27** The yeast two-hybrid assay for detection of the interactions between *Arabidopsis* IMPA2 and TuMV viral proteins.

Positive interactions between *Arabidopsis* IMPA2 and TuMV viral proteins Nib, NIa-Pro, VPg or CI were confirmed in yeast. A series of 10  $\mu$ l aliquots of 10x yeast dilutions co-transformed with bait and prey were spotted onto SD selection plates and incubated for 2-4 days at 30°C. Yeast cultures were plated on SD/-Leu/-Trp or SD/-Ade/-His/-Leu/-Trp dropout medium to observe yeast growth and to identify positive interactions, respectively. Co-transformation of the pGAD empty vector (prey) with the pGBK empty vector (bait) was used as a negative control, and co-transformation of pGAD-VPg with pGBK-eIF(iso)4E as a positive control.

**Table 10 Summary of tested protein-protein interactions**

	Method	NIb	NIa-Pro	VPg	CI
PRH75	BiFC	+	+	+	+
	FRET	+	+	+	+
	Y2H	+	-	+	+
IMPA1	BiFC	+	+	+	+
	Y2H	+	+	+	+
IMPA2	BiFC	+	+	+	+
	Y2H	+	+	+	+



### 3.5.5 PRH75 colocalizes with *Arabidopsis* importin $\alpha$ , eIF(iso)4E and TuMV viral replicase proteins

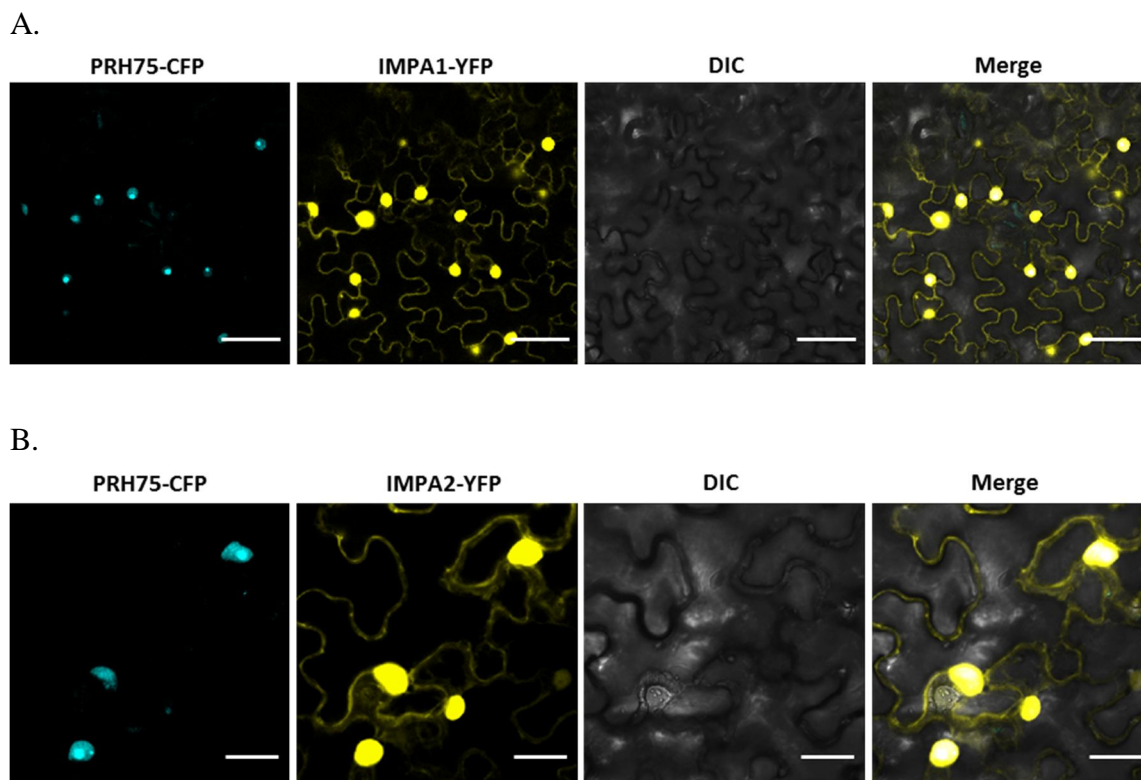
To determine if PRH75 colocalizes with IMPA1 and IMPA2, *N. benthamiana* leaves were co-agroinfiltrated with vectors expressing PRH75-CFP and IMPA1-YFP or IMPA2-YFP, respectively. At 48 h post agroinfiltration, observation was taken by a confocal microscopy and revealed that the cyan fluorescence of PRH75 predominantly overlapped the IMPA1-YFP and IMPA2-YFP fluorescence in the nucleus (Figure 28).

*Arabidopsis* eIF(iso)4E, the isoform of eIF4E, which functions as a cap-binding protein that initiates translation of mRNA (Wang and Krishnaswamy, 2012). eIF(iso)4E was reported to interact with TuMV VPg and its precursor VPg-Pro (NIa) and was required for TuMV infection (Lellis *et al.*, 2002). When expressed alone, eIF(iso)4E was found mainly in the cytoplasm, around the nuclear membrane and in the ER network. eIF(iso)4E was redistributed to the nucleus when co-expressed with VPg-Pro (NIa) (Beauchemin *et al.*, 2007; Beauchemin and Laliberté, 2007). The colocalization study of PRH75 with eIF(iso)4E indicated that PRH75 overlaps the localization of eIF(iso)4E in the nucleus (Figure 29).

To investigate whether the intracellular distributions of TuMV viral replicase proteins change in the presence of PRH75, we co-expressed PRH75-CFP with NIB-YFP, NIa-Pro-YFP, VPg-YFP and CI-YFP, respectively in *N. benthamiana* leaves. No different subcellular distribution patterns were found when viral protein was expressed alone or co-expressed with PRH75. These data suggested that PRH75 colocalized with TuMV viral replicase proteins in the nucleus (Figure 30).

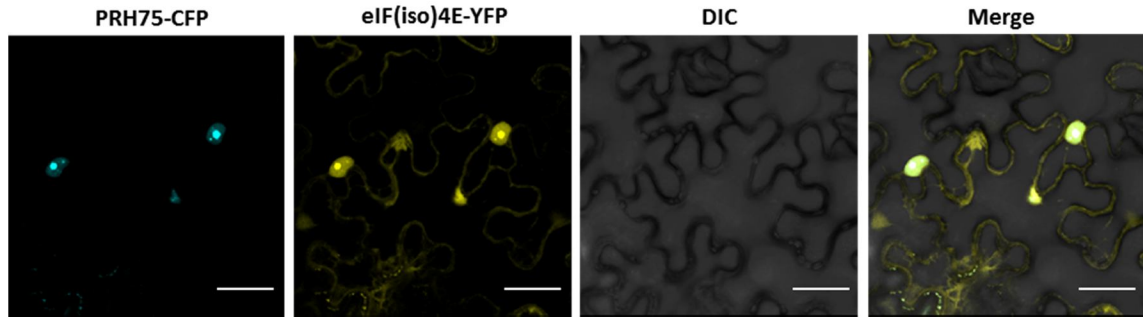
### 3.5.6 Distribution of BiFC signals between PRH75 and TuMV viral replicase proteins is altered in the presence of TuMV infection

To assess whether the interactions between PRH75 and TuMV viral replicase proteins are altered during TuMV infection, the BiFC assay was carried out. Four viral proteins, NIB, NIa-Pro, VPg and CI and PRH75 were introduced into N- or C- terminal half of YFP, respectively, and co-expressed into *N. benthamiana* leaves infected with a TuMV



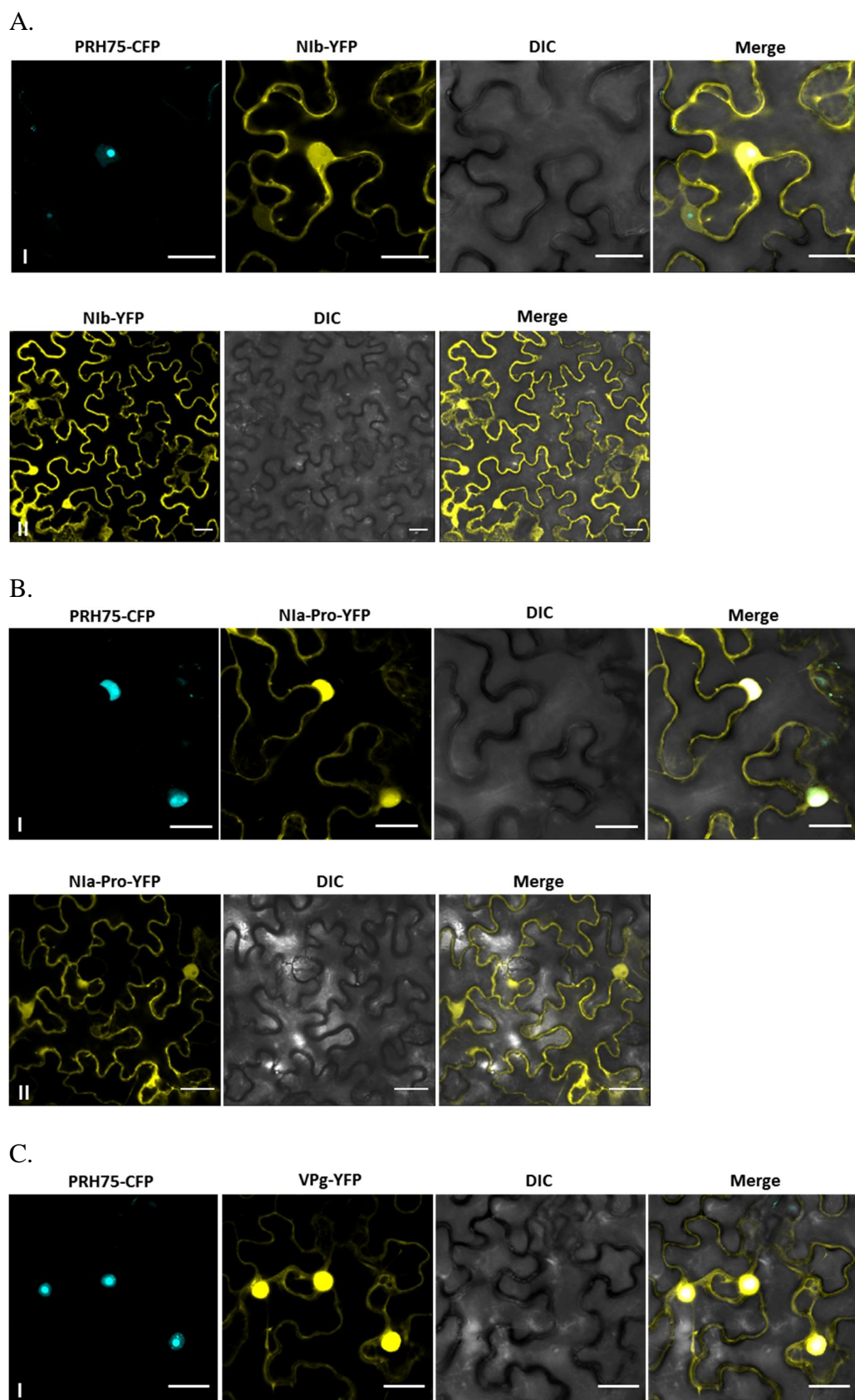
**Figure 28** Colocalization of PRH75 and *Arabidopsis* importin  $\alpha$ .

*N. benthamiana* leaves were co-agroinfiltrated with constructs to co-express (A) PRH75-CFP and IMPA1-YFP, (B) PRH75-CFP and IMPA2-YFP. Observations were recorded 48 h post agroinfiltration using a confocal microscopy. DIC, differential interference contrast. Bars in (A), 50  $\mu\text{m}$ , and in (B) 25  $\mu\text{m}$ .



**Figure 29 Colocalization of PRH75 and *Arabidopsis* host proteins.**

*N. benthamiana* leaves were co-agroinfiltrated with constructs expressing PRH75-CFP and eIF(iso)4E-YFP. Images were taken 48 h post agroinfiltration using a confocal microscopy. DIC, differential interference contrast. Bars, 30  $\mu\text{m}$ .



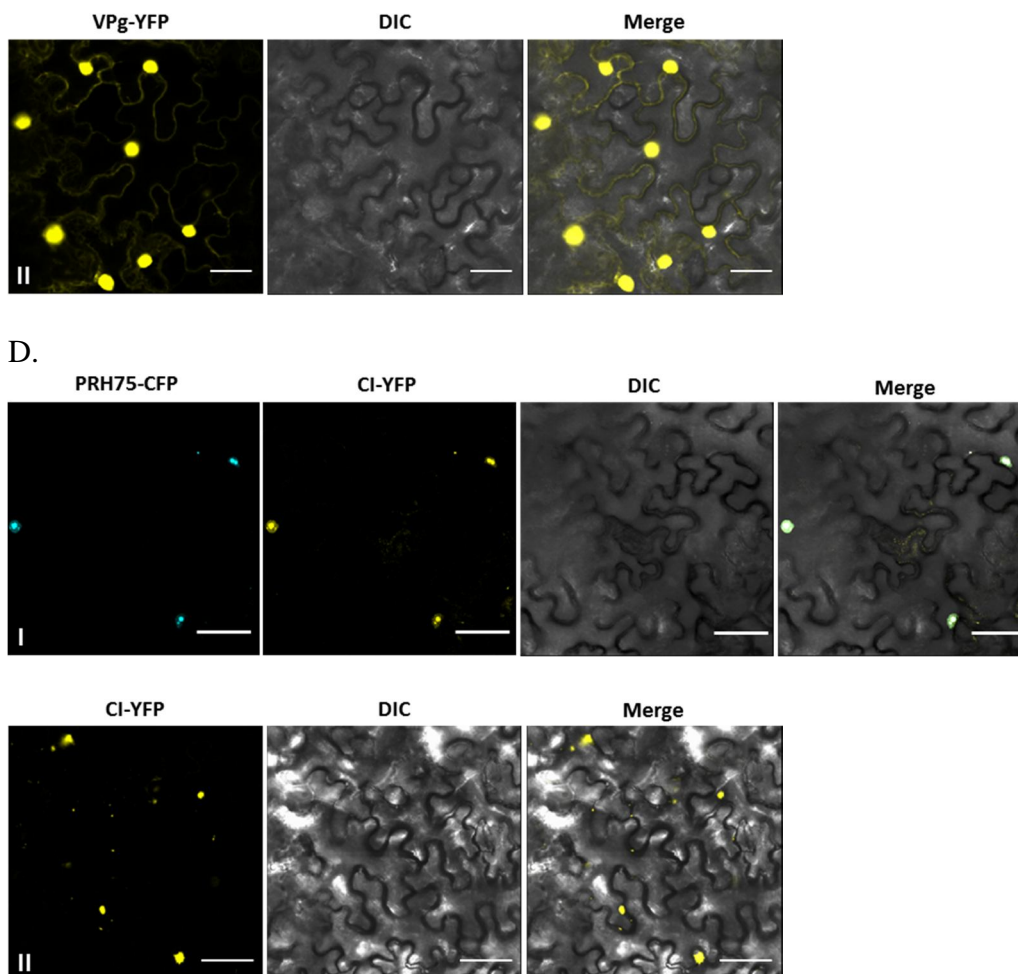


**Figure 30 Colocalization of PRH75 and TuMV viral proteins.**

*N. benthamiana* leaves were co-agroinfiltrated with constructs to co-express (A-I) PRH75-CFP and NIb-YFP, (B-I) PRH75-CFP and NIa-Pro-YFP, (C-I) PRH75-CFP and VPg-YFP, and (D-I) PRH75-CFP and CI-YFP. Transient expression of TuMV viral protein alone in *N. benthamiana*. (A-II) NIb-YFP, (B-II) NIa-Pro-YFP, (C-II) VPg-YFP, and (D-II) CI-YFP. Images were recorded 48 h post agroinfiltration using a confocal microscopy. DIC, differential interference contrast. Bars in (A), 20  $\mu\text{m}$ , in (B), 25  $\mu\text{m}$ , in (C), 30  $\mu\text{m}$  and in (D), 50  $\mu\text{m}$ .

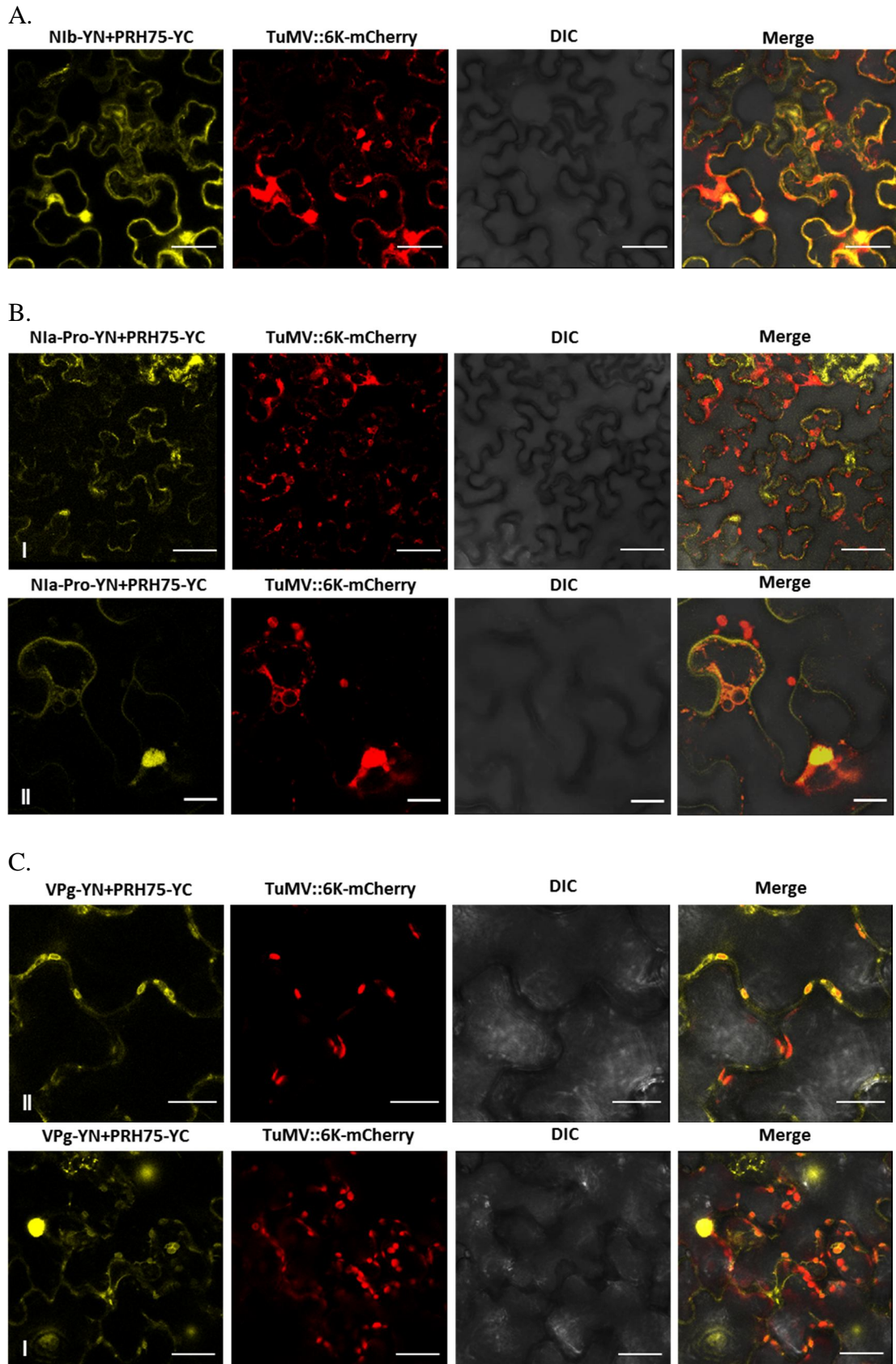
infectious clone expressing a 6K2-mCherry fusion protein (TuMV::6K2-mCherry). The TuMV infectious clone was engineered to carry an in-frame translational fusion of 6K2-mCherry between P1 and HC-Pro. The TuMV::6K2-mCherry infectious clone can induce the formation of discrete fluorescent structures, designated as the viral vesicles. Moreover, the motility of 6K2-induced vesicle suggests that the virus movement determinant lies on 6K2 protein. dsRNA was detected within the virus-induced vesicles by staining with antibodies (Cotton *et al.*, 2009). Further, host factors such as eIF(iso)4E (Beauchemin *et al.*, 2007), PABP (Beauchemin and Laliberté, 2007), Hsc70-3 (Dufresne *et al.*, 2008), eEF1A (Dufresne *et al.*, 2008) and AtRH8 (Huang *et al.*, 2010) were previously demonstrated to be enclosed within the 6K2-induced vesicles, indicating that TuMV 6K2 vesicles represent the sites of viral genome replication. Thus, the 6K2-mCherry induced vesicles can serve as a marker for TuMV replication complexes.

In the presence of TuMV infection, PRH75 indeed interacted with TuMV viral replicase proteins NIB, NIa-Pro, VPg and CI. Moreover, those positive interactions were colocalized with 6K2- induced vesicles (Figure 31). The colocalization of PRH75 with viral replicase proteins and 6K2-induced replication vesicles in TuMV-infected cells strongly indicated that PRH75 was translocated from the nucleus to the cytoplasm through the interactions with viral replicase proteins and PRH75 was required for successful TuMV replication.

### 3.5.7 PRH75 is associated with TuMV replication vesicles that are bound to chloroplasts and contain dsRNA

Previous studies have shown that 6K2-induced mobile vesicles are derived from the ER and traffic from the ER to the periphery of chloroplasts for viral replication (Wei and Wang, 2008; Wei *et al.*, 2010). To determine if PRH75 is also transported to the chloroplast-associated 6K2 vesicles during TuMV infection, colocalization studies of PRH75-CFP and a TuMV infectious clone with a YFP fused to the viral protein marker 6K2 of the replication complex (TuMV::6K2-YFP), were performed. The infectious clone of TuMV was engineered to carry an in-frame translational fusion of 6K2-YFP between P1 and HC-Pro (Huang *et al.*, 2010).





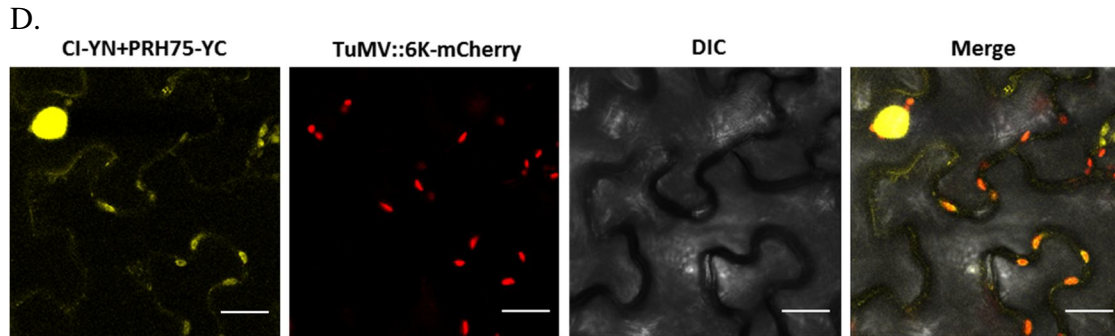


**Figure 31 The BiFC assay of interactions between PRH75 and TuMV viral proteins during TuMV infection.**

Co-agroinfiltration with constructs to co-express (A) NIb and PRH75 fused with the N- and C- terminal moiety of YFP (YN and YC), respectively, into *N. benthamiana* leaves infected by TuMV::6K2-mCherry. (B) NIa-Pro-YN and PRH75-YC, (C) VPg-YN and PRH75-YC, and (D) CI-YN and PRH75-YC. DIC, differential interference contrast. Bars in (A), 30  $\mu\text{m}$ ; in (B-I), 30  $\mu\text{m}$ , in (B-II), 20  $\mu\text{m}$ ; in (C-I), 30  $\mu\text{m}$ , in (C-II), 20  $\mu\text{m}$  and in (D), 20  $\mu\text{m}$ .



*N. benthamiana* leaves were co-agroinfiltrated with PRH75-CFP and TuMV::6K2-YFP, and the localization of PRH75 as well as the movement of the viral vesicles were monitored by a confocal microscopy 3 days and 4 days post agroinfiltration. Indeed, the 6K2-YFP induced yellow fluorescent vesicles were observed on the outer membrane of chloroplast and closely aligned with the chloroplast in TuMV-infected *N. benthamiana* leaf epidermal cells. Cyan fluorescence from PRH75-CFP overlapped with the 6K2-induced vesicles at 3 days and 4 days post agroinfiltration (Figure 32). The presence of PRH75 associated with TuMV replication vesicles strongly supported the idea that PRH75 was recruited to the viral replication complexes via its binding to viral proteins and was essential for TuMV infection.

Virus replication takes places in the virus-induced vesicles that shelter viral RNA from degradation. Before replication, the viral replication complexes (VRCs) are assembled, in a process associated with intracellular membranes. The VRC contains the proteins synthesized from the viral RNA as well as host proteins to facilitate viral replication and translation (Sanfaçon, 2005). Template viral RNAs, as well as double-stranded RNA regions formed when the complementary negative-sense RNA is synthesized, are also enclosed within the vesicles. During viral replication, RNA helicases are recruited to the vesicles and considered to catalyze the separation of dsRNA. As discussed before, PRH75 colocalized and interacted with NIB, the RNA-dependent RNA polymerase of TuMV, raising the possibility that PRH75 is recruited to the VRCs and plays a role of unwinding the viral dsRNA during replication.

To confirm that the colocalization of PRH75 matched with viral RNA replication sites, a novel strategy for localizing plant viral RNAs and VRCs *in planta* using an RNA-binding protein, coupled to the BiFC vectors, referred to a dsRNA-binding dependent fluorescence complementation (dRBFC) assay, has been developed (Tilsner *et al.*, 2009) (Cheng, unpublished data). To validate the sensitivity of dsRNA detection, PRH75-CFP was co-expressed along with the dRBFC assay. The yellow fluorescence signal of the dRBFC was visualized as small, discrete aggregates distributed throughout the cytoplasm, as well as concentrated in the nucleus. The cyan fluorescence of PRH75 overlapped with the dRBFC-labelled dsRNA in the nucleus (Figure 33). In comparison with the

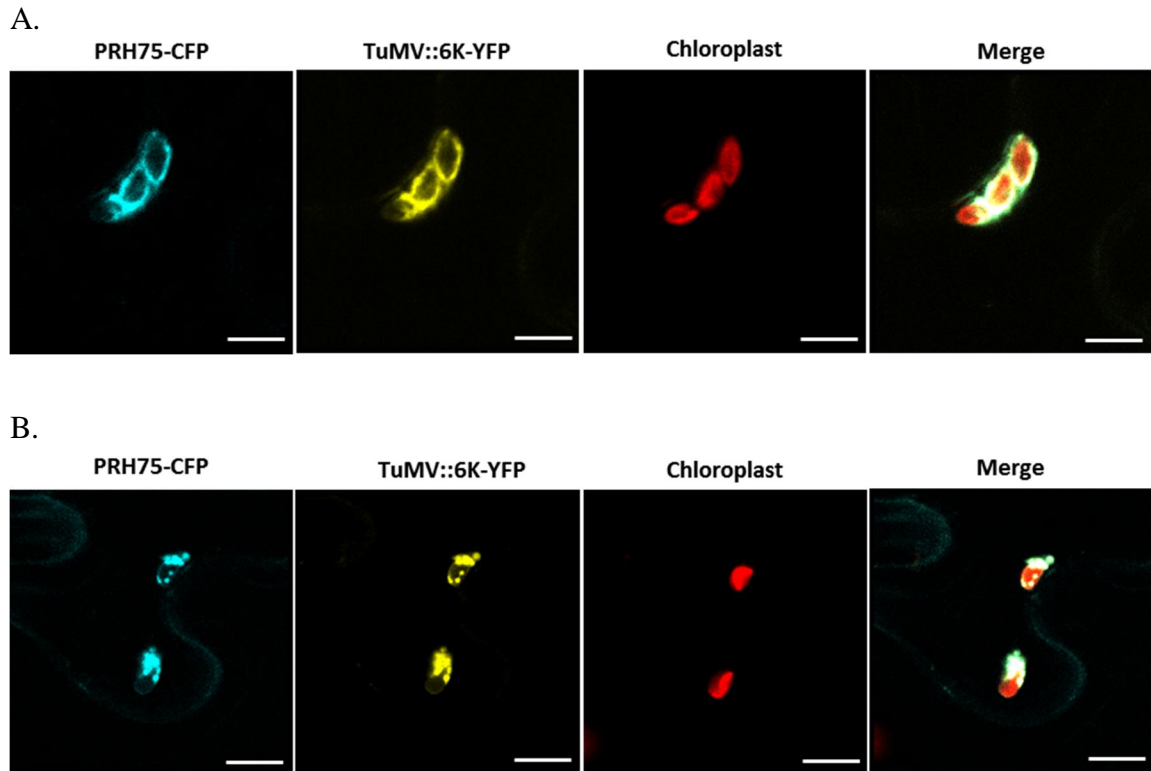


**Figure 32 PRH75-CFP colocalized with the chloroplast-bound 6K-YFP vesicles.**

*N. benthamiana* leaves were co-agroinfiltrated with constructs expressing PRH75-CFP and TuMV::6K2-YFP. (A) Images were taken 3 days post infiltration using a confocal microscopy. (B) Images were recorded 4 days post infiltration. DIC, differential interference contrast. Bars in (A), 10  $\mu\text{m}$ , and in (B), 5  $\mu\text{m}$ .

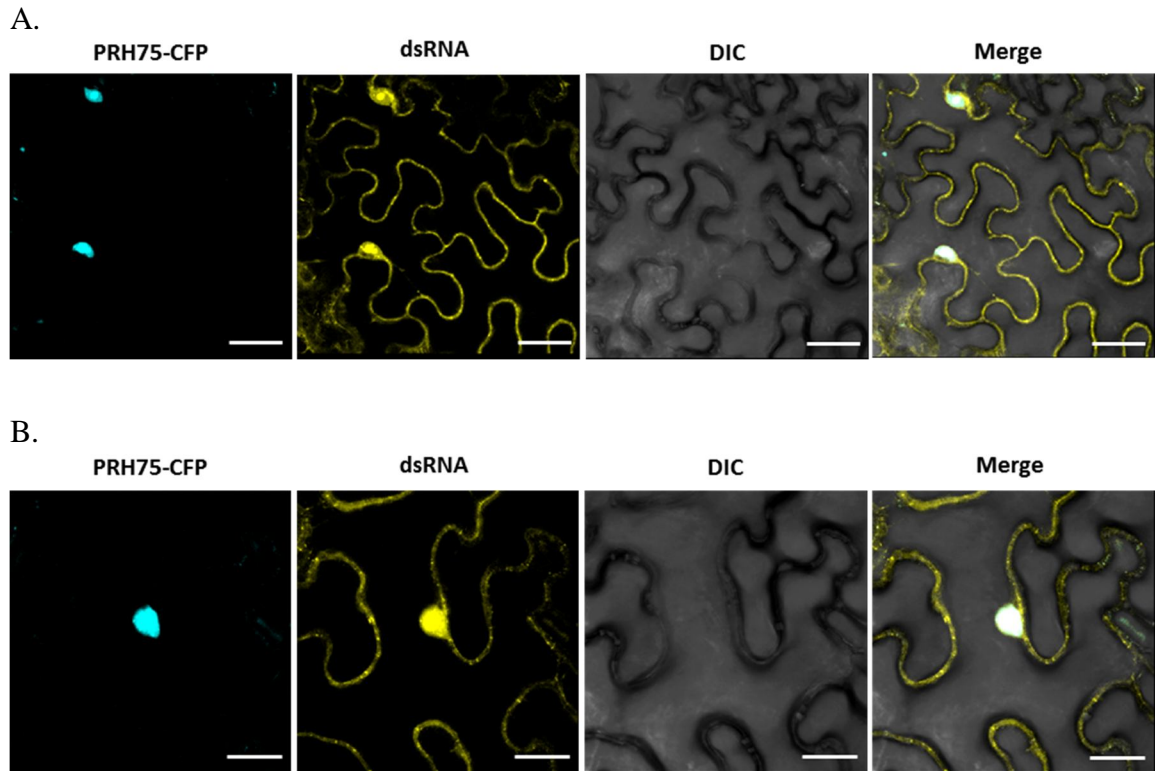


**Figure 33 PRH75-CFP colocalized with dsRNA-containing foci.**

*N. benthamiana* leaves were co-agroinfiltrated with constructs to co-express PRH75-CFP and the dRBFC assay. Observation was recorded 48 h post agroinfiltration using a confocal microscopy. DIC, differential interference contrast. Bars in (A), 30 μm, and in (B), 20 μm.

localization pattern in the absence of viral infection, coexpression of PRH75 and the dRBFC assay into *N. benthamiana* leaves infected with the TuMV infectious clone (TuMV::6K2-mCherry), resulted in observing dRBFC yellow fluorescence signals in a granular aggregation or discrete structures in the cytoplasm, resembling the described VRC during TuMV infection (Grangeon *et al.*, 2012). Since the dRBFC assay can bind both plant and viral dsRNA, dRBFC signal was also detected in the nucleus. PRH75-CFP was found to form punctate structures and colocalize with viral dsRNA in the labelled VRC (Figure 34). Collectively, these results indicated that PRH75 was recruited to VRC, namely viral dsRNA containing foci, during viral replication. In addition to unwinding the viral dsRNA intermediate, PRH75 may remain and serve other functions in the nucleus.

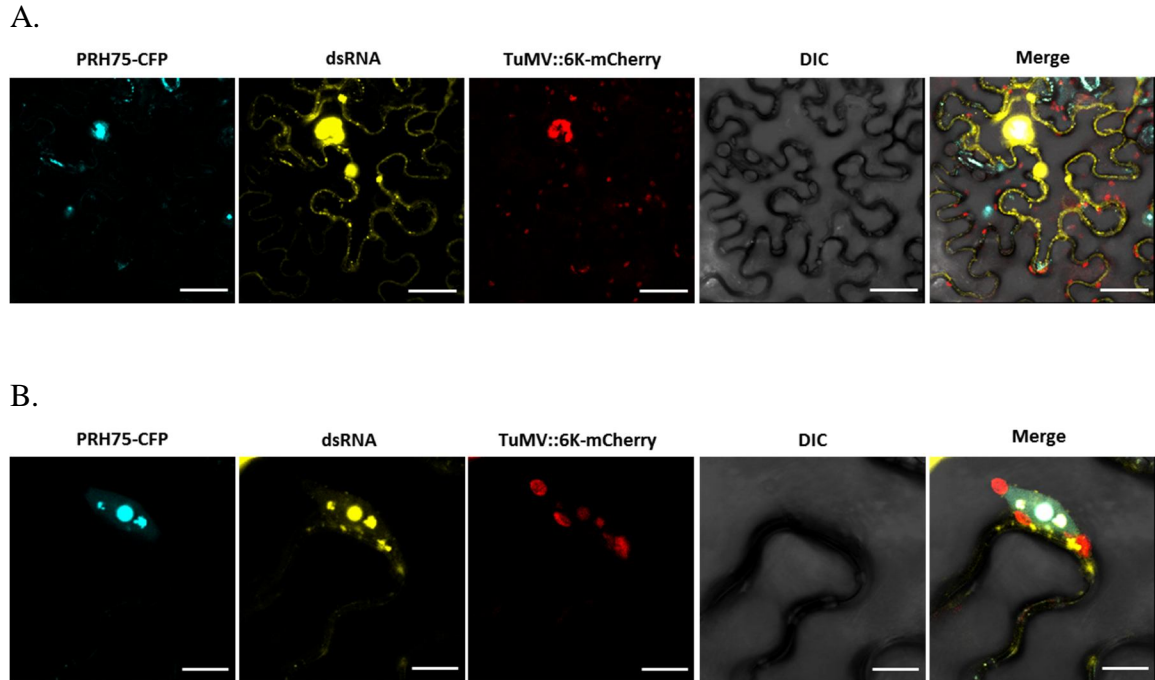


**Figure 34 PRH75-CFP colocalized with dsRNA-containing foci in the presence of TuMV infection.**

Co-agroinfiltration with constructs to co-express PRH75-CFP and the dRBFC assay into *N. benthamiana* leaves infected with TuMV::6K2-mCherry. Images were taken 48 h post agroinfiltration using a confocal microscopy. DIC, differential interference contrast. Bars in (A), 30  $\mu\text{m}$ , and in (B), 10  $\mu\text{m}$ .

## Chapter 4: Discussion

### 4.1 Identification of *Arabidopsis* DEAD-box RNA helicases as host factors required for TuMV infection

In this study, a functional genomics-based screening was performed to identify *Arabidopsis* DEAD-box RNA helicases (*AtRH* or *RH*) that are required for TuMV infection. From 42 selected putative *AtRH* genes in the *Arabidopsis* genome, homozygous T-DNA insertion lines for 26 *AtRH* genes were available. In an initial screening based on symptom severity after TuMV infection, three *Arabidopsis* T-DNA insertion lines, corresponding to the genes *AtRH9*, *AtRH26* and *PRH75*, were identified as showing less susceptibility to TuMV infection than wild-type controls. Although there was some variability in symptom development among individual plants within the same genotype, *atrh9*, *atrh26* and *prh75* T-DNA mutants showed suppressed TuMV infection in comparison with wild-type plants (Figure 4). Since the preliminary BiFC experiments did not find positive interactions between *AtRH26* and TuMV viral proteins (data not shown), I selected *AtRH9* and *PRH75* for further analysis.

ELISA assays of TuMV coat protein (CP) accumulation showed remarkably reduced amounts of CP in both *atrh9* and *prh75* T-DNA mutants (Figure 4). Consistently, quantitative RT-PCR analysis of viral RNA accumulation in newly-emerged leaves of TuMV-challenged *atrh9* and *prh75* T-DNA mutants suggested that viral replication was drastically inhibited compared with that in TuMV-infected WT plants (Figures 6, 13). This conclusion was further supported by the weak green fluorescence observed from the newly-emerged leaves of *atrh9* and *prh75* T-DNA insertion mutants infected by a GFP-tagged TuMV infectious clone, indicative of a delayed viral spread relative to WT controls (Figures 6, 13). Thus, these results strongly suggest that *AtRH9* and *PRH75* are required for TuMV infection.

Both *AtRH9* and *PRH75* belong to the family of DEAD-box RNA helicase proteins that have both RNA-binding and helicase activities. As briefly discussed in Chapter 1, several *AtRH*s, for example, *AtRH8* (Huang *et al.*, 2010), *AtRH20* (Kovalev *et al.*, 2012) *AtRH2* and *AtRH5* (Kovalev and Nagy, 2014) have been found to play functional roles in viral

infection. Here, our study has shown that AtRH9 and PRH75 are two potential host factors in the DEAD-box RNA helicase family associated with TuMV infection. The involvement of AtRH9 and PRH75 in TuMV infection and the mechanism underlying the association between DEAD-box RNA helicase and potyvirus infection, therefore became the main objective of the remainder of this thesis.

#### **4.2 AtRH9 and its recruitment for TuMV infection**

AtRH9 is a mitochondrial protein and may be involved in RNA metabolism in mitochondria as an RNA chaperon (Köhler *et al.*, 2010). The subcellular localization of AtRH9 was visualized as punctate particles in the cytoplasm (Figure 8), consistent with the reported mitochondrial distribution (Matthes *et al.*, 2007). It is worth noting that AtRH9 mRNA level is enhanced in response to biotic stress caused by different pathogens (Matthes *et al.*, 2007). Likewise, AtRH9 is involved in plant-pathogen interactions but its functional role therein is currently unknown.

To explore the functional role of AtRH9 in TuMV infection, the BiFC assay was conducted to test protein-protein interactions between AtRH9 and TuMV viral proteins. This analysis revealed that AtRH9 interacts with NIa-Pro (Figure 9), a virus-encoded protease. TuMV NIa-Pro is present in the VRC and is also responsible for catalyzing the cleavage of P3/6K1, 6K1/CI, CI/6K2, 6K2/NIa, NIa/NIb, NIb/CP and the cleavage site between VPg and NIa-Pro domains in NIa protein (Li *et al.*, 1997). However, no interaction between AtRH9 and NIa-Pro was detected by the Y2H assay (data not shown). It is possible that the interaction between AtRH9 and NIa-Pro found in the BiFC assay was either transient or mediated by one more host protein that binds to both AtRH9 and NIa-Pro and thus serves as a bridging interactor. Further study is needed to confirm the AtRH9 and NIa-Pro interaction and to elucidate the functional role played by AtRH9 in TuMV infection.

While our results demonstrate that AtRH9 is associated with TuMV infection through interaction with NIa-Pro, the biological mechanism is unclear at present. It is possible that AtRH9 may participate in the separation of RNA duplexes during viral genome

replication. Alternatively, AtRH9 is also likely to facilitate the proteolytic cleavage of TuMV polyprotein via interacting with NIa-Pro.

### 4.3 PRH75 and its roles in TuMV infection

#### 4.3.1 PRH75 is a nuclear-localized ATP-dependent DEAD-box RNA helicase

In this study, we have shown that PRH75 is a nuclear-localized DEAD-box RNA helicase in *Arabidopsis* and that it is associated with TuMV infection (Figures 17, 18). This conclusion is based on an intensive screening of *Arabidopsis atrh* T-DNA insertion lines for their susceptibility to TuMV infection. Consistent with the previous findings, the sequence analysis clearly demonstrates that PRH75 contains the conserved DEAD domain and RNA-binding domain characterized as RGG repeats at the carboxyl-terminal extension, which is also found in nucleolar fibrillarin and nucleolin (Figure 16). In addition, all the conserved domains for ATP-dependent RNA helicase activity are present in PRH75 (Figure 15). Recently, ATP-dependent RNA unwinding activity of PRH75 has been reported (Nayak *et al.*, 2013). *Arabidopsis PRH75* encodes an essential enzyme which is required for embryo development, thus *PRH75* is referred to as an *embryo defective* gene (Nayak *et al.*, 2013). Given the lethality of *prh75* T-DNA knockout mutant, it is suggested there is no functional redundancy between PRH75 and other DEAD-box RNA helicase.

#### 4.3.2 PRH75 interacts with multiple viral proteins that are essential for TuMV replication

In this study, BiFC assays revealed a positive interaction between PRH75 and several viral proteins, including NIa-Pro, VPg, CI and NIB, respectively (Figure 19). The intimate association between PRH75 and these viral proteins was confirmed by FRET analysis (Figure 21). However, Y2H assays only detected the positive interactions of PRH75 with NIB, VPg, and CI, respectively, but not with NIa-Pro (Figure 20). The absence of the expected protein-protein interaction between PRH75 and NIa-Pro is probably due to weak or transient interaction intensity or lack of protein partners required for the interaction. Nonetheless, PRH75 interacts with TuMV NIa-Pro, VPg, CI and NIB,



which represent four primary components involved in the viral replication complex (VRC) (Wei *et al.*, 2010).

Potyviral NIa contains two nuclear localization signals (NLS) and localizes in the nucleus where NIa may induce nuclear inclusions. Mutation of NIa NLS results in a significant decrease of viral genome amplification, which indicates that nuclear localization and transport of NIa plays an essential role for viral infection (Restrepo *et al.*, 1990; Schaad *et al.*, 1996; Rajamäki and Valkonen, 2009). NIa contains an N-terminal VPg domain and a C-terminal NIa-Pro protease domain. NIa is processed into two functional proteins VPg and NIa-Pro, during proteolytic cleavage by the C-terminal NIa-Pro protease (Carrington and Dougherty, 1987). The nuclear localization of PRH75 supports the hypothesis that its interaction with NIa-Pro and/or VPg in the nucleus is critical for viral infection. Furthermore, two identified TuMV host factors, namely *Arabidopsis* PABP and eIF(iso)4E, have been found to interact and associate with TuMV VPg-Pro (NIa) in the nucleus during TuMV infection (Beauchemin *et al.*, 2007; Beauchemin and Laliberté, 2007), providing precedent for this type of interaction. Consistently, NIa has recently been observed to interact with nucleolar fibrillain and this interaction may play a role in suppression of virus-induced gene silencing during PVA infection (Rajamäki and Valkonen, 2009).

Potyviral VPg is a multifunctional protein implicated in viral RNA replication and translation, cell-to-cell and long-distance movement, and virulence determination (Schaad *et al.*, 1996; Schaad *et al.*, 1997; Keller *et al.*, 1998; Lellis *et al.*, 2002). Potyviral VPg can be uridylated by NIb, the RNA-dependent RNA polymerase and serve as a primer for viral RNA synthesis during replication (Puustinen and Mäkinen, 2004). Given its intrinsic structure flexibility (Grzela *et al.*, 2008; Hébrard *et al.*, 2009), VPg could function as a hub protein to interact with diverse viral and host proteins to regulate different functions during viral infection (Jiang and Laliberté, 2011; Rantalainen *et al.*, 2011). The presence of VPg at the 5' end of the TuMV genome and its ability to interact with host factors eIF4E or eIF(iso)4E, which belong to the host translation machinery, strongly demonstrates that VPg is essential for viral RNA translation (Wittmann *et al.*, 1997; Schaad *et al.*, 2000; Lellis *et al.*, 2002; Roudet-Tavert *et al.*, 2007). In addition,

host proteins such as PVIP (Dunoyer *et al.*, 2004), PABP (Dufresne *et al.*, 2008), eEF1A (Thivierge *et al.*, 2008) and AtRH8 (Huang *et al.*, 2010) have also been reported to interact with VPg. The self-interaction of VPg (Guo *et al.*, 2001) and interactions between P1 (Merits *et al.*, 1999), HC-Pro (Roudet-Tavert *et al.*, 2007), P3 (Merits *et al.*, 1999), CI (Tavert-Roudet *et al.*, 2012), Nib (Li *et al.*, 1997) and CP (Zilian and Maiss, 2011) have been discovered in potyviruses as well. It is worth noting that the interactome between VPg and potyviral proteins reveals the importance of co-ordinated functions with other potyviral proteins during viral infection. The ability of PRH75 to bind to VPg suggests the possibility that PRH75 may play a role in viral genome translation via interaction with VPg. Since VPg has been shown to promote viral translation by increasing the stability of viral RNA (Eskelin *et al.*, 2011), PRH75 may be required for stabilization of viral RNA to secure efficient translation as an RNA chaperone.

Potyviral CI possesses ATPase and RNA helicase activities, which are involved in the unfolding of RNA secondary structures during viral genome replication. Mutation of conserved helicase domain residues of CI causes a significant reduction of viral RNA replication (Carrington *et al.*, 1998). Together with VPg and Nib, CI and host translation factors eIF(iso)4E were observed to associate with the VRC in TuMV-infected leaves (Cotton *et al.*, 2009; Tavert-Roudet *et al.*, 2012). It was also found that CI colocalized with dsRNA punctates in the VRC (Cotton *et al.*, 2009) and assisted cell-to-cell transport of virions through the PD by interacting with P3N-PIPO (Wei *et al.*, 2010). These findings have revealed a pivotal role for CI in viral genome replication, translation and intercellular movement. That is, CI not only acts as an RNA helicase to catalyse the separation of RNA duplexes but also coordinates viral RNA replication and translation by association with both viral RNA polymerase (Nib) and eIF(iso)4E as well as to facilitate viral movement by association with P3N-PIPO. The interaction between PRH75 and CI reinforces the idea of the involvement of PRH75 in the VRC and suggested that PRH75 associated with CI and Nib to form the protein complex which was responsible for viral genome replication. Moreover, the association of PRH75 with TuMV CI may raise the possibility that both viral helicase and cellular helicase are required for viral replication and suggest that PRH75 may work synergistically with viral helicase CI.

TuMV Nib is a viral RNA-dependent RNA polymerase which catalyzes the synthesis of new viral genomic RNA. The Nib protein accumulates predominantly in the nucleus as nuclear inclusions and is also recruited into the cytoplasmic membrane-bound vesicles that house the VRC during viral infection (Restrepo *et al.*, 1990; Dufresne *et al.*, 2008; Thivierge *et al.*, 2008). Recently, Nib has been identified to be the interacting partner of SCE1, a SUMO-conjugating enzyme by the Wang laboratory (Xiong and Wang, 2013). As a result, Nib is SUMOylated. Silencing *SCE1* could confer resistance to potyvirus infection. Thus, SUMOylation plays a crucial role in the potyvirus replication process, which may directly regulate the function of Nib (Xiong and Wang, 2013). More recent data suggest that Nib is predominantly SUMOylated with small ubiquitin-like modifier 3 (SUMO3), and mimicking SUMOylation of Nib changes its partition between the nucleus and cytoplasm (Xiong *et al.*, unpublished data). Intriguingly, using SCE1 as bait, the Y2H screening identified PRH75 as one of SUMO substrates in *Arabidopsis* and the SUMOylation assay showed that PRH75 is SUMOylated by SUMO3 (Elrouby and Coupland, 2010). Given that Nib and PRH75 interact with each other and both are SUMOylated, it is tempting to speculate that PRH75 is involved in Nib SUMOylation to regulate TuMV infection. Alternatively, as SUMOylation of Nib facilitates its cytoplasm localization and recruitment to the VRC through interacting with 6K2-VPg-Pro, it is also possible that the SUMOylated form of PRH75 allows its redistribution from the nucleus to the cytoplasm and the cytoplasmic PRH75-Nib complex can be brought to the VRC by PRH75 or Nib through interacting with viral replicase components essential for TuMV replication.

#### 4.3.3 Localization of PRH75 and its recruitment to viral replication complex (VRC)

To establish the subcellular localization of the various protein complexes of PRH75 with different viral proteins during TuMV infection, the BiFC assay was conducted with co-expression of Nib-YN, NIa-Pro-YN, VPg-YN or CI-YN with PRH75-YC, respectively, in TuMV-infected leaves. The distribution of BiFC interacting signals between PRH75 with Nib, NIa-Pro, VPg or CI was observed in the nucleus as well as along with 6K2-induced vesicles in the presence of TuMV infection (Figure 31). This is in contrast with the observation that PRH75 mainly interacted with viral proteins in the nucleus in the

absence of TuMV infection (Figure 19). These results have demonstrated that the interactions of PRH75 with TuMV viral replicase proteins occur in the nucleus and in the cytoplasmic 6K2-induced vesicles during viral infection. This is consistent with the previously published data that, during viral genome replication, TuMV replicase proteins such as NIb and VPg-Pro (NIa) are localized in the cytoplasm and, to a greater extent, in the nucleus of infected cells (Restrepo *et al.*, 1990; Li *et al.*, 1997). Although the primary localization of PRH75 is in the nucleus, PRH75 is likely undergoing intracellular translocation from the nucleus to cytoplasm as a result of interacting with multiple viral proteins essential for viral replication in the VRC or is intercepted to join the VRC before it is targeted to the nucleus. The association of PRH75 with the viral replicase components in the nucleus and cytoplasm was further confirmed by the colocalization studies of PRH75 and TuMV NIb, NIa-Pro, VPg and CI (Figures 30).

The cytoplasmic 6K2-induced vesicles have been reported to be membrane-associated vesicular structures that contain the viral RNA and the viral and host proteins required for viral replication (Grangeon *et al.*, 2010). The host translation machinery components such as eIF(iso)4E, PABP and eEF1A have also been shown to be present in the 6K2-induced vesicles, suggesting 6K2-induced vesicles may represent the site for viral protein synthesis as well as viral genome replication (Beauchemin *et al.*, 2007; Beauchemin and Laliberté, 2007; Thivierge *et al.*, 2008). Observations using confocal microscopy have identified the overlap localization pattern between PRH75 and 6K2-induced membranous vesicles along the outer chloroplast envelope (Figure 32). Furthermore, TuMV VPg-Pro (NIa), NIb and CI have been reported to be associated with viral dsRNA within the VRC (Cotton *et al.*, 2009). Consistently, PRH75 colocalizes with dsRNA foci during viral infection which indicates the presence of PRH75 in the VRC and may play a functional role during viral replication (Figure 34).

In this study, I was able to demonstrate that PRH75 colocalized with 6K2-induced vesicles and viral dsRNA (Figures 32, 34). Moreover, the intimate association with four primary components of viral replication complexes indicates that PRH75 may serve as an important host component of the VRC. Collectively, these data support a possible functional role of PRH75 in TuMV genome translation and/or replication. It is certainly

noteworthy that recruitment of PRH75 to the VRC is favourable for TuMV infection. Given the biological function of PRH75 as an efficient RNA helicase that can unwind the RNA duplexes, the emerging picture of PRH75 associated with TuMV infection is that PRH75 may alternate or remodel the secondary structure of the viral genomic RNA during viral translation or separate the viral dsRNA intermediates during the process of viral RNA replication.

#### 4.3.4 *Arabidopsis* PRH75 is highly dynamic

It is well known that nuclear and nucleolar proteins are highly dynamic. Nucleolar proteins are in a constant flux, moving in and out of the nucleolus. As a result many of them may exhibit altered distribution patterns during interactions with different proteins or complexes, especially in response to stresses (Mayer and Grummt, 2005).

*Arabidopsis* PRH75 is predominantly localized in the nucleus, preferentially targeting to the nucleolus under normal conditions (Figure 17). In the presence of TuMV infection, PRH75 was found to be recruited to the cytoplasmic VRC (Figure 31, 32). Therefore, we speculate that the subsequent recruitment of PRH75 to the VRC may indicate a constant association with viral replicase components for TuMV genome replication under viral infection. Similarly, another DEAD-box protein, AtRH2, which is the *Arabidopsis* ortholog of the mammalian DEAD-box helicase eIF4A-III, is relocalized from the nucleoplasm to the nucleolus and splicing speckles under hypoxic stress (Koroleva *et al.*, 2009). In a recent study, it was reported that, as a component of the cytoplasmic tombusvirus VRC, AtRH2 destabilizes viral dsRNA replication intermediates and promotes bringing the 5' and 3' terminal negative-sense RNA sequences in close vicinity via long-range RNA-RNA base pairing. The newly formed RNA structure promoted by AtRH2 together with AtRH20 might facilitate the recycling of the viral replicase components for multiple rounds of positive-sense viral RNA synthesis (Kovalev and Nagy, 2014). It is not clear if PRH75 plays a similar role in TuMV infection or if there are any overlapping functions between PRH75 and AtRH2.

#### 4.4 Nucleus, nucleolus and virus life cycle

##### 4.4.1 The nucleolus functions as a stress sensor in response to viral infection

The notion that the nucleolus could function as a stress sensor is well documented (Boulon *et al.*, 2010). The nucleolus is the ribosome factory where most events of ribosome biogenesis, such as ribosomal RNA synthesis, processing, and ribosome subunit assembly, take place. Apart from ribosome subunit biogenesis, the nucleolus appears to be involved in other cellular functions such as stress signalling, viral infection response and DNA repair (Mayer and Grummt, 2005).

After exposure to environmental or cellular stress, the nucleolus plays a critical role in monitoring and sensing the cellular stress signals (Olson, 2004). The nucleolar stress response includes profound alteration in the composition or organization of the nucleolus. For example, nucleolar proteins could translocate to the nucleoplasm under stress conditions. It is anticipated that the dynamic sequestration of nucleolar proteins between different sub-nuclear compartments is crucial for nucleolar stress response (Koroleva *et al.*, 2009).

Although the relation between nucleus, nucleolus and virus infection has been a research interest in the last decade, it is still far beyond our understanding of a clear picture. However, it is well established that, during viral infection, various viral components could traffic in and out of the nucleolus or the nucleus, and some nucleolar proteins are translocated out the nucleolus or non-nucleolar proteins enter the nucleolus to fulfill their functions (Salveti and Greco, 2014).

##### 4.4.2 Nuclear import of TuMV viral proteins is mediated by *Arabidopsis* importin $\alpha$

Although most RNA viruses are predominantly cytoplasmic during their life cycle, there are diverse strategies utilized by RNA viruses in which they can recruit nuclear and nucleolar components, or direct host cellular functions within the nucleus, in order to facilitate their reproductive processes, such as viral genome replication, virus assembly and intracellular trafficking (Hiscox, 2003; Weidman *et al.*, 2003). An increasing number of studies have highlighted the importance of the functions of nucleus and nucleolus, with

special regards to some RNA virus families, namely, positive-sense, single-stranded RNA viruses belonging to the *Flaviviridae*, *Coronaviridae* and *Togaviridae* families. For example, members of *Flaviviridae* include HCV, DENV, WNV (Rice, 1996). Members of *Coronaviridae* include SARS-CoV and *Infectious bronchitis virus* (IBV) (Siddell, 1995).

Indeed, many positive-sense, single-stranded RNA viruses can interact with proteins associated with host nucleus or induce the translocation of host proteins from the nucleus. The functional relevance between nucleus or nucleolus localization of viral proteins and viral genome replication remains less well understood. However, the need of efficient trafficking of viral proteins from the cytoplasm to the nucleus has been shown to be essential for viral infection (Restrepo *et al.*, 1990).

Despite the fact that virus-encoded proteins are usually small in size and thus could passively diffuse through the nuclear pores, active transport of viral proteins into the nucleus has been well demonstrated (Kamata *et al.*, 2005). The localization of proteins to the nucleus or nucleolus is mediated by dedicated targeting mechanisms that recognize specific protein motifs and contribute to the efficiency of nuclear or nucleolar transport of the proteins. Most proteins that are imported to the nucleus or the nucleolus contain the nuclear localization signal (NLS) or nucleolar localization signal (NoLS). Similarly, viral NLS or NoLS have been identified within potyviral NIb and NIa (Carrington *et al.*, 1991; Li and Carrington, 1993; Schaad *et al.*, 1996). Furthermore, many studies have suggested that viruses can recognize and utilize the host's nuclear import machinery to gain access to the nucleus (Krichevsky *et al.*, 2006).

Plant nuclear import and export machinery is composed of a network of proteins that shuttle between the nucleus and the cytoplasm, allowing substrate exchange through the nuclear pore complexes (NPC) (Doye and Hurt, 1997). Among them, importin  $\alpha$  and importin  $\beta$  are two of the best characterized nuclear import receptors that can bind to the substrates and translocate them into the nucleus (Goldfarb *et al.*, 2004). In the cytoplasm, importin  $\alpha$  could bind to proteins containing NLS or NoLS via its NLS- or NoLS-binding region. The importin  $\alpha$  complex is then targeted and transported into the nucleus through

the nuclear pore complexes. In *Arabidopsis*, importin  $\alpha$  is capable of mediating the nuclear import of proteins without the requirement for importin  $\beta$  (Krichevsky *et al.*, 2006).

Our data demonstrate that two *Arabidopsis* importin  $\alpha$  isoforms, IMPA1 and IMPA2 directly interact with TuMV NIB, NIa-Pro, VPg and CI *in vivo* and *in vitro* (Figures 24-27). Interestingly, our study also shows that PRH75 interacts with both IMPA1 and IMPA2 in the nucleus which is consistent with the colocalization result between PRH75 with IMPA1 and IMPA2 (Figures 22, 23, 28). The reason for the association between importin  $\alpha$ , TuMV viral proteins and PRH75 is not clear. It is possible that the function of importin  $\alpha$  is to serve as an adaptor that links TuMV viral proteins to PRH75 to form the ternary complex at the periphery of the NPC. Attempts to knockdown both *IMPA1* and *IMPA2* using VIGS were not successful (data not shown). *Arabidopsis* has nine importin  $\alpha$  isoforms and functional redundancy is very likely (Bhattacharjee *et al.*, 2008). Our study is the first to investigate and provide evidence for the functional roles of *Arabidopsis* importin  $\alpha$  in nuclear import of TuMV viral proteins via the interaction with viral proteins.

Our finding that *Arabidopsis* IMPA1 and IMPA2 directly interact with TuMV NIB, NIa-Pro, VPg and CI is consistent with those studies reported previously. RNA silencing suppressor protein 2b of CMV is imported into the nucleus via the interaction with *Arabidopsis* importin  $\alpha$  to counteract the RNA silencing defence in the host nucleus (Wang *et al.*, 2004). HIV-encoded Rev protein, which is an essential regulator of viral gene expression, is responsible for promoting the nuclear export of unspliced and partially spliced mRNA (Dvorin and Malim, 2003). It is also a nuclear factor that could be imported into the nucleus by direct binding to human importin  $\beta$  (Henderson and Percipalle, 1997). Moreover, recent studies have shown that the nuclear import of HIV-1 integrase is mediated by importin  $\alpha$ . HIV-1 replication is significantly impaired in *importin*  $\alpha$  knockdown HeLa cells (Nitahara-Kasahara *et al.*, 2007; Ao *et al.*, 2010; Levin *et al.*, 2010).



Altogether, this work suggests that the association with *Arabidopsis* importin  $\alpha$  is likely involved in the trafficking of TuMV viral proteins from the cytoplasm to the nucleus. This observation may broaden our understanding of nuclear import strategy employed by potyviruses as well as open a new investigation area for engineering antiviral strategies. However, more research attention should be paid to elucidate the mechanism underlying the nuclear import machinery during potyvirus life cycle.

#### 4.5 Major findings and future directions

Although considerable effort has been made in discovering the host proteins involved in potyvirus infection, the vast majority of components are still unknown. In this study, we screened *Arabidopsis* T-DNA insertion mutants of *AtRHs* against TuMV infection and identified three mutants, *atrh9*, *atrh26* and *prh75* exhibiting reduced symptoms after TuMV infection. Among them, we found that TuMV NIB, NIa-Pro, VPg and CI interact with PRH75, a nuclear-localized DEAD-box RNA helicase, in the nucleus. In TuMV-infected cells, PRH75 also associates with NIB, NIa-Pro, VPg and CI that are primary components of the VRC in the cytoplasm. Moreover, PRH75 colocalized with viral dsRNA in the VRC in the presence of viral infection. Furthermore, we presented evidence that viral accumulation and replication are inhibited if *PRH75* is knocked down and concluded that PRH75 is required for TuMV infection. These findings highlight the important role of DEAD-box RNA helicases in potyvirus life cycle and will certainly shed light into the intricate relation between viruses and their hosts. Future studies should focus on unveiling the underlying molecular mechanism of the functional role DEAD-box RNA helicases play during potyvirus infection.

The involvement of nuclear RNA helicases in the viral infection process has been proposed in several independent studies. For example, RNA helicase DDX56 in the nucleolus can bind to WNV capsid protein and be recruited to the cytoplasm for viral genome replication during WNV infection (Xu *et al.*, 2011; Xu and Hobman, 2012). Nucleolin has been reported to colocalize with the NS5B protein of HCV outside the nucleolus, in the perinuclear region during HCV infection (Shimakami *et al.*, 2006; Kusakawa *et al.*, 2007).

Based on the data presented in this study, we propose a model in which PRH75 has versatile functions in TuMV infection (Figure 35). *Arabidopsis* DEAD-box RNA helicase PRH75 interacts with TuMV Nib, VPg, NIa-Pro and CI in the nucleus. The nuclear transport of viral proteins is mediated by *Arabidopsis* importin  $\alpha$ . During TuMV infection, PRH75 is recruited to 6K2-induced viral replication complex via interacting with the important viral components Nib, VPg, NIa-Pro and CI and may assist in unwinding of viral RNA duplexes during the replication process. Downregulation of *PRH75* in *Arabidopsis* impedes the viral infection. Thus, PRH75 serves as an important host factor required for TuMV infection. However, the precise function of PRH75 in potyvirus infection remains to be further explored in the future.

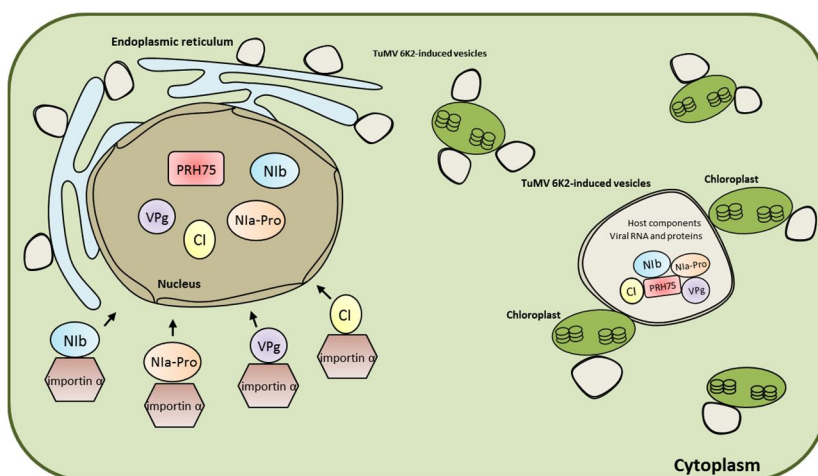


**Figure 35 Working model for *Arabidopsis* PRH75 associated with TuMV infection.**

## Reference

- Abbink TE, Tjernberg PA, Bol JF, Linthorst HJ** (1998) Tobacco mosaic virus helicase domain induces necrosis in N gene-carrying tobacco in the absence of virus replication. *Molecular plant-microbe interactions* **11**: 1242-1246
- Adams MJ, Antoniw JF, Beudoin F** (2005) Overview and analysis of the polyprotein cleavage sites in the family Potyviridae. *Molecular plant pathology* **6**: 471-487
- Ahlquist P, Noueir AO, Lee W-M, Kushner DB, Dye BT** (2003) Host factors in positive-strand RNA virus genome replication. *Journal of Virology* **77**: 8181-8186
- Andreou AZ, Klostermeier D** (2013) The DEAD-box helicase eIF4A. *RNA biology* **10**: 19-32
- Andret-Link P, Fuchs M** (2005) Transmission specificity of plant viruses by vectors. *Journal of Plant Pathology*: 153-165
- Anindya R, Savithri HS** (2004) Potyviral NIa proteinase, a proteinase with novel deoxyribonuclease activity. *Journal of Biological Chemistry* **279**: 32159-32169
- Ao Z, Jayappa KD, Wang B, Zheng Y, Kung S, Rassart E, Depping R, Kohler M, Cohen EA, Yao X** (2010) Importin  $\alpha 3$  interacts with HIV-1 integrase and contributes to HIV-1 nuclear import and replication. *Journal of virology* **84**: 8650-8663
- Ariumi Y, Kuroki M, Abe K-i, Dansako H, Ikeda M, Wakita T, Kato N** (2007) DDX3 DEAD-box RNA helicase is required for hepatitis C virus RNA replication. *Journal of virology* **81**: 13922-13926
- Astier S, Albouy J, Maury Y, Lecoq H** (2001) Principles of plant virology: genome, pathogenicity, virus ecology. Institut National de la Recherche Agronomique
- Aubourg S, Kreis M, Lecharny A** (1999) The DEAD box RNA helicase family in *Arabidopsis thaliana*. *Nucleic Acids Research* **27**: 628-636
- Azevedo J, Garcia D, Pontier D, Ohnesorge S, Yu A, Garcia S, Braun L, Bergdoll M, Hakimi MA, Lagrange T** (2010) Argonaute quenching and global changes in Dicer homeostasis caused by a pathogen-encoded GW repeat protein. *Genes & development* **24**: 904-915
- Baulcombe D** (2004) RNA silencing in plants. *Nature* **431**: 356-363
- Beauchemin C, Boutet N, Laliberté JF** (2007) Visualization of the interaction between the precursors of VPg, the viral protein linked to the genome of Turnip mosaic

virus, and the translation eukaryotic initiation factor iso 4E in planta. *Journal of Virology* **81**: 775-782

**Beauchemin C, Laliberté JF** (2007) The poly(A) binding protein is internalized in virus-induced vesicles or redistributed to the nucleolus during turnip mosaic virus infection. *Journal of Virology* **81**: 10905-10913

**Beijerinck M** (1898) Concerning a contagium viwm fluidum as cause of the spot disease of tobacco leaves.

**Belov GA, Altan-Bonnet N, Kovtunovych G, Jackson CL, Lippincott-Schwartz J, Ehrenfeld E** (2007) Hijacking components of the cellular secretory pathway for replication of poliovirus RNA. *Journal of virology* **81**: 558-567

**Bendahmane A, Kanyuka K, Baulcombe DC** (1999) The Rx gene from potato controls separate virus resistance and cell death responses. *The Plant Cell Online* **11**: 781-791

**Bendahmane A, Querci M, Kanyuka K, Baulcombe DC** (2000) Agrobacterium transient expression system as a tool for the isolation of disease resistance genes: application to the Rx2 locus in potato. *The Plant Journal* **21**: 73-81

**Bent AF, Mackey D** (2007) Elicitors, effectors, and R genes: the new paradigm and a lifetime supply of questions. *Annu. Rev. Phytopathol.* **45**: 399-436

**Bhattacharjee S, Lee L-Y, Oltmanns H, Cao H, Cuperus J, Gelvin SB** (2008) IMPa-4, an Arabidopsis importin  $\alpha$  isoform, is preferentially involved in Agrobacterium-mediated plant transformation. *The Plant Cell Online* **20**: 2661-2680

**Blanc S, López-Moya J-J, Wang R, Garcí a-Lampasona S, Thornbury DW, Pirone TP** (1997) A specific interaction between coat protein and helper component correlates with aphid transmission of a potyvirus. *Virology* **231**: 141-147

**Blevins T, Rajeswaran R, Shivaprasad PV, Beknazariants D, Si-Ammour A, Park H-S, Vazquez F, Robertson D, Meins F, Hohn T** (2006) Four plant Dicers mediate viral small RNA biogenesis and DNA virus induced silencing. *Nucleic acids research* **34**: 6233-6246

**Boller T, Felix G** (2009) A renaissance of elicitors: perception of microbe-associated molecular patterns and danger signals by pattern-recognition receptors. *Annual review of plant biology* **60**: 379-406

**Boudet N, Aubourg S, Toffano-Nioche C, Kreis M, Lecharny A** (2001) Evolution of intron/exon structure of DEAD helicase family genes in Arabidopsis, Caenorhabditis, and Drosophila. *Genome research* **11**: 2101-2114

**Boulon S, Westman BJ, Hutten S, Boisvert F-M, Lamond AI** (2010) The nucleolus under stress. *Molecular cell* **40**: 216-227

- Brodersen P, Voinnet O** (2006) The diversity of RNA silencing pathways in plants. *TRENDS in Genetics* **22**: 268-280
- Burch-Smith TM, Schiff M, Liu Y, Dinesh-Kumar SP** (2006) Efficient virus-induced gene silencing in Arabidopsis. *Plant Physiology* **142**: 21-27
- Burch-Smith TM, Zambryski PC** (2010) Loss of increased size exclusion limit (ise)1 or ise2 increases the formation of secondary plasmodesmata. *Current Biology* **20**: 989-993
- Burgyán J, Havelda Z** (2011) Viral suppressors of RNA silencing. *Trends in plant science* **16**: 265-272
- Bushell M, Sarnow P** (2002) Hijacking the translation apparatus by RNA viruses. *The Journal of cell biology* **158**: 395-399
- Callaway A, Giesman-Cookmeyer D, Gillock E, Sit T, Lommel S** (2001) The multifunctional capsid proteins of plant RNA viruses. *Annual review of phytopathology* **39**: 419-460
- Cao M, Du P, Wang X, Yu Y-Q, Qiu Y-H, Li W, Gal-On A, Zhou C, Li Y, Ding S-W** (2014) Virus infection triggers widespread silencing of host genes by a distinct class of endogenous siRNAs in Arabidopsis. *Proceedings of the National Academy of Sciences* **111**: 14613-14618
- Carrington JC, Dougherty WG** (1987) Small nuclear inclusion protein encoded by a plant potyvirus genome is a protease. *Journal of virology* **61**: 2540-2548
- Carrington JC, Freed DD, Leinicke AJ** (1991) Bipartite signal sequence mediates nuclear translocation of the plant potyviral NIa protein. *The Plant Cell Online* **3**: 953-962
- Carrington JC, Jensen PE, Schaad MC** (1998) Genetic evidence for an essential role for potyvirus CI protein in cell-to-cell movement. *The Plant Journal* **14**: 393-400
- Carter J, Saunders VA** (2007) *Virology: principles and applications*. John Wiley & Sons
- Casteel CL, Yang C, Nanduri AC, Jong HN, Whitham SA, Jander G** (2014) The NIa - Pro protein of Turnip mosaic virus improves growth and reproduction of the aphid vector, *Myzus persicae* (green peach aphid). *The Plant Journal* **77**: 653-663
- Castelló MJ, Carrasco JL, Vera P** (2010) DNA-binding protein phosphatase AtDBP1 mediates susceptibility to two potyviruses in Arabidopsis. *Plant Physiology* **153**: 1521-1525

- Chapman EJ, Prokhnevsky AI, Gopinath K, Dolja VV, Carrington JC** (2004) Viral RNA silencing suppressors inhibit the microRNA pathway at an intermediate step. *Genes & development* **18**: 1179-1186
- Chen Y, Potratz JP, Tijerina P, Del Campo M, Lambowitz AM, Russell R** (2008) DEAD-box proteins can completely separate an RNA duplex using a single ATP. *Proceedings of the National Academy of Sciences* **105**: 20203-20208
- Chinnusamy V, Schumaker K, Zhu JK** (2004) Molecular genetic perspectives on cross-talk and specificity in abiotic stress signalling in plants. *Journal of experimental botany* **55**: 225-236
- Chisholm ST, Mahajan SK, Whitham SA, Yamamoto ML, Carrington JC** (2000) Cloning of the Arabidopsis RTM1 gene, which controls restriction of long-distance movement of tobacco etch virus. *Proceedings of the National Academy of Sciences* **97**: 489-494
- Chisholm ST, Parra MA, Anderberg RJ, Carrington JC** (2001) Arabidopsis RTM1 and RTM2 genes function in phloem to restrict long-distance movement of tobacco etch virus. *Plant Physiology* **127**: 1667-1675
- Chowda-Reddy RV, Sun H, Chen H, Poysa V, Ling H, Gijzen M, Wang A** (2011) Mutations in the P3 protein of Soybean mosaic virus G2 isolates determine virulence on Rsv4-genotype Soybean. *Molecular Plant-Microbe Interactions* **24**: 37-43
- Chung BY-W, Miller WA, Atkins JF, Firth AE** (2008) An overlapping essential gene in the Potyviridae. *Proceedings of the National Academy of Sciences* **105**: 5897-5902
- Collier SM, Moffett P** (2009) NB-LRRs work a “bait and switch” on pathogens. *Trends in plant science* **14**: 521-529
- Cordin O, Banroques J, Tanner NK, Linder P** (2006) The DEAD-box protein family of RNA helicases. *Gene* **367**: 17-37
- Cotton S, Grangeon R, Thivierge K, Mathieu I, Ide C, Wei T, Wang A, Laliberte JF** (2009) Turnip mosaic virus RNA replication complex vesicles are mobile, align with microfilaments, and are each derived from a single viral genome. *Journal of Virology* **83**: 10460-10471
- Cui X, Wei T, Chowda-Reddy RV, Sun G, Wang A** (2010) The Tobacco etch virus P3 protein forms mobile inclusions via the early secretory pathway and traffics along actin microfilaments. *Virology* **397**: 56-63
- Decroocq V, Sicard O, Alamillo JM, Lansac M, Eyquard JP, García JA, Candresse T, Le Gall O, Revers F** (2006) Multiple resistance traits control Plum pox virus

infection in *Arabidopsis thaliana*. *Molecular Plant-Microbe Interactions* **19**: 541-549

- Deleris A, Gallego-Bartolome J, Bao J, Kasschau KD, Carrington JC, Voinnet O** (2006) Hierarchical action and inhibition of plant Dicer-like proteins in antiviral defense. *Science* **313**: 68-71
- Diaz-Pendon JA, Truniger V, Nieto C, Garcia-Mas J, Bendahmane A, Aranda MA** (2004) Advances in understanding recessive resistance to plant viruses. *Molecular plant pathology* **5**: 223-233
- Ding S-W, Voinnet O** (2007) Antiviral immunity directed by small RNAs. *Cell* **130**: 413-426
- Ding SW** (2010) RNA-based antiviral immunity. *Nature Reviews Immunology* **10**: 632-644
- Dodds PN, Rathjen JP** (2010) Plant immunity: towards an integrated view of plant-pathogen interactions. *Nature Reviews Genetics* **11**: 539-548
- Dolja V, Haldeman R, Robertson N, Dougherty W, Carrington J** (1994) Distinct functions of capsid protein in assembly and movement of tobacco etch potyvirus in plants. *The EMBO journal* **13**: 1482
- Doye V, Hurt E** (1997) From nucleoporins to nuclear pore complexes. *Current opinion in cell biology* **9**: 401-411
- Dufresne PJ, Thivierge K, Cotton S, Beauchemin C, Ide C, Ubalijoro E, Laliberté JF, Fortin MG** (2008) Heat shock 70 protein interaction with Turnip mosaic virus RNA-dependent RNA polymerase within virus-induced membrane vesicles. *Virology* **374**: 217-227
- Dufresne PJ, Ubalijoro E, Fortin MG, Laliberte JF** (2008) *Arabidopsis thaliana* class II poly(A)-binding proteins are required for efficient multiplication of turnip mosaic virus. *Journal of General Virology* **89**: 2339-2348
- Dunoyer P, Thomas C, Harrison S, Revers F, Maule A** (2004) A Cysteine-Rich Plant Protein Potentiates Potyvirus Movement through an Interaction with the Virus Genome-Linked Protein VPg. *Journal of Virology* **78**: 2301-2309
- Duprat A, Caranta C, Revers F, Menand B, Browning KS, Robaglia C** (2002) The *Arabidopsis* eukaryotic initiation factor (iso)4E is dispensable for plant growth but required for susceptibility to potyviruses. *Plant Journal* **32**: 927-934
- Durrant W, Dong X** (2004) Systemic acquired resistance. *Annu. Rev. Phytopathol.* **42**: 185-209

- Dvorin J, Malim M** (2003) Intracellular trafficking of HIV-1 cores: journey to the center of the cell. *In* Cellular Factors Involved in Early Steps of Retroviral Replication. Springer, pp 179-208
- Earley KW, Haag JR, Pontes O, Opper K, Juehne T, Song K, Pikaard CS** (2006) Gateway-compatible vectors for plant functional genomics and proteomics. *Plant Journal* **45**: 616-629
- Edwardson JR, Christie R** (1991) A monograph on the potyvirus group. Monograph /Agricultural Experiment Station
- Edwardson JR, Christie RG** (1986) Viruses infecting forage legumes. Vol. 1. Florida Agricultural Experiment Stations Monograph Series: 1-246
- Elrouby N, Coupland G** (2010) Proteome-wide screens for small ubiquitin-like modifier (SUMO) substrates identify Arabidopsis proteins implicated in diverse biological processes. *Proceedings of the National Academy of Sciences* **107**: 17415-17420
- Erickson F, Dinesh-Kumar S, Holzberg S, Ustach C, Dutton M, Handley V, Corr C, Baker B** (1999) Interactions between tobacco mosaic virus and the tobacco N gene. *Philosophical Transactions of the Royal Society of London. Series B: Biological Sciences* **354**: 653-658
- Eskelin K, Hafrén A, Rantalainen KI, Mäkinen K** (2011) Potyviral VPg enhances viral RNA translation and inhibits reporter mRNA translation in planta. *Journal of virology* **85**: 9210-9221
- Fairman-Williams ME, Guenther U-P, Jankowsky E** (2010) SF1 and SF2 helicases: family matters. *Current opinion in structural biology* **20**: 313-324
- Fang J, Acheampong E, Dave R, Wang F, Mukhtar M, Pomerantz RJ** (2005) The RNA helicase DDX1 is involved in restricted HIV-1 Rev function in human astrocytes. *Virology* **336**: 299-307
- Fang J, Kubota S, Yang B, Zhou N, Zhang H, Godbout R, Pomerantz RJ** (2004) A DEAD box protein facilitates HIV-1 replication as a cellular co-factor of Rev. *Virology* **330**: 471-480
- Fauquet CM, Mayo M, Maniloff J, Desselberger U, Ball LA** (2005) Virus taxonomy: VIIIth report of the International Committee on Taxonomy of Viruses. Academic Press
- Fraser R, Van Loon LC** (1986) Genes for resistance to plant viruses. *Critical reviews in plant sciences* **3**: 257-294
- Fuller-Pace FV** (2006) DExD/H box RNA helicases: multifunctional proteins with important roles in transcriptional regulation. *Nucleic acids research* **34**: 4206-4215



- Gaffney T, Friedrich L, Vernooij B, Negrotto D, Nye G, Uknes S, Ward E, Kessmann H, Ryals J** (1993) Requirement of salicylic acid for the induction of systemic acquired resistance. *Science* **261**: 754-756
- Gallois JL, Charron C, Sanchez F, Pagny G, Houvenaghel MC, Moretti A, Ponz F, Revers F, Caranta C, German-Retana S** (2010) Single amino acid changes in the turnip mosaic virus viral genome-linked protein (VPg) confer virulence towards *Arabidopsis thaliana* mutants knocked out for eukaryotic initiation factors eIF(iso)4E and eIF(iso)4G. *Journal of General Virology* **91**: 288-293
- Gancarz BL, Hao L, He Q, Newton MA, Ahlquist P** (2011) Systematic identification of novel, essential host genes affecting bromovirus RNA replication. *PLoS ONE* **6**
- Garcia-Ruiz H, Takeda A, Chapman EJ, Sullivan CM, Fahlgren N, Bremel KJ, Carrington JC** (2010) *Arabidopsis* RNA-dependent RNA polymerases and dicer-like proteins in antiviral defense and small interfering RNA biogenesis during Turnip Mosaic Virus infection. *The Plant Cell Online* **22**: 481-496
- García JA, Glasa M, Cambra M, Candresse T** (2014) Plum pox virus and sharka: a model potyvirus and a major disease. *Molecular plant pathology* **15**: 226-241
- Gardner MW, Kendrick JB** (1921) Turnip mosaic. *Journal of Agricultural Research* **22**: 121
- Gibbs A, Ohshima K** (2010) Potyviruses and the digital revolution. *Annual review of phytopathology* **48**: 205-223
- Gibbs AJ, Ohshima K, Phillips MJ, Gibbs MJ** (2008) The prehistory of potyviruses: their initial radiation was during the dawn of agriculture. *PLoS One* **3**: e2523
- Goldbach R** (1987) Genome similarities between plant and animal RNA viruses. *Microbiological sciences* **4**: 197-202
- Goldfarb DS, Corbett AH, Mason DA, Harreman MT, Adam SA** (2004) Importin  $\alpha$ : a multipurpose nuclear-transport receptor. *Trends in cell biology* **14**: 505-514
- Gong Z, Dong C-H, Lee H, Zhu J, Xiong L, Gong D, Stevenson B, Zhu J-K** (2005) A DEAD box RNA helicase is essential for mRNA export and important for development and stress responses in *Arabidopsis*. *The Plant Cell Online* **17**: 256-267
- Gong Z, Lee H, Xiong L, Jagendorf A, Stevenson B, Zhu J-K** (2002) RNA helicase-like protein as an early regulator of transcription factors for plant chilling and freezing tolerance. *Proceedings of the National Academy of Sciences* **99**: 11507-11512

- Gorbalenya AE, Koonin EV** (1993) Helicases: amino acid sequence comparisons and structure-function relationships. *Current Opinion in Structural Biology* **3**: 419-429
- Govier D, Kassanis B** (1974) A virus-induced component of plant sap needed when aphids acquire potato virus Y from purified preparations. *Virology* **61**: 420-426
- Grangeon R, Agbeci M, Chen J, Grondin G, Zheng H, Laliberté JF** (2012) Impact on the endoplasmic reticulum and Golgi apparatus of turnip mosaic virus infection. *Journal of Virology* **86**: 9255-9265
- Grangeon R, Cotton S, Laliberté J-F** (2010) A model for the biogenesis of turnip mosaic virus replication factories. *Communicative & integrative biology* **3**: 363-365
- Grangeon R, Jiang J, Wan J, Agbeci M, Zheng H, Laliberté JF** (2013) 6K2-induced vesicles can move cell to cell during turnip mosaic virus infection. *Frontiers in Microbiology* **4**
- Grifo J, Tahara S, Leis J, Morgan M, Shatkin A, Merrick W** (1982) Characterization of eukaryotic initiation factor 4A, a protein involved in ATP-dependent binding of globin mRNA. *Journal of Biological Chemistry* **257**: 5246-5252
- Grzela R, Szolajska E, Ebel C, Madern D, Favier A, Wojtal I, Zagorski W, Chroboczek J** (2008) Virulence factor of potato virus Y, genome-attached terminal protein VPg, is a highly disordered protein. *Journal of Biological Chemistry* **283**: 213-221
- Guo D, Rajamäki M-L, Saarma M, Valkonen JP** (2001) Towards a protein interaction map of potyviruses: protein interaction matrixes of two potyviruses based on the yeast two-hybrid system. *Journal of General Virology* **82**: 935-939
- Guo HS, Ding SW** (2002) A viral protein inhibits the long range signaling activity of the gene silencing signal. *The EMBO journal* **21**: 398-407
- Hafrén A, Hofius D, Rönnholm G, Sonnewald U, Mäkinen K** (2010) HSP70 and its cochaperone CPIP promote potyvirus infection in *Nicotiana benthamiana* by regulating viral coat protein functions. *Plant Cell* **22**: 523-535
- Hamilton A, Voinnet O, Chappell L, Baulcombe D** (2002) Two classes of short interfering RNA in RNA silencing. *The EMBO Journal* **21**: 4671-4679
- Hartley JL, Temple GF, Brasch MA** (2000) DNA cloning using in vitro site-specific recombination. *Genome research* **10**: 1788-1795
- Hasiów-Jaroszewska B, Fares MA, Elena SF** (2014) Molecular Evolution of Viral Multifunctional Proteins: The Case of Potyvirus HC-Pro. *Journal of molecular evolution* **78**: 75-86

- Hébrard E, Bessin Y, Michon T, Longhi S, Uversky VN, Delalande F, Van Dorselaer A, Romero P, Walter J, Declerk N, Fargette D** (2009) Intrinsic disorder in Viral Proteins Genome-Linked: Experimental and predictive analyses. *Virology Journal* **6**
- Henderson BR, Percipalle P** (1997) Interactions between HIV Rev and nuclear import and export factors: the Rev nuclear localisation signal mediates specific binding to human importin- $\beta$ . *Journal of molecular biology* **274**: 693-707
- Hilbert M, Karow AR, Klostermeier D** (2009) The mechanism of ATP-dependent RNA unwinding by DEAD box proteins. *Biological chemistry* **390**: 1237-1250
- Himber C, Dunoyer P, Moissiard G, Ritzenthaler C, Voinnet O** (2003) Transitivity-dependent and-independent cell-to-cell movement of RNA silencing. *The EMBO Journal* **22**: 4523-4533
- Hiscox JA** (2003) The interaction of animal cytoplasmic RNA viruses with the nucleus to facilitate replication. *Virus research* **95**: 13-22
- Hofius D, Maier AT, Dietrich C, Jungkunz I, Börnke F, Maiss E, Sonnewald U** (2007) Capsid protein-mediated recruitment of host DnaJ-like proteins is required for Potato virus Y infection in tobacco plants. *Journal of virology* **81**: 11870-11880
- Hong X-Y, Chen J, Shi Y-H, Chen J-P** (2007) The '6K1' protein of a strain of Soybean mosaic virus localizes to the cell periphery. *Archives of virology* **152**: 1547-1551
- Hong Y, Hunt AG** (1996) RNA polymerase activity catalyzed by a potyvirus-encoded RNA-dependent RNA polymerase. *Virology* **226**: 146-151
- Hsieh Y-C, Omarov RT, Scholthof HB** (2009) Diverse and newly recognized effects associated with short interfering RNA binding site modifications on the Tomato bushy stunt virus p19 silencing suppressor. *Journal of virology* **83**: 2188-2200
- Huang TS, Wei T, Laliberté JF, Wang A** (2010) A host RNA helicase-like protein, AtRH8, interacts with the potyviral genome-linked protein, VPg, associates with the virus accumulation complex, and is essential for infection. *Plant Physiology* **152**: 255-266
- Hyodo K, Okuno T** (2014) Host factors used by positive-strand RNA plant viruses for genome replication. *Journal of General Plant Pathology* **80**: 123-135
- Ishibashi K, Masuda K, Naito S, Meshi T, Ishikawa M** (2007) An inhibitor of viral RNA replication is encoded by a plant resistance gene. *Proceedings of the National Academy of Sciences* **104**: 13833-13838

- Ivanov KI, Eskelin K, Lõhmus A, Mäkinen K** (2014) Molecular and Cellular Mechanisms Underlying Potyvirus Infection. *Journal of General Virology*: vir. 0.064220-064220
- Ivanov KI, Mäkinen K** (2012) Coat proteins, host factors and plant viral replication. *Current opinion in virology* **2**: 712-718
- Jackson RJ, Hellen CU, Pestova TV** (2010) The mechanism of eukaryotic translation initiation and principles of its regulation. *Nature reviews Molecular cell biology* **11**: 113-127
- Jenner CE, Wang X, Tomimura K, Ohshima K, Ponz F, Walsh JA** (2003) The dual role of the potyvirus P3 protein of Turnip mosaic virus as a symptom and avirulence determinant in brassicas. *Molecular plant-microbe interactions* **16**: 777-784
- Jiang J, Laliberté JF** (2011) The genome-linked protein VPg of plant viruses -A protein with many partners. *Current Opinion in Virology* **1**: 347-354
- Jiang Y, Serviène E, Gal J, Panavas T, Nagy PD** (2006) Identification of essential host factors affecting tombusvirus RNA replication based on the yeast Tet promoters Hughes Collection. *Journal of virology* **80**: 7394-7404
- Jiménez I, López L, Alamillo JM, Valli A, García JA** (2006) Identification of a Plum pox virus CI-interacting protein from chloroplast that has a negative effect in virus infection. *Molecular Plant-Microbe Interactions* **19**: 350-358
- Jin H** (2008) Endogenous small RNAs and antibacterial immunity in plants. *FEBS letters* **582**: 2679-2684
- Johansen IE, Lund OS, Hjulsager CK, Laursen J** (2001) Recessive resistance in *Pisum sativum* and potyvirus pathotype resolved in a gene-for-cistron correspondence between host and virus. *Journal of virology* **75**: 6609-6614
- Jones JD, Dangl JL** (2006) The plant immune system. *Nature* **444**: 323-329
- Kamata M, Nitahara-Kasahara Y, Miyamoto Y, Yoneda Y, Aida Y** (2005) Importin- $\alpha$  promotes passage through the nuclear pore complex of human immunodeficiency virus type 1 Vpr. *Journal of virology* **79**: 3557-3564
- Kang B-C, Yeam I, Jahn MM** (2005) Genetics of plant virus resistance. *Annu. Rev. Phytopathol.* **43**: 581-621
- Kant P, Kant S, Gordon M, Shaked R, Barak S** (2007) STRESS RESPONSE SUPPRESSOR1 and STRESS RESPONSE SUPPRESSOR2, two DEAD-box RNA helicases that attenuate Arabidopsis responses to multiple abiotic stresses. *Plant physiology* **145**: 814-830

- Karimi M, Inzé D, Depicker A** (2002) GATEWAY™ vectors for Agrobacterium-mediated plant transformation. *Trends in Plant Science* **7**: 193-195
- Karpova T, McNally JG** (2006) Detecting Protein-Protein Interactions with CFP-YFP FRET by Acceptor Photobleaching. *Current Protocols in Cytometry*: 12.17. 11-12.17. 11
- Kasschau KD, Carrington JC** (2001) Long-distance movement and replication maintenance functions correlate with silencing suppression activity of potyviral HC-Pro. *Virology* **285**: 71-81
- Kasschau KD, Cronin S, Carrington JC** (1997) Genome amplification and long-distance movement functions associated with the central domain of tobacco etch potyvirus helper component-proteinase. *Virology* **228**: 251-262
- Katiyar-Agarwal S, Jin H** (2010) Role of small RNAs in host-microbe interactions. *Annual review of phytopathology* **48**: 225
- Keller KE, Johansen E, Martin RR, Hampton R** (1998) Potyvirus genome-linked protein (VPg) determines pea seed-borne mosaic virus pathotype-specific virulence in *Pisum sativum*. *Molecular plant-microbe interactions* **11**: 124-130
- Khan JA, Dijkstra J** (2006) *Handbook of plant virology*. Food Products Press
- Kim JS, Kim KA, Oh TR, Park CM, Kang H** (2008) Functional characterization of DEAD-box RNA helicases in *Arabidopsis thaliana* under abiotic stress conditions. *Plant and cell physiology* **49**: 1563-1571
- King AM, Adams MJ, Lefkowitz EJ, Carstens EB** (2012) Virus taxonomy: classification and nomenclature of viruses: Ninth Report of the International Committee on Taxonomy of Viruses, Vol 9. Elsevier
- Knight H, Knight MR** (2001) Abiotic stress signalling pathways: specificity and cross-talk. *Trends in plant science* **6**: 262-267
- Kobayashi K, Otegui MS, Krishnakumar S, Mindrinos M, Zambryski P** (2007) INCREASED SIZE EXCLUSION LIMIT2 encodes a putative DEVH box RNA helicase involved in plasmodesmata function during *Arabidopsis* embryogenesis. *The Plant Cell Online* **19**: 1885-1897
- Köhler D, Schmidt-Gattung S, Binder S** (2010) The DEAD-box protein PMH2 is required for efficient group II intron splicing in mitochondria of *Arabidopsis thaliana*. *Plant molecular biology* **72**: 459-467
- Koroleva OA, Brown J, Shaw PJ** (2009) Localization of eIF4A-III in the nucleolus and splicing speckles is an indicator of plant stress. *Plant signaling & behavior* **4**: 1148-1151

- Koroleva OA, Calder G, Pendle AF, Kim SH, Lewandowska D, Simpson CG, Jones IM, Brown JWS, Shawa PJ** (2009) Dynamic behavior of Arabidopsis eIF4A-III, putative core protein of exon junction complex: Fast relocation to nucleolus and splicing speckles under hypoxia. *Plant Cell* **21**: 1592-1606
- Kovalev N, Barajas D, Nagy PD** (2012) Similar roles for yeast Dbp2 and Arabidopsis RH20 DEAD-box RNA helicases to Ded1 helicase in tombusvirus plus-strand synthesis. *Virology* **432**: 470-484
- Kovalev N, Nagy PD** (2014) The Expanding Functions of Cellular Helicases: The Tombusvirus RNA Replication Enhancer Co-opts the Plant eIF4AIII-Like AtRH2 and the DDX5-Like AtRH5 DEAD-Box RNA Helicases to Promote Viral Asymmetric RNA Replication. *PLoS pathogens* **10**: e1004051
- Kovalev N, Pogany J, Nagy PD** (2012) A co-opted DEAD-box RNA helicase enhances tombusvirus plus-strand synthesis. *PLoS Pathogens* **8**
- Krichevsky A, Kozlovsky SV, Gafni Y, Citovsky V** (2006) Nuclear import and export of plant virus proteins and genomes. *Molecular plant pathology* **7**: 131-146
- Kusakawa T, Shimakami T, Kaneko S, Yoshioka K, Murakami S** (2007) Functional interaction of hepatitis C Virus NS5B with Nucleolin GAR domain. *Journal of biochemistry* **141**: 917-927
- Kushner DB, Lindenbach BD, Grdzlishvili VZ, Noueiry AO, Paul SM, Ahlquist P** (2003) Systematic, genome-wide identification of host genes affecting replication of a positive-strand RNA virus. *Proceedings of the National Academy of Sciences* **100**: 15764-15769
- Laliberté J-F, Sanfaçon H** (2010) Cellular remodeling during plant virus infection. *Annual review of phytopathology* **48**: 69-91
- Lellis AD, Kasschau KD, Whitham SA, Carrington JC** (2002) Loss-of-susceptibility mutants of Arabidopsis thaliana reveal an essential role for eIF(iso)4E during potyvirus infection. *Current Biology* **12**: 1046-1051
- Leonard S, Plante D, Wittmann S, Daigneault N, Fortin MG, Laliberte JF** (2000) Complex formation between potyvirus VPg and translation eukaryotic initiation factor 4E correlates with virus infectivity. *Journal of Virology* **74**: 7730-7737
- Léonard S, Viel C, Beauchemin C, Daigneault N, Fortin MG, Laliberté J-F** (2004) Interaction of VPg-Pro of Turnip mosaic virus with the translation initiation factor 4E and the poly (A)-binding protein in planta. *Journal of general virology* **85**: 1055-1063
- Levin A, Hayouka Z, Friedler A, Loyter A** (2010) Transportin 3 and importin  $\alpha$  are required for effective nuclear import of HIV-1 integrase in virus-infected cells. *Nucleus* **1**: 422

- Levy A, Dafny-Yelin M, Tzfira T** (2008) Attacking the defenders: plant viruses fight back. *Trends in microbiology* **16**: 194-197
- Li D, Liu H, Zhang H, Wang X, Song F** (2008) OsBIRH1, a DEAD-box RNA helicase with functions in modulating defence responses against pathogen infection and oxidative stress. *Journal of experimental botany* **59**: 2133-2146
- Li S-C, Chung M-C, Chen C-S** (2001) Cloning and characterization of a DEAD box RNA helicase from the viable seedlings of aged mung bean. *Plant molecular biology* **47**: 761-770
- Li XH, Carrington JC** (1993) Nuclear transport of tobacco etch potyviral RNA-dependent RNA polymerase is highly sensitive to sequence alterations. *Virology* **193**: 951-958
- Li XH, Valdez P, Olvera RE, Carrington JC** (1997) Functions of the tobacco etch virus RNA polymerase (NIb): subcellular transport and protein-protein interaction with VPg/proteinase (NIa). *Journal of virology* **71**: 1598-1607
- Lin L, Luo Z, Yan F, Lu Y, Zheng H, Chen J** (2011) Interaction between potyvirus P3 and ribulose-1, 5-bisphosphate carboxylase/oxygenase (RubisCO) of host plants. *Virus genes* **43**: 90-92
- Linder P, Jankowsky E** (2011) From unwinding to clamping the DEAD box RNA helicase family. *Nature Reviews Molecular Cell Biology* **12**: 505-516
- Lorković Z, Herrmann RG, Oelmüller R** (1997) PRH75, a new nucleus-localized member of the DEAD-box protein family from higher plants. *Molecular and cellular biology* **17**: 2257-2265
- Lorsch JR** (2002) RNA chaperones exist and DEAD box proteins get a life. *Cell* **109**: 797-800
- Lu Q, Tang X, Tian G, Wang F, Liu K, Nguyen V, Kohalmi SE, Keller WA, Tsang EWT, Harada JJ, Rothstein SJ, Cui Y** (2010) Arabidopsis homolog of the yeast TREX-2 mRNA export complex: Components and anchoring nucleoporin. *Plant Journal* **61**: 259-270
- Lu W-T, Wilczynska A, Smith E, Bushell M** (2014) The diverse roles of the eIF4A family: you are the company you keep. *Biochemical Society transactions* **42**: 166-172
- Lucas WJ** (2006) Plant viral movement proteins: agents for cell-to-cell trafficking of viral genomes. *Virology* **344**: 169-184
- Mallory A, Vaucheret H** (2010) Form, function, and regulation of ARGONAUTE proteins. *The Plant Cell Online* **22**: 3879-3889

- Mandadi KK, Scholthof K-BG** (2013) Plant immune responses against viruses: how does a virus cause disease? *The Plant Cell Online* **25**: 1489-1505
- Matthes A, Schmidt-Gattung S, Köhler D, Forner J, Wildum S, Raabe M, Urlaub H, Binder S** (2007) Two DEAD-box proteins may be part of RNA-dependent high-molecular-mass protein complexes in Arabidopsis mitochondria. *Plant physiology* **145**: 1637-1646
- Matthews REF, Hull R** (2002) *Matthews' plant virology*. Gulf Professional Publishing
- Mayer C, Grummt I** (2005) Extra View Cellular Stress and Nucleolar Function. *Cell Cycle* **4**: 1036-1038
- Mérai Z, Kerényi Z, Kertész S, Magna M, Lakatos L, Silhavy D** (2006) Double-stranded RNA binding may be a general plant RNA viral strategy to suppress RNA silencing. *Journal of Virology* **80**: 5747-5756
- Merits A, Guo D, Järvekülg L, Saarma M** (1999) Biochemical and genetic evidence for interactions between potato A potyvirus-encoded proteins P1 and P3 and proteins of the putative replication complex. *Virology* **263**: 15-22
- Moffett P** (2009) Mechanisms of Recognition in Dominant R Gene Mediated Resistance. *Advances in virus research* **75**: 1-229
- Nagy PD, Pogany J** (2010) Global Genomics and Proteomics Approaches to Identify Host Factors as Targets to Induce Resistance Against Tomato Bushy Stunt Virus. *Advances in virus research* **76**: 123-177
- Nagy PD, Pogany J** (2011) The dependence of viral RNA replication on co-opted host factors. *Nature Reviews Microbiology* **10**: 137-149
- Nakahara KS, Shimada R, Choi S-H, Yamamoto H, Shao J, Uyeda I** (2010) Involvement of the P1 cistron in overcoming eIF4E-mediated recessive resistance against Clover yellow vein virus in pea. *Molecular plant-microbe interactions* **23**: 1460-1469
- Nayak NR, Putnam AA, Addepalli B, Lowenson JD, Chen T, Jankowsky E, Perry SE, Dinkins RD, Limbach PA, Clarke SG** (2013) An Arabidopsis ATP-Dependent, DEAD-Box RNA Helicase Loses Activity upon IsoAsp Formation but Is Restored by PROTEIN ISOASPARTYL METHYLTRANSFERASE. *The Plant Cell* **25**: 2573-2586
- Nicaise V, Gallois JL, Chafiai F, Allen LM, Schurdi-Levraud V, Browning KS, Candresse T, Caranta C, Le Gall O, German-Retana S** (2007) Coordinated and selective recruitment of eIF4E and eIF4G factors for potyvirus infection in Arabidopsis thaliana. *FEBS Letters* **581**: 1041-1046



- Nishikiori M, Dohi K, Mori M, Meshi T, Naito S, Ishikawa M** (2006) Membrane-bound tomato mosaic virus replication proteins participate in RNA synthesis and are associated with host proteins in a pattern distinct from those that are not membrane bound. *Journal of virology* **80**: 8459-8468
- Nitahara-Kasahara Y, Kamata M, Yamamoto T, Zhang X, Miyamoto Y, Muneta K, Iijima S, Yoneda Y, Tsunetsugu-Yokota Y, Aida Y** (2007) Novel nuclear import of Vpr promoted by importin  $\alpha$  is crucial for human immunodeficiency virus type 1 replication in macrophages. *Journal of virology* **81**: 5284-5293
- Noueiry AO, Chen J, Ahlquist P** (2000) A mutant allele of essential, general translation initiation factor DED1 selectively inhibits translation of a viral mRNA. *Proceedings of the National Academy of Sciences* **97**: 12985-12990
- Novak JE, Kirkegaard K** (1994) Coupling between genome translation and replication in an RNA virus. *Genes & development* **8**: 1726-1737
- Ohshima K, Yamaguchi Y, Hirota R, Hamamoto T, Tomimura K, Tan Z, Sano T, Azuhata F, Walsh JA, Fletcher J** (2002) Molecular evolution of Turnip mosaic virus: evidence of host adaptation, genetic recombination and geographical spread. *Journal of General Virology* **83**: 1511-1521
- Olson MO** (2004) Sensing cellular stress: another new function for the nucleolus? *Science's STKE [electronic resource] : signal transduction knowledge environment* **2004**
- Owtrim GW** (2006) RNA helicases and abiotic stress. *Nucleic acids research* **34**: 3220-3230
- Panavas T, Serviene E, Brasher J, Nagy PD** (2005) Yeast genome-wide screen reveals dissimilar sets of host genes affecting replication of RNA viruses. *Proceedings of the National Academy of Sciences of the United States of America* **102**: 7326-7331
- Patarroyo C, Laliberté J-F, Zheng H** (2012) Hijack it, change it: how do plant viruses utilize the host secretory pathway for efficient viral replication and spread? *Frontiers in plant science* **3**
- Poole RL** (2007) The TAIR database. In *Plant Bioinformatics*. Springer, pp 179-212
- Porebski S, Bailey LG, Baum BR** (1997) Modification of a CTAB DNA extraction protocol for plants containing high polysaccharide and polyphenol components. *Plant molecular biology reporter* **15**: 8-15
- Puustinen P, Mäkinen K** (2004) Uridylylation of the potyvirus VPg by viral replicase N1b correlates with the nucleotide binding capacity of VPg. *Journal of Biological Chemistry* **279**: 38103-38110

- Pyle AM** (2008) Translocation and unwinding mechanisms of RNA and DNA helicases. *Annu. Rev. Biophys.* **37**: 317-336
- Qi X, Bao FS, Xie Z** (2009) Small RNA deep sequencing reveals role for Arabidopsis thaliana RNA-dependent RNA polymerases in viral siRNA biogenesis. *PLoS One* **4**: e4971
- Qu F, Morris TJ** (2002) Efficient infection of *Nicotiana benthamiana* by Tomato bushy stunt virus is facilitated by the coat protein and maintained by p19 through suppression of gene silencing. *Molecular plant-microbe interactions* **15**: 193-202
- Qu F, Morris TJ** (2005) Suppressors of RNA silencing encoded by plant viruses and their role in viral infections. *FEBS letters* **579**: 5958-5964
- Qu F, Ye X, Hou G, Sato S, Clemente TE, Morris TJ** (2005) RDR6 has a broad-spectrum but temperature-dependent antiviral defense role in *Nicotiana benthamiana*. *Journal of virology* **79**: 15209-15217
- Rajamäki ML, Valkonen JPT** (2009) Control of nuclear and nucleolar localization of nuclear inclusion protein a of picorna-like potato virus a in *nicotiana* species. *Plant Cell* **21**: 2485-2502
- Rana TM** (2007) Illuminating the silence: understanding the structure and function of small RNAs. *Nature reviews Molecular cell biology* **8**: 23-36
- Rantalainen KI, Eskelin K, Tompa P, Mäkinen K** (2011) Structural flexibility allows the functional diversity of potyvirus genome-linked protein VPg. *Journal of Virology* **85**: 2449-2457
- Restrepo-Hartwig MA, Carrington JC** (1992) Regulation of nuclear transport of a plant potyvirus protein by autoproteolysis. *Journal of virology* **66**: 5662-5666
- Restrepo MA, Freed DD, Carrington JC** (1990) Nuclear transport of plant potyviral proteins. *The Plant Cell Online* **2**: 987-998
- Rice C** (1996) Flaviviridae: the viruses and their replication. *Fields virology* **3**: 931-959
- Robaglia C, Caranta C** (2006) Translation initiation factors: A weak link in plant RNA virus infection. *Trends in Plant Science* **11**: 40-45
- Rocak S, Linder P** (2004) DEAD-box proteins: the driving forces behind RNA metabolism. *Nature reviews Molecular cell biology* **5**: 232-241
- Rogers GW, Richter NJ, Merrick WC** (1999) Biochemical and kinetic characterization of the RNA helicase activity of eukaryotic initiation factor 4A. *Journal of Biological Chemistry* **274**: 12236-12244

- Rohožková J, Navrátil M** (2011) P1 peptidase-a mysterious protein of family Potyviridae. *Journal of biosciences* **36**: 189-200
- Ross AF** (1961) Localized acquired resistance to plant virus infection in hypersensitive hosts. *Virology* **14**: 329-339
- Ross AF** (1961) Systemic acquired resistance induced by localized virus infections in plants. *Virology* **14**: 340-358
- Roudet-Tavert G, Michon T, Walter J, Delaunay T, Redontot E, Le Gall O** (2007) Central domain of a potyvirus VPg is involved in the interaction with the host translation initiation factor eIF4E and the viral protein HCPro. *Journal of General Virology* **88**: 1029-1033
- Ruiz-Ferrer V, Voinnet O** (2009) Roles of plant small RNAs in biotic stress responses. *Annual review of plant biology* **60**: 485-510
- Ryals JA, Neuenschwander UH, Willits MG, Molina A, Steiner H-Y, Hunt MD** (1996) Systemic acquired resistance. *The Plant Cell* **8**: 1809
- Sáenz P, Cervera MT, Dallot S, Quiot L, Quiot J-B, Riechmann JL, Garcí a JA** (2000) Identification of a pathogenicity determinant of Plum pox virus in the sequence encoding the C-terminal region of protein P3+ 6K1. *Journal of General Virology* **81**: 557-566
- Salonen A, Ahola T, Kääriäinen L** (2005) Viral RNA replication in association with cellular membranes. In *Membrane trafficking in viral replication*. Springer, pp 139-173
- Salvador B, SaENZ P, Yangüez E, Quiot JB, Quiot L, Delgadillo MO, Garcia JA, Simón-Mateo C** (2008) Host-specific effect of P1 exchange between two potyviruses. *Molecular plant pathology* **9**: 147-155
- Salvetti A, Greco A** (2014) Viruses and the nucleolus: The fatal attraction. *Biochimica et Biophysica Acta (BBA)-Molecular Basis of Disease* **1842**: 840-847
- Sánchez F, Wang X, Jenner CE, Walsh JA, Ponz F** (2003) Strains of Turnip mosaic potyvirus as defined by the molecular analysis of the coat protein gene of the virus. *Virus Research* **94**: 33-43
- Sanfaçon H** (2005) Replication of positive-strand RNA viruses in plants: contact points between plant and virus components. *Botany* **83**: 1529-1549
- Sanfaçon H** (2012) Investigating the role of viral integral membrane proteins in promoting the assembly of nepovirus and comovirus replication factories. *Frontiers in plant science* **3**

- Sato M, Nakahara K, Yoshii M, Ishikawa M, Uyeda I** (2005) Selective involvement of members of the eukaryotic initiation factor 4E family in the infection of *Arabidopsis thaliana* by potyviruses. *FEBS Letters* **579**: 1167-1171
- Schaad MC, Anderberg RJ, Carrington JC** (2000) Strain-specific interaction of the tobacco etch virus NIa protein with the translation initiation factor eIF4E in the yeast two-hybrid system. *Virology* **273**: 300-306
- Schaad MC, Haldeman-Cahill R, Cronin S, Carrington JC** (1996) Analysis of the VPg-proteinase (NIa) encoded by tobacco etch potyvirus: effects of mutations on subcellular transport, proteolytic processing, and genome amplification. *Journal of Virology* **70**: 7039-7048
- Schaad MC, Jensen PE, Carrington JC** (1997) Formation of plant RNA virus replication complexes on membranes: role of an endoplasmic reticulum-targeted viral protein. *The EMBO journal* **16**: 4049-4059
- Schaad MC, Lellis AD, Carrington JC** (1997) VPg of tobacco etch potyvirus is a host genotype-specific determinant for long-distance movement. *Journal of virology* **71**: 8624-8631
- Schiestl RH, Gietz RD** (1989) High efficiency transformation of intact yeast cells using single stranded nucleic acids as a carrier. *Current genetics* **16**: 339-346
- Schoelz JE, Harries PA, Nelson RS** (2011) Intracellular transport of plant viruses: Finding the door out of the cell. *Molecular Plant* **4**: 813-831
- Scholthof KBG, Adkins S, Czosnek H, Palukaitis P, Jacquot E, Hohn T, Hohn B, Saunders K, Candresse T, Ahlquist P** (2011) Top 10 plant viruses in molecular plant pathology. *Molecular Plant Pathology* **12**: 938-954
- Seo J-K, Lee S-H, Kim K-H** (2009) Strain-specific cylindrical inclusion protein of Soybean mosaic virus elicits extreme resistance and a lethal systemic hypersensitive response in two resistant soybean cultivars. *Molecular plant-microbe interactions* **22**: 1151-1159
- Serva S, Nagy PD** (2006) Proteomics analysis of the tombusvirus replicase: Hsp70 molecular chaperone is associated with the replicase and enhances viral RNA replication. *Journal of virology* **80**: 2162-2169
- Sharma N, Sahu PP, Puranik S, Prasad M** (2013) Recent Advances in Plant-Virus Interaction with Emphasis on Small Interfering RNAs (siRNAs). *Molecular biotechnology* **55**: 63-77
- Shiboleth YM, Haronsky E, Leibman D, Arazi T, Wassenegger M, Whitham SA, Gaba V, Gal-On A** (2007) The conserved FRNK box in HC-Pro, a plant viral suppressor of gene silencing, is required for small RNA binding and mediates symptom development. *Journal of virology* **81**: 13135-13148

- Shimakami T, Honda M, Kusakawa T, Murata T, Shimotohno K, Kaneko S, Murakami S** (2006) Effect of hepatitis C virus (HCV) NS5B-nucleolin interaction on HCV replication with HCV subgenomic replicon. *Journal of virology* **80**: 3332-3340
- Shukla DD, Ward CW, Brunt AA** (1994) *The Potyviridae*. Cab International
- Siddell SG** (1995) *The coronaviridae*. Springer
- Silhavy D, Molnár A, Lucioli A, Szittyá G, Hornyik C, Tavazza M, Burgyán J** (2002) A viral protein suppresses RNA silencing and binds silencing-generated, 21-to 25-nucleotide double-stranded RNAs. *The EMBO Journal* **21**: 3070-3080
- Singleton MR, Dillingham MS, Wigley DB** (2007) Structure and mechanism of helicases and nucleic acid translocases. *Annu. Rev. Biochem.* **76**: 23-50
- Sochor J, Babula P, Adam V, Krska B, Kizek R** (2012) Sharka: The past, the present and the future. *Viruses* **4**: 2853-2901
- Sonenberg N, Hinnebusch AG** (2009) Regulation of translation initiation in eukaryotes: mechanisms and biological targets. *Cell* **136**: 731-745
- Song S-K, Ryu KH, Kang YH, Song JH, Cho Y-H, Yoo S-D, Schiefelbein J, Lee MM** (2011) Cell fate in the Arabidopsis root epidermis is determined by competition between WEREWOLF and CAPRICE.
- Soosaar JL, Burch-Smith TM, Dinesh-Kumar SP** (2005) Mechanisms of plant resistance to viruses. *Nature Reviews Microbiology* **3**: 789-798
- Sorel M, Garcia JA, German-Retana S** (2014) The potyviridae cylindrical inclusion helicase: A key multipartner and multifunctional protein. *Molecular Plant-Microbe Interactions* **27**: 215-226
- Sparkes IA, Runions J, Kearns A, Hawes C** (2006) Rapid, transient expression of fluorescent fusion proteins in tobacco plants and generation of stably transformed plants. *Nature protocols* **1**: 2019-2025
- Suehiro N, Natsuaki T, Watanabe T, Okuda S** (2004) An important determinant of the ability of Turnip mosaic virus to infect Brassica spp. and/or Raphanus sativus is in its P3 protein. *Journal of general virology* **85**: 2087-2098
- Svitkin YV, Pause A, Haghighat A, Pyronnet S, Witherell G, Belsham GJ, Sonenberg N** (2001) The requirement for eukaryotic initiation factor 4A (eIF4A) in translation is in direct proportion to the degree of mRNA 5' secondary structure. *Rna* **7**: 382-394
- Sztuba-Solińska J, Stollar V, Bujarski JJ** (2011) Subgenomic messenger RNAs: mastering regulation of (+)-strand RNA virus life cycle. *Virology* **412**: 245-255

- Takken FL, Albrecht M, Tameling WI** (2006) Resistance proteins: molecular switches of plant defence. *Current opinion in plant biology* **9**: 383-390
- Tanner NK, Cordin O, Banroques J, Doère M, Linder P** (2003) The Q motif: a newly identified motif in DEAD box helicases may regulate ATP binding and hydrolysis. *Molecular cell* **11**: 127-138
- Tavert-Roudet G, Abdul-Razzak A, Doublet B, Walter J, Delaunay T, German-Retana S, Michon T, le Gall O, Candresse T** (2012) The C terminus of lettuce mosaic potyvirus cylindrical inclusion helicase interacts with the viral VPg and with lettuce translation eukaryotic initiation factor 4E. *Journal of General Virology* **93**: 184-193
- Thivierge K, Cotton S, Dufresne PJ, Mathieu I, Beauchemin C, Ide C, Fortin MG, Laliberté JF** (2008) Eukaryotic elongation factor 1A interacts with Turnip mosaic virus RNA-dependent RNA polymerase and VPg-Pro in virus-induced vesicles. *Virology* **377**: 216-225
- Thresh J** (2006) Crop viruses and virus diseases: a global perspective. *Virus Diseases and Crop Biosecurity*. Springer, pp 9-32
- Tilsner J, Linnik O, Christensen NM, Bell K, Roberts IM, Lacomme C, Oparka KJ** (2009) Live-cell imaging of viral RNA genomes using a Pumilio-based reporter. *The Plant Journal* **57**: 758-770
- Tomlinson J** (1987) Epidemiology and control of virus diseases of vegetables. *Annals of Applied Biology* **110**: 661-681
- Tran EJ, Zhou Y, Corbett AH, Wentz SR** (2007) The DEAD-box protein Dbp5 controls mRNA export by triggering specific RNA: protein remodeling events. *Molecular cell* **28**: 850-859
- Truniger V, Aranda M** (2009) Recessive resistance to plant viruses. *Advances in virus research* **75**: 119-231
- Umate P, Tuteja R, Tuteja N** (2010) Genome-wide analysis of helicase gene family from rice and Arabidopsis: a comparison with yeast and human. *Plant molecular biology* **73**: 449-465
- Urcuqui-Inchima S, Haenni A-L, Bernardi F** (2001) Potyvirus proteins: a wealth of functions. *Virus research* **74**: 157-175
- Valli A, Martín-Hernández AM, López-Moya JJ, García JA** (2006) RNA silencing suppression by a second copy of the P1 serine protease of Cucumber vein yellowing ipomovirus, a member of the family Potyviridae that lacks the cysteine protease HCPro. *Journal of virology* **80**: 10055-10063

- van Regenmortel MH, Fauquet C, Bishop D, Carstens E, Estes M, Lemon S, Maniloff J, Mayo M, McGeoch D, Pringle C** (2000) Virus taxonomy: classification and nomenclature of viruses. Seventh report of the International Committee on Taxonomy of Viruses. Academic Press
- Vashisht AA, Tuteja N** (2006) Stress responsive DEAD-box helicases: a new pathway to engineer plant stress tolerance. *Journal of Photochemistry and Photobiology B: Biology* **84**: 150-160
- Vaucheret H** (2006) Post-transcriptional small RNA pathways in plants: mechanisms and regulations. *Genes & Development* **20**: 759-771
- Verchot J, Koonin EV, Carrington JC** (1991) The 35-kDa protein from the N-terminus of the potyviral polyprotein functions as a third virus-encoded proteinase. *Virology* **185**: 527-535
- Vijayapalani P, Maeshima M, Nagasaki-Takekuchi N, Miller WA** (2012) Interaction of the trans-frame potyvirus protein P3N-PIPO with host protein PCaP1 facilitates potyvirus movement. *PLoS Pathogens* **8**
- Voinnet O, Lederer C, Baulcombe DC** (2000) A Viral Movement Protein Prevents Spread of the Gene Silencing Signal in *Nicotiana benthamiana*. *Cell* **103**: 157-167
- Wagner EK, Hewlett MJ, Bloom DC, Camerini D** (1999) Basic virology. Blackwell Science Malden
- Walsh JA, Jenner CE** (2002) Turnip mosaic virus and the quest for durable resistance. *Molecular Plant Pathology* **3**: 289-300
- Wang A** (2013) Molecular isolation and functional characterization of host factors required in the virus infection cycle for disease control in plants. *CAB Reviews: Perspectives in Agriculture, Veterinary Science, Nutrition and Natural Resources* **8**
- Wang A, Krishnaswamy S** (2012) Eukaryotic translation initiation factor 4E-mediated recessive resistance to plant viruses and its utility in crop improvement. *Molecular Plant Pathology* **13**: 795-803
- Wang H, Kim S, Ryu W-S** (2009) DDX3 DEAD-Box RNA helicase inhibits hepatitis B virus reverse transcription by incorporation into nucleocapsids. *Journal of virology* **83**: 5815-5824
- Wang Y, Tzfira T, Gaba V, Citovsky V, Palukaitis P, Gal-On A** (2004) Functional analysis of the Cucumber mosaic virus 2b protein: pathogenicity and nuclear localization. *Journal of general virology* **85**: 3135-3147

- Wei T, Huang TS, McNeil J, Laliberté JF, Hong J, Nelson RS, Wang A** (2010) Sequential recruitment of the endoplasmic reticulum and chloroplasts for plant potyvirus replication. *Journal of Virology* **84**: 799-809
- Wei T, Wang A** (2008) Biogenesis of cytoplasmic membranous vesicles for plant potyvirus replication occurs at endoplasmic reticulum exit sites in a COPI- and COPII-dependent manner. *Journal of Virology* **82**: 12252-12264
- Wei T, Zhang C, Hong J, Xiong R, Kasschau KD, Zhou X, Carrington JC, Wang A** (2010) Formation of complexes at plasmodesmata for potyvirus intercellular movement is mediated by the viral protein P3N-PIPO. *PLoS Pathogens* **6**
- Weidman MK, Sharma R, Raychaudhuri S, Kundu P, Tsai W, Dasgupta A** (2003) The interaction of cytoplasmic RNA viruses with the nucleus. *Virus research* **95**: 75-85
- Wen R-H, Hajimorad M** (2010) Mutational analysis of the putative pipo of soybean mosaic virus suggests disruption of PIPO protein impedes movement. *Virology* **400**: 1-7
- Wen RH, Maroof MS, Hajimorad M** (2011) Amino acid changes in P3, and not the overlapping pipo-encoded protein, determine virulence of Soybean mosaic virus on functionally immune Rsv1-genotype soybean. *Molecular plant pathology* **12**: 799-807
- Whitham SA, Wang Y** (2004) Roles for host factors in plant viral pathogenicity. *Current opinion in plant biology* **7**: 365-371
- Wittmann S, Chatel H, Fortin MG, Laliberté JF** (1997) Interaction of the viral protein genome linked of turnip mosaic potyvirus with the translational eukaryotic initiation factor (iso) 4E of *Arabidopsis thaliana* using the yeast two-hybrid system. *Virology* **234**: 84-92
- Xie Z, Johansen LK, Gustafson AM, Kasschau KD, Lellis AD, Zilberman D, Jacobsen SE, Carrington JC** (2004) Genetic and functional diversification of small RNA pathways in plants. *PLoS biology* **2**: e104
- Xiong R, Wang A** (2013) SCE1, the SUMO-conjugating enzyme in plants that interacts with NIB, the RNA-dependent RNA polymerase of Turnip mosaic virus, is required for viral infection. *Journal of Virology* **87**: 4704-4715
- Xu Z, Anderson R, Hobman TC** (2011) The capsid-binding nucleolar helicase DDX56 is important for infectivity of West Nile virus. *Journal of virology* **85**: 5571-5580
- Xu Z, Hobman TC** (2012) The helicase activity of DDX56 is required for its role in assembly of infectious West Nile virus particles. *Virology* **433**: 226-235

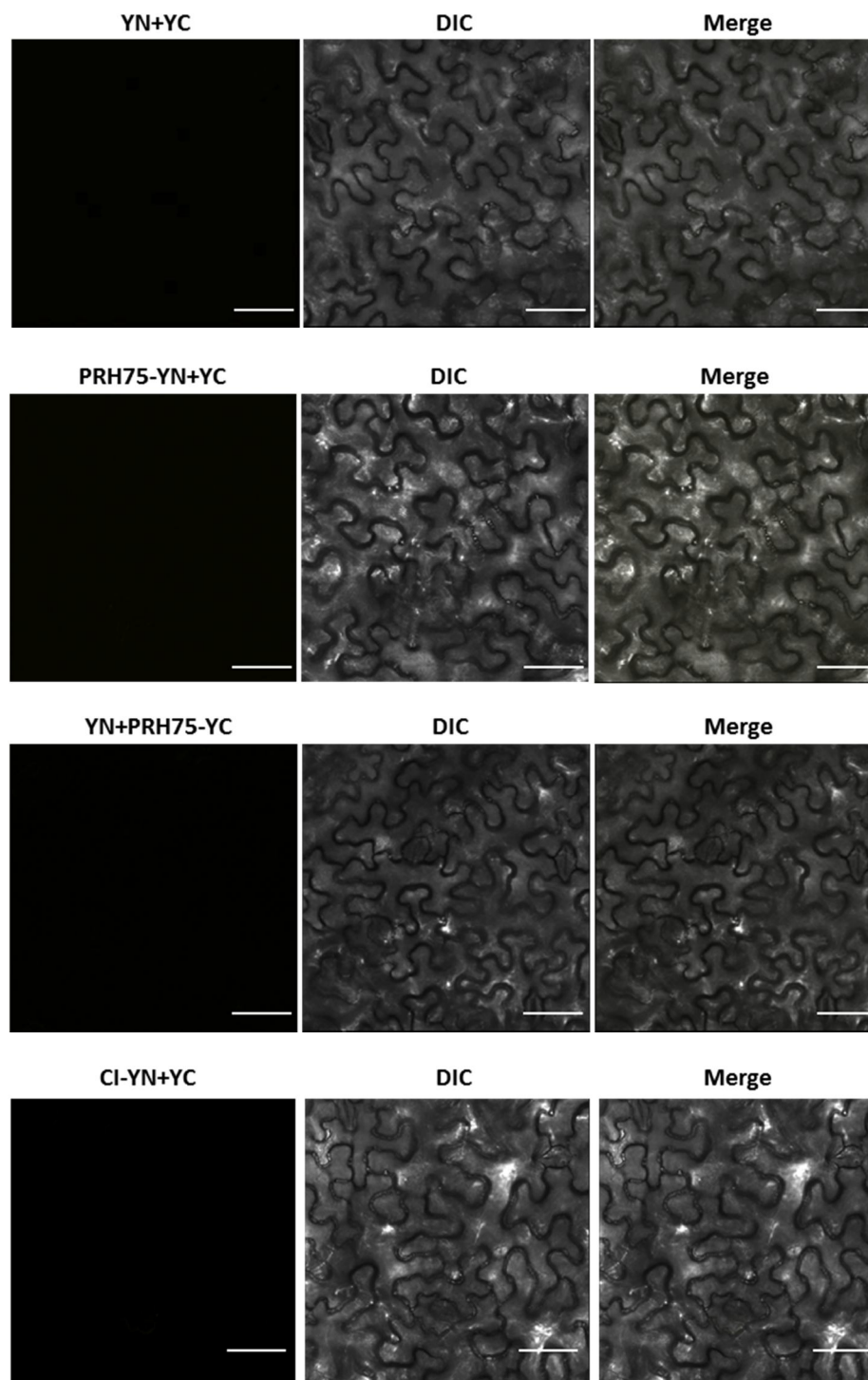


- Yamaji Y, Maejima K, Komatsu K, Shiraishi T, Okano Y, Himeno M, Sugawara K, Neriya Y, Minato N, Miura C, Hashimoto M, Namba S** (2012) Lectin-mediated resistance impairs plant virus infection at the cellular level. *Plant Cell* **24**: 778-793
- Yang Q, Del Campo M, Lambowitz AM, Jankowsky E** (2007) DEAD-box proteins unwind duplexes by local strand separation. *Molecular cell* **28**: 253-263
- Yedavalli VS, Neuveut C, Chi Y-h, Kleiman L, Jeang K-T** (2004) Requirement of DDX3 DEAD box RNA helicase for HIV-1 Rev-RRE export function. *Cell* **119**: 381-392
- Yoshii M, Nishikiori M, Tomita K, Yoshioka N, Kozuka R, Naito S, Ishikawa M** (2004) The Arabidopsis cucumovirus multiplication 1 and 2 loci encode translation initiation factors 4E and 4G. *Journal of virology* **78**: 6102-6111
- Zhang C, Hajimorad M, Eggenberger A, Tsang S, Whitham S a, Hill, JH.** 2009. Cytoplasmic inclusion cistron of Soybean mosaic virus serves as a virulence determinant on Rsv3-genotype soybean and a symptom determinant. *Virology* **391**: 240-248
- Zhu J, Dong C-H, Zhu J-K** (2007) Interplay between cold-responsive gene regulation, metabolism and RNA processing during plant cold acclimation. *Current opinion in plant biology* **10**: 290-295
- Zilian E, Maiss E** (2011) Detection of plum pox potyviral protein-protein interactions in planta using an optimized mRFP-based bimolecular fluorescence complementation system. *Journal of General Virology* **92**: 2711-2723

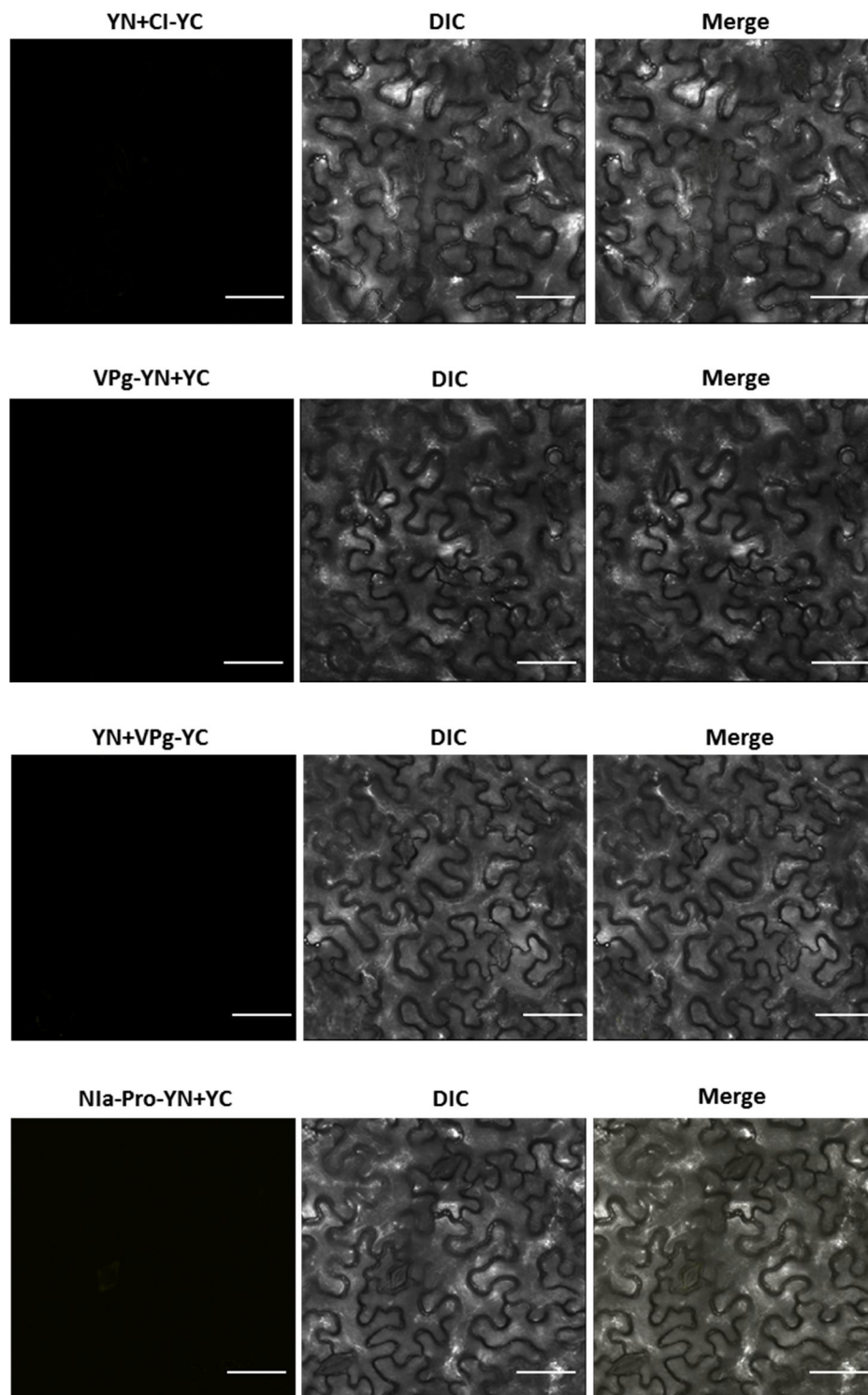
## Appendices

### Appendix I: List of DEAD-box RNA helicases in *Arabidopsis*.

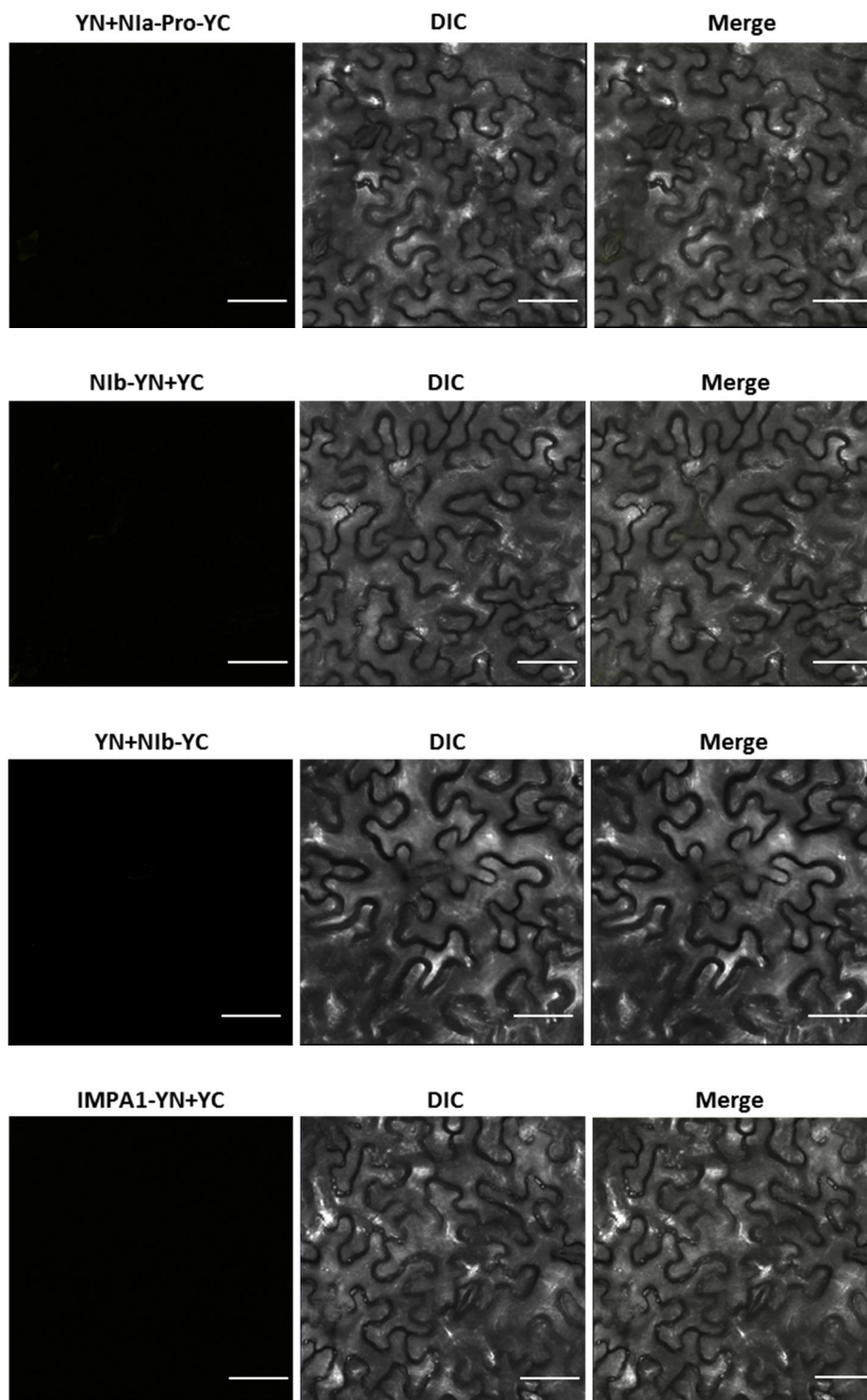
Gene Names	Locus	Gene Names	Locus
RH1	AT4G15850	RH46	AT5G14610
DRH1	AT3G01540	RH47	AT1G12770
RH2(eIF-4A-III)	AT3G19760	RH48	AT1G63250
RH3	AT5G26742	RH49	AT1G71370
RH4(eIF-4A)	AT3G13920	RH50	AT3G06980
eIF-4A-2	AT1G54270	RH51	AT3G18600
eIF-4A-3	AT1G72730	RH52	AT3G58570
RH5	AT1G31970	RH53	AT3G22330
RH6	AT2G45810	RH55	AT1G71280
RH8	AT4G00660	RH56	AT5G11200
RH9	AT3G22310	RH57	AT3G09720
RH10	AT5G60990	RH58	AT5G19210
RH11	AT3G58510	PRH75	AT5G62190
RH12	AT3G61240		
RH13	AT3G16840		
RH15	AT5G11170		
RH16	AT4G34910		
RH17	AT2G40700		
RH18	AT5G05450		
RH20	AT1G55150		
RH21	AT2G33730		
RH22	AT1G59990		
RH24	AT2G47330		
RH25	AT5G08620		
RH26	AT5G08610		
RH27	AT5G65900		
RH28	AT4G16630		
RH29	AT1G77030		
RH30	AT5G63120		
RH31	AT5G63630		
RH32	AT5G54910		
RH33	AT2G07750		
RH34	AT1G51380		
RH35	AT5G51280		
RH36	AT1G16280		
RH37	AT2G42520		
RH38	AT3G53110		
RH39	AT4G09730		
RH40	AT3G06480		
RH41	AT3G02065		
RH42	AT1G20920		
RH43	AT4G33370		
RH45	AT3G09620		

**Appendix II: Negative controls of the BiFC assays.**

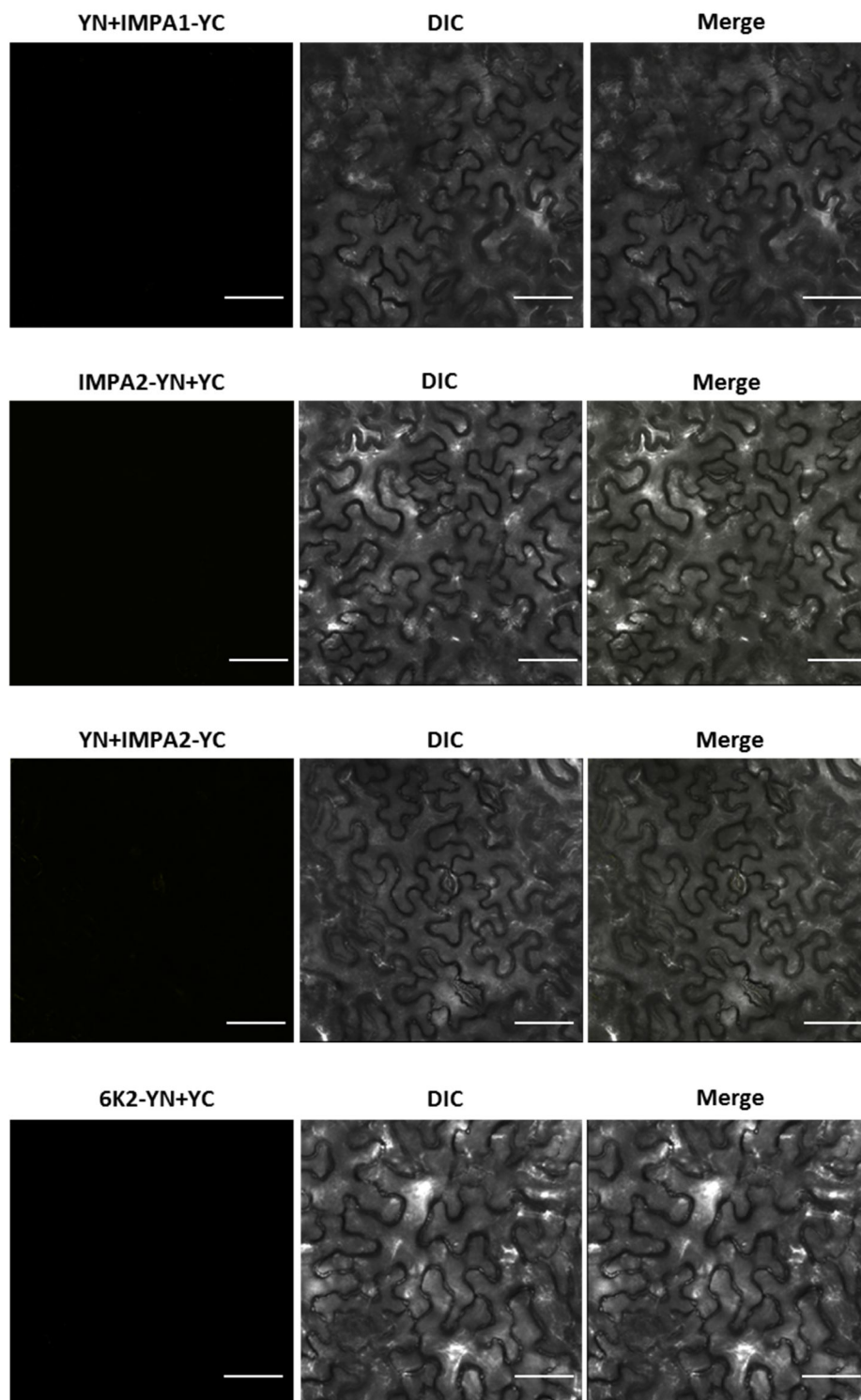
Bars, 50  $\mu$ m.



Bars, 50 µm.



Bars, 50  $\mu$ m.



Bars, 50  $\mu$ m.

**CURRICULUM VITAE****Yinzi Li****Education**


---

 The University of Western Ontario

London, Ontario, Canada

2009 ~ present, Ph.D candidate

Nanjing Agricultural University

Nanjing, Jiangsu, China

2005 ~ 2009, Bachelor's Degree of Agronomy (Honors)

**Honors/Awards**


---

 2009 ~ 2014 Western Graduate Research Scholarship

2011 American Society For Virology (ASV) Travel Award

**Post presentation**


---

**Li, Yinzi**, Zhang, Changwei, Bernards, Mark, Wang, Aiming (2010) Screening for DEAD-box RNA helicases in *Arabidopsis* that are required for *Turnip mosaic virus* (TuMV) infection. Joint Annual Meetings of the American Society of Plant Biologists and the Canadian Society of Plant Physiologists, Montréal, Canada.

**Li, Yinzi**, Chowda-Reddy, R.V., Bernards, Mark, Wang, Aiming (2011) Molecular identification of host membrane-associated proteins that interact with potyviral P3. The 2011 Annual Meeting of the American Society for Virology, University of Minnesota, Minneapolis, Minnesota.
**Oral presentation**


---

**Li, Yinzi**, Bernards, Mark, Wang, Aiming (2012) Molecular identification and characterization of host proteins associated with potyvirus infection. The 2012 Annual Meeting of the American Society for Virology, University of Wisconsin-Madison, Madison, Wisconsin.